Developing Antiviral Platforms And Assessing Interferon Against Kyasanur Forest Disease Virus

by

Bradley William Michael Cook

A Thesis submitted to the Faculty of Graduate Studies of The University of Manitoba in partial fulfilment of the requirements of the degree of

Doctor of Philosophy

Department of Microbiology, University of Manitoba Winnipeg, Manitoba, Canada

Abstract

Kyasanur Forest disease virus (KFDV) of the *Flaviviridae* virus family has caused seasonal infections and periodic outbreaks in Karnataka, India. First identified in 1957, KFDV annually infects 400-500 people and has a fatality rate of 3-5%; there are no approved antivirals and the existing licensed vaccine's effectiveness appears to be questionable. Many tools for KFDV research are limited and this work sought to develop methods for analysing antivirals, including interferon (IFN)-α/β species. The BHK-21 (ATCC) cell line allowed for high virus propagation and distinguishable cytopathic effects (CPE) for determining antiviral effectiveness. The additional tool of a reverse genetics system expressing a full-length cDNA KFDV genome with a GFP reporter failed to propagate, despite numerous GFP genome-insertion strategies. The clinically approved IFN-α2a or IFN-α2b has had variable success at combatting flavivirus diseases in people, especially in the immuno-compromised. The continued passaging of KFDV-infected cells with repeated IFN-α2a treatment did not eliminate KFDV and had little effect on infectious particle production. IFN-α species, αWA and αK were more effective than IFN-α2a and α2b at reducing KFDV; however dose ranges indicated that while low concentrations could limit CPE, higher concentrations were needed to inhibit virion release. Avoidance of IFN-α/β through Jak/STAT signalling repression was attributed to the NS5 protein, specifically the RdRp domain based on data obtained with luciferase and vesicular stomatitis virus (VSV) recovery assays. However, the mechanism appears to act subsequently to STAT1/2 activation without NS5 binding to any Jak/STAT components. A non-infectious, replicative system serving as a platform for antiviral drug testing against KFDV in a high throughput manner could only provide

luciferase signals when the NS proteins capable of driving replication, were supplied *in cis* (subgenomic) but not *in trans* (antigenome). To conclude, IFN-α species such as IFN-αWA may be better suited than the licensed IFN-α2a for treatment of KFDV infections; however, IFN effects appear to be subdued *in vitro* due to the actions of the NS5 protein. While IFN may not be a successful antiviral against KFDV, the work in this thesis provides a foundation for evaluating other potential anti-KFDV therapeutics.

List Of Abbreviations

AHFV-Alkhurma hemorrhagic fever virus

BHK-Baby Hamster Kidney

C-Capsid protein

CAT-chloramphenicol-acetyl-transferase

CC-Cytotoxicity concentration

cDNA-Complementary Deoxyribonucleic acid

CL-2-Containment level 2

CL-4-Containment level 4

CM-Convoluted membranes

CPE-Cytopathic effect

DENV-Dengue virus

DLR-Dual luciferase reporter

DMEM-Dulbecco's minimal essential medium

DNA-Deoxyribonucleic acid

E-Envelope protein

E. coli-Escherichia coli

EDTA-ethylene-diamine-tetra-acetic acid

EMCV-Encephalomyocarditis Virus

EMEM-Eagle's minimal essential medium

ER-Endoplasmic reticulum

FACS-Fluorescence-associated cell sorting

FBS-Fetal bovine serum

GFP-Green fluorescent protein

GTP-Guanosine tri-phosphate

HA-Hemagglutinin

HCV-Hepatitis C virus

HEK 293T-Human embryonic kidney 293 T-antigen

HIV-Human immunodeficiency virus

HRP-Horse-radish peroxidase

HRV-Human rhinovirus

hScrib-Human scribble

IC-Inhibitory concentration

IFN-Interferon

IFNAR1-Interferon alpha receptor 1

IRES-Internal ribosome entry sequence

IRF-9-Interferon regulatory factor – 9

ISG-Interferon stimulated genes

ISGF3-Interferon-stimulated growth factor 3

ISRE-Interferon-stimulated response element

Jak-Janus kinase

JEV-Japanese encephalitis virus

Kb-Kilo base

kDa-Kilo Dalton

KFDV-Kyasanur Forest disease virus

LGTV-Langat virus

M-Membrane protein

Mda5-Melanoma differentiation-association gene 5

MDCK-Madin-Darby canine kidney

MEM-Minimal essential medium

MOI-Multiplicity of infection

MTase-Methyl-transferase

NML-National Microbiology Laboratory

NS-Non-Structural proteins

NTPase-Nucleoside tri-phosphatase

PBS-Phosphate-buffered saline

PC-Paracrystalline membranes

PCR-Polymerase chain reaction

PKR-Protein kinase R

PMSF-Phenyl-methane-sulfonyl-fluoride

prM-Pre-Membrane protein

PS-Porcine stable kidney

RC-Replication complex

RdRp-RNA-dependent RNA polymerase

RGS-Reverse genetics system

RIG-I-Retinoic acid-inducible gene I

RLU-Raw light units

RNA-Ribonucleic Acid

RT-PCR-Reverse transcription polymerase chain reaction

SDS-Sodium dodecyl sulfate

SDS-PAGE-Sodium dodecyl sulfate-polyacrylamide gel electrophoresis

SeAP-Secreted alkaline phosphatase

STAT-Signal transducer and activator of transcription

TBE serocomplex-Tick-borne encephalitis serocomplex

TBEV-Tick-borne encephalitis virus

TCID-Tissue culture infectious dose

TRIM-Tripartite motif

UTR-Untranslated Region

VLP-Virus-like particle

VP-Vesicle packets

VSV-Vesicular stomatitis virus

VSV-GFP-Vesicular stomatitis virus-green fluorescent protein

WNV-West Nile virus

YFV-Yellow fever virus

Acknowledgements

I would like to thank Dr. Steven Theriault and Dr. Deborah Court for the opportunity to follow the research endeavors that I wanted and for their unwavering support throughout this process. Thank you to my remaining committee members Dr. Darwyn Kobasa and Dr. Teresa de Kievit for their candor, which undoubtedly, shaped my project and helped to improve myself as a scientist. I would like to thank the external examiner Dr. Michael Holbrook for his constructive criticisms, which undeniably helped to shape this thesis. Thank you to our technician Mr. Todd Cutts, we may not always see "eye to eye" but the success of this project can be attributed to your technical expertise, advice and support. Thank you to Mr. Aidan Nikiforuk for help with many aspects of the project, but most importantly for aiding in the dreaded minigenome/subgenomic clone systems. I hope we never have to talk about that project ever again! I would also like to extend thanks to all of the former members of the ABRP group who have supported me throughput this process, specifically Mr. Jay Krishnan and Mrs. Diane Gordon-Pappis. Special thank you to the CL-4 support staff: Mrs. Lisa Fernando, Mr. Allen Grolla, Mr. Shane Jones and Mr. Jason Gren, for their fantastic CL-4 training and technical expertise. A big thank you for the rest of Special Pathogens program, I cannot thank you all enough for the support and the guidance that I have received over the years!! I would finally like to thank everyone at the National Microbiology Laboratory, especially the DNA core and Proteomics departments and the department of Microbiology at the University of Manitoba.

Dedication

My work is dedicated to my lord and savior Jesus Christ and to the loving memories of my grandmother, mother and sister. I would also like to dedicate this work to my wife My Kim Tran, her endless support and encouragement really drove this degree. This work is also dedicated to the rest of my close friends/brothers in team Showtime!

List Of Tables.

List Of Figures.

List Of Copyrighted Materials.

Figures 3.4.1.a. and Figure 3.4.2.1.b. were obtained from: Cook, B. W. M., Cutts, T. A., Court, D. A., Theriault, S. (2012) The generation of a reverse genetics system for Kyasanur Forest disease virus and the ability to antagonize the induction of the antiviral state. Virus Research 163:2. Reproduced with permission.

Chapter 1. Thesis Introduction

Viral hemorrhagic fevers have come to the forefront of global consciousness with the 2013-2015 West African ebola virus outbreak, which has killed more people than all of the previous outbreaks combined (Cohen & Kupferschmidt 2014). Unfortunately, the number of cases continues to increase and importation of cases into Europe and United States, and transmission within hospital settings have occurred (Kuhn et al. 2014). Much like ebola virus, there are hemorrhagic fever-causing flaviviruses, include those that cause yellow fever, dengue, Alkhumra hemorrhagic fever, Omsk hemorrhagic fever and Kyasanur Forest diseases (Go et al. 2014). In recent times, flaviviruses have been expanding their geographical ranges as increased travel, shipping of goods and animals, and human expansion into virus-endemic areas may provide new opportunities for the spread of vectors, animal reservoirs and ecological niches (Singh & Gajadhar 2014; Jones et al. 2008). Examples of such expansion have been documented with the emergence or re-emergence of flaviviruses in new geographical locations, as demonstrated by the detection of West Nile virus in North America (Lanciotti et al. 1999; Campbell et al. 2002), Alkhumra hemorrhagic fever virus in Egypt (Carletti et al. 2010; Ravanini et al. 2011; Musso et al. 2015) and Kyasanur Forest disease virus in three other Indian states (Mourya et al. 2013; Tandale et al. 2015; ProMED-mail 2015) and possibly China (Wang et al. 2009), Powassan virus in Russia and North America (Deardorff et al. 2013), Omsk hemorrhagic fever virus in Russia (Karan et al. 2014), and Japanese encephalitis virus into New Guinea and Australia (Ritchie & Rochester 1998). Overlooking viral hemorrhagic fever viruses has proven costly, as exemplified by the ebola outbreak in West Africa. While Kyasanur Forest disease virus remains in a localized area in India, the threat of increased dissemination into new locations is

concerning, especially since the closely-related Alkhumra hemorrhagic fever has spread from Saudi Arabia into Egypt.

Since the discovery of Kyasanur Forest disease virus research focused mainly on vectors of transmission, defining causes of the intermittent outbreaks, clinical aspects of the disease and vaccine development. Work on KFDV from a research perspective was minimal from the 1960s onwards, until recent years with increased research in the areas of phylogenetics, small animal model development, vaccine efficacy and genetic manipulations. In spite of this exciting upsurge in KFDV investigation, there are many unanswered questions. This thesis is devoted to not only continuing such studies but, also encouraging further pursuits for KFDV examination. The research described in this thesis was designed to address many aspects of KFDV that remain unresolved, with a focus on antiviral exploration. The starting point was to define suitable tissue culture cell lines to detect and quantify KFDV infection, visually with a microscope. Attempts were made to greatly enhance this process by adding a reporter gene, expressed like the other viral proteins, so that during replication the reporter could give an indication of virus replication and be measured empirically. Interferon (IFN) is a commonly used antiviral and has been used to treat many flavivirus diseases. This work evaluated the likelihood of IFN to be a successful antiviral treatment option against KFDV *in vitro*, after the infection has occurred. Building on IFN studies demonstrating that many flaviviruses can inhibit the antiviral properties of IFN, assessing the ability of KFDV to also do this was undertaken. Finally, several methodologies were created to allow for a tool that enables quick and reliable testing conditions for antivirals against KFDV. An additional benefit of such a system is to eliminate the need for high containment laboratories for initial antiviral compound screenings. Taken together, the work

described in this thesis will help to determine the value of IFN as a post-exposure treatment against KFDV infection and in developing the tools needed for analyzing other antivirals by *in vitro* methods. Such antivirals may be used individually or in combinational treatments with IFN.

1.1. Introduction To Kyasanur Forest Disease Virus (KFDV)

Kyasanur Forest disease virus (herein referred to as KFDV) is a member of the *Flaviviridae* virus family and *Flavivirus* genus, which includes many mosquito- and tick-borne viruses. Within the genus there are many serocomplexes of viruses based on their antigenic and genetic relatedness; KFDV falls within the tick-borne encephalitis (TBE) serocomplex, as determined by antibody cross-reactivity among all of the tick-borne viruses. This serocomplex includes: tick-borne encephalitis, Russian spring-summer encephalitis, Omsk hemorrhagic fever, Powassan, Langat and Louping-Ill viruses (Calisher et al. 1989). With the exception of Powassan virus, the tick-borne serocomplex viruses are located throughout Eurasia, but for the most part each member of the complex is restricted to specific geographical areas (Gould et al. 2004). Interestingly, the majority of the TBE viruses are predominantly associated with neurological disorders, while Omsk hemorrhagic fever, Alkhumra hemorrhagic fever and KFD virus-diseases primarily cause hemorrhagic fever manifestations with infrequent neurological disease (Gritsun et al. 2003).

KFDV is a containment level-4 (CL-4) virus (Cook et al. 2012), and like other flaviviruses, it is composed of a spherical-shaped, lipid-enveloped particle of 45 nm in diameter,

encasing an icosahedral nucleocapsid that contains the positive-stranded RNA genome of 10.8 kilobases (Cook et al. 2012; Pattnaik 2006).

The virus was first discovered in 1957 during an outbreak that occurred in monkeys followed by humans within the Kyasanur Forest of the Shimoga district in Karnataka state (Work et al. 1959). Over time, sporadic outbreaks continued in monkeys and humans within Shimoga and spread into six neighboring districts, despite the introduction of a vaccine in 1990 (Mourya et al. 2013). More recently, KFDV cases have been documented in three adjacent states, as there were sporadic human and monkey laboratory-confirmed cases in Kerala state, one confirmed monkey case in Tamil Nadu state (Mourya et al. 2013; Tandale et al. 2015) and 18 human cases in Goa (ProMED-mail 2015). Most of these cases interestingly occurred within a national park that is 400 kilometers away from the endemic Shmoga district of Karnataka state, straddling Karnataka, Kerala and Tamil Nandu states (Stone 2014). Furthermore, serological surveys of people suggest that KFDV may be more widespread, with high proportions of seropositive people in northern India, specifically Gujrat and West Bengal states (Pattnaik 2006). The transmission of the virus to humans and monkeys occurs primarily during blood meal uptake of KFDV-infected ticks of the *Haemaphysalis* species (Trapido et al. 1959), thus KFDV is of arthropod-borne origin. The virus is maintained in these forested areas by cycling the virus with reservoir animals, including rats, shrews (Boshell & Rajagopalan 1968), bats (Bhat et al. 1978) and possibly cattle (Anderson & Singh 1971). KFDV is a zoonotic virus as humans may acquire the virus through handling and interactions with infected or deceased monkeys (Mourya et al. 2013) and perhaps with reservoir animals, although this has not been documented (Pattnaik 2006). Incidence of human infection occurs in two peaks: the dry season (December to May) and

the start of the monsoon season (June to September), albeit at lower levels as human and monkey activities on the forest floor are reduced (Work et al. 1959). Villagers enter the forested areas to plant crops such as rice, allow livestock to graze and, collect firewood and leaves (Trapido et al. 1959). In this venue, close contact with infected ticks and potentially infected or dead monkeys such as red-faced bonnets (*Macaca radiata*) and black-faced langurs (*Semnopithecus entellus*) (Pattnaik 2006) is possible. Monkeys leave the forest canopy to pillage from crops or when they die; during this time ticks on their faces, ears, hands and feet and pelvic regions are able drop off onto the forest floor, thereby aiding in the dissemination of the virus, not only to humans but, to other monkeys, reservoir animals and naïve ticks (Trapido et al. 1964). Additionally, factors including climate change, increased deforestation and agricultural practices, may lead to more interactions between ticks, monkeys and humans within KFD-endemic areas (Singh & Gajadhar 2014).

The vaccination strategy against KFDV is intended to be administered to humans residing within 5 kilometers of a human, monkey or tick laboratory-confirmed positive case (Kasabi, Murhekar, Sandhya, et al. 2013). This vaccine was first administered in one or two doses a month apart and was evaluated for protection during the 1990-1992 endemic periods (Dandawate et al. 1994). In summation of the campaigns starting in 1990-1992, of the 349-confirmed cases: 325 were unvaccinated (93%) and 24 (7%) received either one (14 cases) or two (10 cases) doses (Dandawate et al. 1994). The importance of two doses was noticed, however the next documented vaccination strategy included a booster administered after the two-dose regime. During the 2005-2010 endemic period, there were a total of 168 laboratory-confirmed cases including 134 unvaccinated (accounting for 80% of cases), 18 (11%) received either one or two

doses and 16 (9%) obtained two doses with the booster (Kasabi, Murhekar, Sandhya, et al. 2013). The minor difference in positive cases in people who obtained two doses and two doses with the booster seems to highlight this vaccines' short-lived immunogenicity. Despite this weakness, it appears that the best strategy is continued or consecutive dosing, a booster shortage during the 2011-2012 endemic season accentuates this as only the two-dose approach was available. Of the 61 confirmed cases, 39 (64%) did not receive any of the vaccine regimen, 22 (33%) cases received one or two doses (Kasabi, Murhekar, Yadav, et al. 2013). More recently in 2013-2014, 106 cases were confirmed for KFDV with 95 (90%) unvaccinated, 10 (9%) receiving one or two doses and 1 case (~1%) receiving the full vaccination complement (Kiran et al. 2015). Thus of the 684 documented laboratory confirmed cases since the beginning of the vaccination campaign, the total amount of cases which had not received any of the vaccine's doses were 595 (87%) versus 89 (13%) which had received one or more doses. The major issues with the vaccination scheme are immunogenicity [multiple doses within 9 months give a 82.9% effectiveness (Kasabi, Murhekar, Sandhya, et al. 2013)] and compliance (more than 50% of at-risk individuals do not receive any vaccine doses). Many people believe that there are adverse side effects associated with the vaccine (Kiran et al. 2015), however only "minor burning" at the injection site and "temporary giddiness" have been reported (Dandawate et al. 1994). The estimated annual cases of KFDV in humans range from 400-500 with 3-5% of those becoming fatal (Holbrook 2012). Although KFDV has remained contained within southern India with respect to infections, the discovery of two variants of KFDV in Saudi Arabia in 1994 and China in 1989 demonstrate the potential for more widespread dissemination. Alkhumra (sometimes incorrectly referred to as Alkhurma) hemorrhagic fever virus (AHFV) shares 97% amino acid

identity with KFDV (Dodd et al. 2011), and causes a similar hemorrhagic disease with limited neurological involvement (Memish et al., 2014). Contrary to what is known about KFDV transmission, AHFV is transmitted by primarily by soft ticks (*Ornithodoros savignyi*) or through contact with infected sheep or goat blood and/or raw milk (Madani 2005). The virus appears to no longer be restricted to Saudi Arabia, as four Italian travellers, independently, acquired the virus at markets in southern Egypt (Carletti et al. 2010; Ravanini et al. 2011; Musso et al. 2015). The incidence rate of AHFV is believed to be around 100 cases per year with a mortality rate of 0.5% (Memish et al., 2014) and not 25-30%, as previously reported (Charrel et al. 2005). The second variant of KFDV, the Nanjianyin virus, is 99.7% and 91.5% identical at the nucleotide level to KFDV and AHFV, respectively. It should be noted that only one person in 1989 has been reported as being infected with this variant and although the symptoms were reported to be similar to KFD, no other confirmed cases have since been reported, as of 2009. Despite this, serological surveys during 1987 – 1990 of the mountain regions of Yunnan province, where the lone patient resided, discovered sero-positive humans, birds, rodents and monkeys (Wang et al. 2009). One report has called into question the authenticity of Nanjianyin, since it is very similar to KFDV reference strain P9605. The strain was given to arbovirus reference laboratories in China for serological surveys testing for KFDVs expansion; the original "Nanjianyin isolate" from the infected patient may have been confused with the P9605 reference strain (Mehla et al. 2009). Thus, the report insinuates that the patient never had KFDV, although that does not explain the serological survey data.

In terms of the KFD characteristics, there have been few reports that outline the clinical descriptions; however a summary has been compiled from the bedside monitoring of tick

flaggers, who became infected during the initial 1957 outbreak (Work et al. 1957) and from suspected cases during an outbreak in 1983-1984 in southern Shimoga (Adhikari Prabha et al. 1993). The disease can be characterized as having four stages, each of about a week in duration. After the incubation period of three to eight days, the first "fever" stages' symptom onset begins with flu-like symptoms, including fever or headache, back and extremity myalgia, diarrhea, vomiting, conjunctivitis, prostration and hypotension. More than half (~54%) of those afflicted will progress into the second "complication" stage, led by hemorrhagic manifestations in the gastro-intestinal, genitourinary, and respiratory tracts and buccal/nasal cavity. Common disorders include, eruption on the palate, nose bleeding and, bloody vomit, urine and stool. Neurological disease may occur during this stage in the form of convulsions, neck stiffness and altered sensorium. However, the literature is confusing on whether or not neurological signs are a common feature (Adhikari Prabha et al. 1993) or a rare or limited occurrence (Work et al. 1957), and therefore, not a prominent feature of the disease. This is in contrast to the situation in Red-Bonnet monkeys in which central nervous system involvement is a common feature in an otherwise similar disease to that of humans (Webb & Chaterjea 1962). A significant subset of patients (~14%) will endure a second-wave of fever following the complication stage for another week before progressing into convalescence. The third "convalescence" stage is a recovery period of about a week in length and patients are typically very weak and bed-ridden with muscle tremors, twitching or shaking. While the mortality rate of KFD is quite low (3-5%), any deaths that are associated with complications are due to hemorrhaging, encephalitis, bronchopneumonia (secondary bacterial infections), shock (congealing or clotting of blood within the blood vessels)

leading to multi-organ system failure and renal or hepatic failure (Work et al. 1957; Adhikari Prabha et al. 1993).

The propagation of KFDV in cell culture has been limited to chick embryo fibroblasts for vaccine production (Mansharamani et al. 1967; Mansharamani & Dandawate 1967), monkey cell lines: VeroE6 (Dodd et al. 2014; Dodd et al. 2011), Vero and LLC-MK2, porcine stable kidney (PS) cells (Calisher et al. 1989) for virus stock preparation and human lung carcinoma (A549) cells for virus stock preparation and antiviral assays (Flint et al. 2014). Baby Hamster Kidney cells (BHK-21) are the cell line of choice for stock generation and titrations for the closely-related AHF (Madani et al. 2014), Omsk hemorrhagic fever and tick-borne encephalitis viruses (Yoshii et al. 2014). However, there does not appear to be a consensus on an optimal cell line for *in vitro* culturing methods for stock preparation or for the observable cytopathic effects (CPE) needed for virus titrations with KFDV. Thus, there is a need for developing tools for analysis of KFDV replication. As part of this thesis, I undertook experiments to address this need using various cell lines to identify the most useful for KFDV replication, judged by visual CPE development and the highest yields for virion production.

1.2. Developing Kyasanur Forest Disease Virus That Expresses A Green Fluorescent Protein During Replication

The green fluorescent protein (GFP) was first described by Shimomura *et al*. in 1962 in jellyfish (*Aequorea victoria*) (Shimomura et al. 1962). Since that time, GFP has been characterized further as 11 β-strands forming a barrel-like structure with an α-helix-containing

fluorophore in the center, which is responsible for the green-coloured fluorescence upon excitation with ultraviolet light (Tsien 1998). Due to the short intensity of emission by the original GFP, mutations within the fluorophore have been generated that produce an enhanced GFP with improved color stability (Heim et al. 1995) and more colours, including cyan, yellow and blue (Tsien 1998; Shaner et al. 2007). Reporter genes like GFP, have been exploited by virologists for use in several, reporter-based assay systems, including ones for flaviviruses. GFP and *Renilla* luciferase-based systems have been produced to evaluate pathogenesis and tissue tropism (Pierson et al. 2005), antiviral drug screening, and diagnostic purposes (neutralizing antibody determination) (Pierson et al. 2005). Unfortunately, when reporter genes were inserted in flavivirus genomes using three different strategies to create a replication-competent, full-length genome virus encoding GFP, the results were met with limited success. Beginning with West Nile virus, a cassette of an internal-ribosome entry sequence (IRES) and gene encoding GFP was inserted in the 3' UTR (untranslated region), thus outside of the open reading frame for the polyprotein (Pierson et al. 2005) (Figure 1.2.1.a.). The IRES allows for the ribosome to initiate translation (cap-independent) of the GFP gene (Moss et al. 1990; Jang & Wimmer 1990). In tissue culture, the GFP-expressing West Nile virus, when compared to control wild-type virus, demonstrated a reduction in virus titres by 10-20 fold and loss of GFP signal after 96 hours. Interestingly, there appeared to be no decline in virus propagation when signal loss was occurring. Investigating this further, RT-PCR and sequencing indicated that there were large deletions and point mutations within both the IRES and GFP, as early as 36 hours post-infection (Pierson et al. 2005). For these experiments, the authors introduced the *NotI*-IRES-GFP-*NotI* cassette 24 nucleotides into the 3' UTR. Perhaps the mutations within the cassette are indicative

of problems with the circularization between the 3' UTR with the 5' UTR and C, as this is an absolutely required step for replication (Villordo & Gamarnik 2009). Furthermore, manipulations in these cyclization sequences have been shown experimentally to cause detrimental effects in propagation (Alvarez et al. 2008). The second strategy involved insertion of the GFP within the polyprotein coding sequence with a cassette of a duplicate C gene followed by GFP and 2A protease coding sequences, preceding the entire polyprotein open reading frame (McGee et al. 2010) (Figure 1.2.1.b.). This recombinant virus was presented for blood meal uptake by mosquitoes and then evaluated for virus and GFP presence over time throughout the body. Delayed replication kinetics was observed for the GFP-incorporated virus through the course of the 14-day study, when compared to the wild type virus. Impaired dissemination of the GFP virus from the midgut into the body and, most notably, into the salivary glands of mosquitoes was observed, with 4% being positive for West Nile-GFP virus and 60% positive for wild-type virus controls. On a small minority of sample days, there was a loss of GFP signal even though viral titres remained high. Samples prepared for RT-PCR and sequencing revealed a mixed population of GFP gene-deletion mutants, ranging from 198 to 618 nucleotides missing (McGee et al. 2010). A similar cloning method for dengue virus, exhibited instability with GFP within 5 passages, but remained stable with *Renilla* luciferase up to 5 passages without any loss in signal. However, the luciferase-dengue virus generated titres 10-fold lower than those of the wild type (Zou et al. 2011). Another approach to the inclusion of the GFP reporter gene into the yellow fever virus genome, involved positioning the GFP gene in between the E and NS1 (Bonaldo et al. 2007) (Figure 1.2.1.c.). The C-terminus of GFP was fused to a duplicate of the 30 amino acid long, E protein-transmembrane domain and the following 9 amino acids of the NS1 ensuring

efficient cleavage. The transmembrane domain of the E will allow GFP to associate with the ER during replication and cleavage of the E and NS1 will occur as normally anticipated. When compared to the wild type yellow fever vaccine strain 17D, the GFP-virus displayed significant titre reduction at 2, 3 and 4 days post-infection. However, the GFP-fused version did recover to wild type levels, 5 days post-infection. It was observed that the GFP gene was stable up to, but not beyond, 10 passages (Bonaldo et al. 2007). Therefore, it would appear that the addition of a reporter cassette, regardless of size, blunts replication and virion production of flavivirus, especially in earlier time points and may become eliminated in subsequent replication cycles.

In response to those previous attempts, I utilized three different configurations to insert GFP into the KFDV reverse genetics system. Upon expression, a full-length KFDV genome featuring GFP would be visualized with a fluorescent microscope. Two different GFP positional placements within the polyprotein were attempted in the first of two methods (Figure 1.2.2.a. and b.). These methods differ from the literature in that there are no major genome duplications or new ORFs outside of the polyprotein region. The third attempt followed the yellow fever study (Bonaldo et al. 2007) in which GFP was incorporated into the polyprotein at the junction of the structural and non structural genes. This strategy appeared to enable GFP to be more stable than the previously published methods of GFP-genome incorporation (Figure 1.2.2.c.).

Figure 1.2.1. Flavivirus Genome And Examples Of GFP-Inclusion Strategies From Literature. Flavivirus genome is depicted in the 5' to 3' orientation. Three different strategies: **a.** Pierson *et. al.* 2005, **b.** McGee *et. al.* 2010 and **c.** Bonaldo *et. al.* 2007, summarize inserting a GFP reporter into the flavivirus genome.

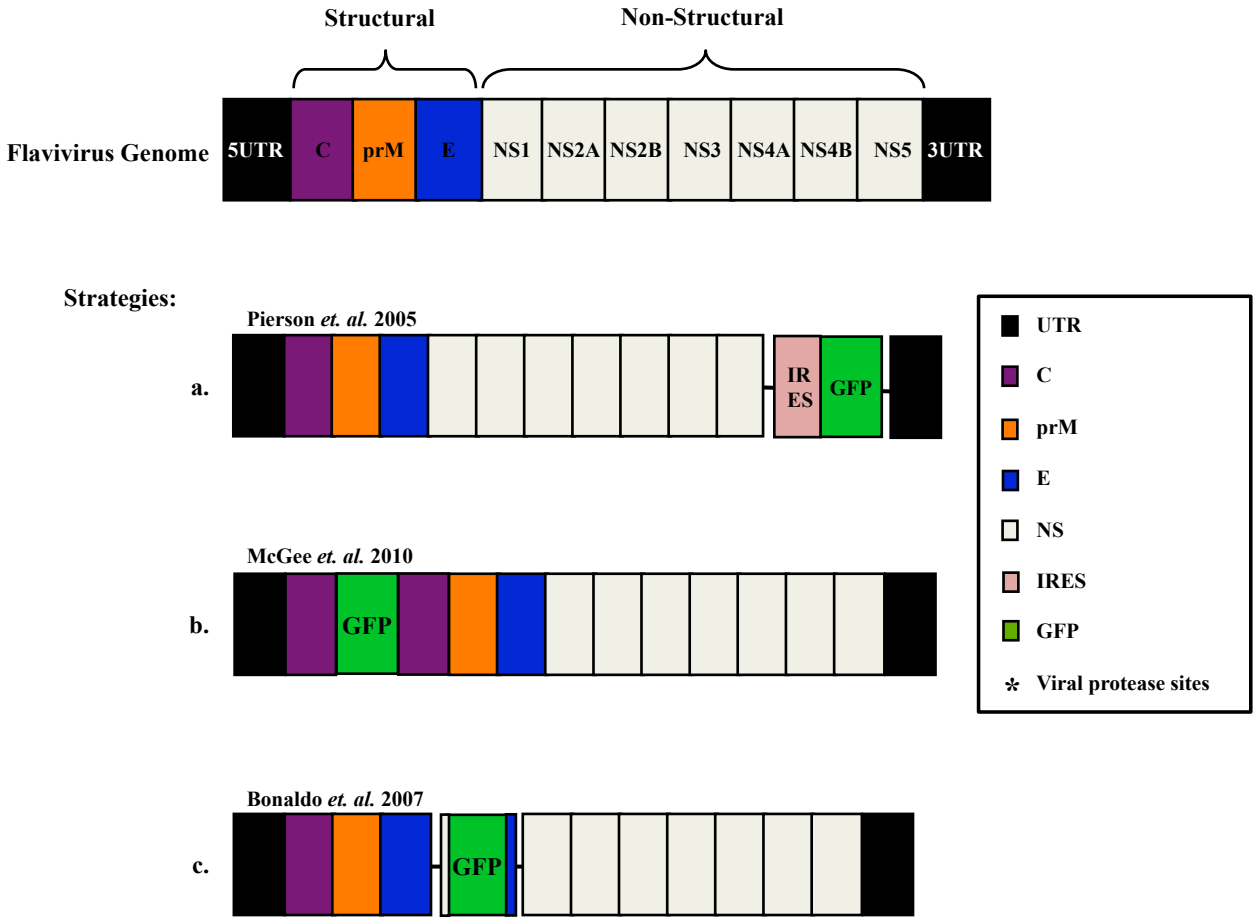

Figure 1.2.2. Flavivirus Genome And Insertion Of The GFP Reporter Gene. Flavivirus genome is depicted in the native positive-sensed orientation. Three different strategies were employed: **(a).** KFDV-RGS-ribo-NSGFP clone has GFP flanked by NS4B/NS5 protease sites into the polyprotein region, **(b).** KFDV-RGS-ribo-NS5-GFP has GFP fused with the polyprotein flanked by NS4B/NS5 protease cut sites with minor deletion of 3' UTR, **(c).** KFDV-RGS-ribo-ENS1-GFP mimics the Bonaldo *et. al*. 2007 methodology, in which GFP is surrounded by duplications of portions of the NS1 and E proteins embedded at the structural and non-structural protein junction.

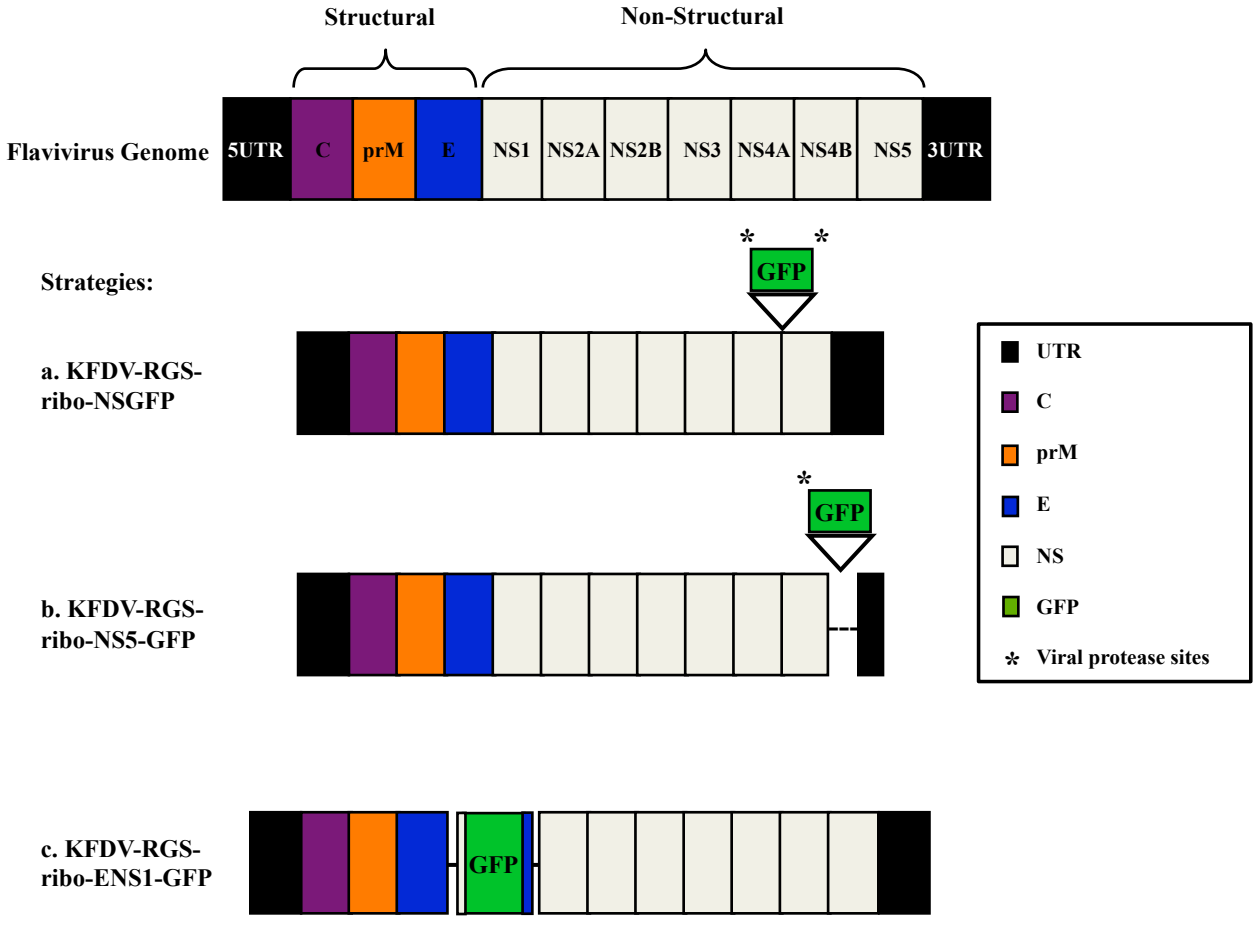

1.3. Introduction To Interferon And Interferon As A Treatment For Viral Disease

The innate immune response has many facets to protect against microorganism infections, including viruses. Generally speaking, there are four main components: atomic barriers (skin and mucous membranes), physiologic barriers (temperature, pH and chemical mediators), phagocytic/endocytic barriers and inflammatory barriers (Kuby 1997). One of the chemical mediators released upon infection is interferon (IFN), which was first characterized in 1957, following the addition of a heat-inactivated influenza virus to chick embryo membranes. An "unknown factor" termed "Interferon" could be released from membranes when incubated at 37^{o}C and it restricted infection by non-heat treated influenza virus upon challenge. IFN was detected in culture medium, membrane extracts and when fresh un-treated membrane was added, albeit in lower amounts. Interestingly, the heat-inactivated virus was only effective at stimulating IFN when it had been heat-treated for 1 hour at 56^{o}C, but not at 60^{o}C. The authors concluded IFN seemed to be a metabolic by-product of the membrane, as it could be "liberated" into culture medium and to other naïve membranes in a time-dependent manner and that single-round replication or abortive replication of the 56^{o}C-treated virus was required for this antiviral action (Isaacs & Lindenmann 1957; Isaacs et al. 1957). As time passed, these astute conclusions would prove to be very accurate.

There are many varieties of IFN in mammals and they are represented by three types: type I has IFN-α (14 species) and IFN-β (one species), type II has IFN-γ and type III has IFN-λ. The focus of this project is on the type I class, whose members share low amino-acid sequence identity, despite having similar three-dimensional structures (Meager 2002).

Induction of the type I IFNs occurs in many cell types upon either direct virus infection or indirectly in response to IFN itself. When a virus enters a cell, the envelope proteins or genetic material can be recognized by the Toll-like receptors (TLR) during the endosomal-fusion process or the genomes can be recognized as replication proceeds via Retinoic acid-inducible gene I (RIG-I)/Melanoma differentiation-association gene 5 (Mda5). Initiation of signalling cascades results in expression of type I IFNs (IFN α/β), co-stimulatory molecules and pro-inflammatory mediators (Takeuchi & Akira 2009). Generally, flaviviruses are identified through the 5' cap structure by RIG-I and through the double-strand RNA intermediate formed during replication by Mda5 and possibly by RIG-I, as well (Takeuchi & Akira 2009). When the afflicted cell excretes the IFN signal, neighbouring naïve cells are able to respond via the Jak/STAT pathway (Figure 1.3.). Initiation of the antiviral state begins with IFN binding to the interferon-alpha receptors 1 and 2 (IFNAR1/2) (step 1), Tyrosine Kinase 2 (Tyk2) phosphorylates IFNAR1 and allows STAT2 to dock to become phosphorylated as well (step 2). Then, Janus kinase (Jak) phosphorylates signal transducer and activator of transcription (STAT) proteins, this activation of STAT1 and STAT2, becomes the driving force for dimerization and translocation into the nucleus via their nuclear localization signal (step 3). Once inside the nucleus, hetero-trimerization with interferon-regulatory factor 9 (IRF-9) is the final step to create the interferon-stimulated growth factor (ISGF3) complex (step 4), which behaves as an enhancer element. As a result, hundreds of IFN-stimulated genes (ISG) are activated (step 5). The antiviral properties allow the cell to be in an "antiviral state" (Randall & Goodbourn 2008) (Figure 1.3.). Some examples of common ISGs are: protein kinase R (PKR) that inhibits translation, RNaseL which

cleaves mRNA (Meager 2002) and Mx proteins that prevent replication and nucleocapsid formation (Verhelst et al. 2013).

Figure 1.3. Antiviral State Induction In Response To Interferon (Adapted From Randall & Goodbourn 2008). 1. Induction of the antiviral state begins with IFN protein binding to IFNAR1/2. **2.** Tyk2 phosphorylates IFNAR1, establishing a docking site and subsequent phosphorylation of STAT2 in step 3. **3.** Jak phosphorylates STAT1 and STAT2, which then form a heterodimer and through a nuclear localization signal, translocate into the nucleus. **4.** The ISGF3 transcriptional enhancer element is formed with the binding of IRF-9 to the STAT1-STAT2 complex. **5.** ISG gene expression is activated.

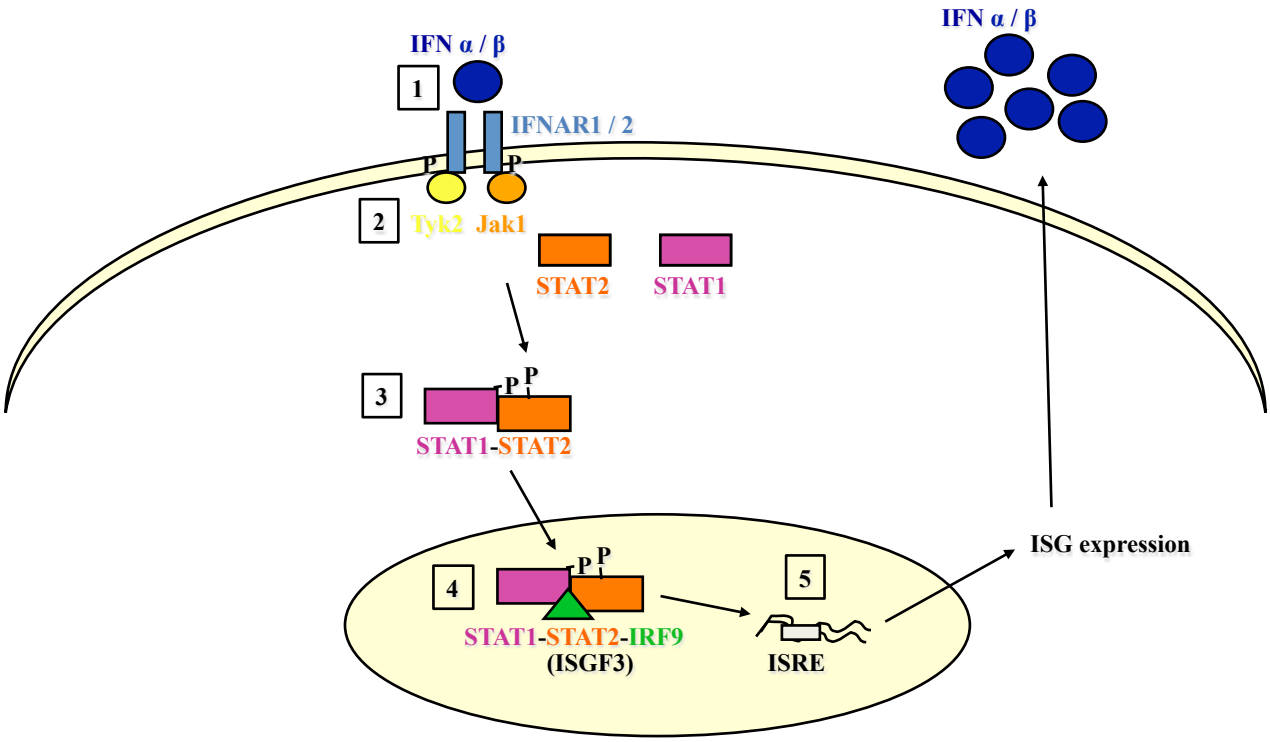

The use of IFN, namely IFN-α species 2a and 2b for the treatment of many ailments besides virus infections was approved by the Federal Drug Administration (FDA) in 1981 (Pestka 2007). With respect to a few flaviviruses, IFN has had varying success rates in human treatment. In this summary of West Nile and Japanese encephalitis virus infected patients' case reports, it is important to note the lengthy incubation period of these flaviviruses can vary from 2-8 days or up to 14 or 21 days post-exposure (Petersen & Barrett 2009). This will certainly influence when patients may seek medical attention, most likely during the presentation of the more severe symptoms. Beginning with cases with positive patient outcomes, a 43 year-old male diagnosed with West Nile virus was administered IFN-α2b daily, from day 3 of hospital admittance until he was discharged (hospital day 17). The patient became alert and orientated by day 2 after starting IFN treatment and improved daily. However, some motor skills were impaired beyond 3 months post-discharge (Kalil et al. 2005). Similarly, a 54 year-old woman had weeklong symptoms of West Nile virus before becoming hospitalized. She became comatose within 24 hours of admittance, at which time laboratory results confirmed West Nile virus infection and IFN-α2b was administered. Her condition improved over the 8 days of daily IFN treatment and she was released. Much like in the previous case, sequelae continued for up to 9 months (Kalil et al. 2005). Case reports of patients with negative-events have also been produced for West Nile and Japanese encephalitis viruses. A 76 year-old male entered a hospital after having flu-like illness with fever, confusion, weakness and respiratory distress for approximately 17 days. A daily-dosing regimen of IFN-α2b began and unfortunately, the patient passed away 14 days later (Chan-Tack & Forrest 2005). A random study of IFN-α2a versus a placebo in children aged 1-15 years of age with suspected Japanese encephalitis virus were scored based on

the presence of fever and signs of neurologic distress, including convulsions (typically 7-14 days post-exposure). The 7-day treatment course of IFN, given daily, did not demonstrate a protective effect in the 87 laboratory-confirmed Japanese encephalitis virus patients, as overall death rates and severity of long-term sequelae (up to 3 months post-discharge) were not significantly different from IFN treated to placebo groups (Solomon et al. 2003). It should be noted that these patients received different doses and routes of injection of IFN, had various days post-exposure before seeking medical intervention and, immune-compromised people had poorer outcomes despite IFN treatment. Thus in clinical situations, the success of IFN-treatment as it relates to patient outcomes is quite complex with many factors to consider. A brief summary of experimental investigations of IFN treatment against numerous viruses, *in vivo* and *in vitro* are described below.

Within the laboratory, Rhesus monkeys (*Macaca mulatta*) challenged with dengue virus, were used to compare single-dose injections of the typical purified IFN-α2a and a pegylated version (PEG-IFN-α2a), delivered 24 hours after viremia was detectable. Pegylation involves the addition of one or more polyethylene glycol moieties to IFN, increasing IFN half-life, tolerability, and reducing proteolysis of IFN (Kieseier & Calabresi 2012). Thus, the serum half-life is prolonged from 2-8 hours to 65 hours, eliminating the need for daily IFN dosing schedules (Baker et al. 2010). The use of pegylated IFN led to decreases in maximum viremia (0.6 – 1.4 orders of magnitude) and faster viral clearance, when compared to the placebo treatment. The non-pegylated IFN only delayed maximal viremia by 3 days and had no observable benefit compared to the placebo control (Ajariyakhajorn et al. 2005).

In cell culture, the different species of IFN-α/β have demonstrated various levels of effectiveness against many viruses, including human immunodeficiency virus (HIV), vesicular stomatitis virus (VSV) (Sperber et al. 1992) and rhinovirus A serotypes (HRV-1A) and (HRV-39) (Sperber et al. 1993). Viruses within the same *Flaviviridae* family demonstrate drastically different susceptibilities to IFN-α2b. Such variation can be seen in the concentrations required to result in 50% (nearly 2-fold differences) and 90% (up to 10-fold differences) inhibition (Crance et al. 2003). Adding to this variability, IFN-α2a has a strain-dependent activity profile as 30 U/mL to as high as 150, 000 U/mL needed to reduce the replication of four different strains of Japanese encephalitis virus (Harinasuta et al. 1984). Langat virus was shown to be sensitive to the effects of IFN-α, however the effects of IFN dwindled once the infection was established (Best et al. 2005). The lack of consistency in the antiviral nature of the type I IFN-α/β species is thought to be associated with different receptor-binding affinities or through the induction of different subsets of ISGs, with preference for the latter scenario (Lavoie et al. 2011). One specific ISG, tripartite motif (TRIM) 79α was shown to be induced by IFN-β and restricted Langat virus and tick-borne encephalitis virus replication in mouse cells (Taylor et al. 2011). This is in contrast to some ISGs that appear to promote flavivirus replication (Schoggins et al. 2011). However the potential of any beneficial effects caused by ISGs for the tick-borne flaviviruses have not been tested.

Since there is no approved therapeutic against KFDV, it would be of interest to assess the IFN-α/β species as the susceptibilities of flaviviruses to IFN are highly variable. The major component of this thesis was to evaluate the utility of IFN-α2a and the other type I IFN-α/β species for their potency against KFDV in cell culture. The success or failure of each IFN

species was judged with respect to limiting CPE damage and virus generation in two different cell lines.

1.4. Flaviviruses And Their Ability To Halt Cellular Interferon Responses

In general, viruses can circumvent the host immune response and the interferon (IFN)-α/β response by influencing host gene expression (IFN, various cytokines or IFN-stimulated genes), directly blocking the IFN signalling cascade and evading the pathogen-associated recognition aspects leading to IFN induction. Innate immune response evasion is thought to be crucial for establishing infection and causing viral pathogenesis (Hanley & Weaver 2010; Randall & Goodbourn 2008). The prevailing thought is that all flaviviruses have IFN-antagonism capabilities with respect to the Jak/STAT pathway; some examples include: West Nile, Langat, tick-borne encephalitis, Japanese encephalitis and dengue viruses. This disruption appears to be vital for flaviviruses, due to the fact that the type I IFNs have been shown to be very strong repressors of flaviviruses (Best et al. 2005; Laurent-Rolle et al. 2010; Samuel & Diamond 2005) by limiting their ability to replicate (Robertson et al. 2009). The typical proteins utilized for Jak/STAT pathway interruption are the non-structural (NS) proteins, mainly the NS5, as found with the following flaviviruses: dengue, yellow fever, Langat, West Nile, tick-borne encephalitis and Japanese encephalitis viruses (Ashour et al. 2009; Best et al. 2005; Laurent-Rolle et al. 2010; Laurent-Rolle et al. 2014), and NS4B-2k: dengue, West Nile and yellow fever viruses (Laurent-Rolle et al. 2010; Liu et al. 2006; Munoz-Jordan et al. 2005). The NS5 is a versatile protein of approximately 900 amino acids with two main functions for replication. The ~260 amino acid

long methyltransferase (MTase) domain works in tandem with the replication machinery, adding and methylating the guanine cap needed for translation-initiation, on the nascent genomes upon the next round of infection. Separated from the MTase by a 10 residue "linker region", the majority of the NS5 protein (~630 amino acids) is dedicated to the RNA-dependent RNA polymerase domain (RdRp) which adds nucleosides to the nascent genomes (Lu & Gong 2013). Besides the roles in genomic capping and replication, an estimated 30-40% of expressed NS5 can accumulate within the nucleus (Davidson 2009). Nuclear entry is possible through nuclear localization signals within the RdRp region (Yap et al. 2007; Johansson et al. 2001; Brooks et al. 2002) and this translocation ability is thought to somehow be involved in pathogenesis (Davidson 2009), and not exclusive to blocking IFN-signalling.

The most interesting aspect of the NS5 protein is that the method used to circumvent the Jak/STAT pathway appears unique for each flavivirus. These viruses have been experimentally shown to block the activation (phosphorylation) of many of the signalling proteins through various mechanisms, therefore preventing the dimerization of STAT1 and STAT2 and their subsequent nuclear translocation and eventual ISG expression, as summarized in Figure 1.4. The NS5 of dengue virus targets STAT2 for ubiquitin-dependent degradation by UBR4-binding and subsequent ubiquitin tagging of STAT2 via ligase-mediated, proteosomal degradation. The NS5 has been shown to interact with both UBR4 and STAT2 independently, and STAT2 degradation cannot occur without all three proteins interacting with each other (Morrison et al. 2013; Ashour et al. 2009). The regions involved are within the first 10 amino acids of NS5 (MTase region), and specifically T2 and G3 for STAT2 degradation (Morrison et al. 2013). Similarly for yellow fever, the NS5 also uses the first 10 amino acids, specifically K6 to bind to STAT2, indifferent to

its phosphorylation state. However, unlike the case during dengue infection, STAT2 does not become degraded rather STAT2 is unable to form a dimer with STAT1, thus stopping Jak/STAT signalling. While the NS5 can be immunoprecipitated with STAT2, it was not observed as a binding partner of UBR4 (Laurent-Rolle et al. 2014), suggesting that STAT2 is not tagged for ubiquitin-degradation. In the case of the NS5 from Langat virus, the phosphorylation of STAT1 can be impeded, but STAT1 and STAT2 are not targeted for destruction. Immunoprecipitation analysis of NS5 found that it was associated with the IFNAR2. The assumption is that this binding prevents the auto-phosphorylation of Jak and therefore impedes the incitement of Jak/STAT signalling (Best et al. 2005). Mutational analysis attributed the anti-IFN activity to the RdRp region of Langat virus and not the MTase, as for dengue and yellow fever viruses. There are two amino acid sequences required 374-380 and 624-647 for blocking STAT1-phosphorylation (Park et al. 2007). West Nile virus' NS5 protein can inhibit the phosphorylation of STAT1, without any apparent binding to any Jak/STAT pathway proteins. Scanning alanine mutagenesis of the same regions as the NS5 of Langat virus revealed 4 amino acids within the RdRp were required for this anti-IFN activity. Unlike Langat, these amino acids were not in 2 separate stretches and the authors acknowledge that their deletion framework was incomplete (Laurent-Rolle et al. 2010). Other studies have indicated that the MTase region of the NS5 is important for anti-IFN activity. Through mutational analysis of the NS5 of tick-borne encephalitis virus, it was found that the latter amino acids of the MTase domain were needed to bind to a plasma membrane protein, human Scribble (hScrib) and this interaction prevented STAT1 phosphorylation. However, the authors speculate that the RdRp may still be important for STAT1 phosphorylation-inhibition, as the RdRp portion of the NS5 of both tick-borne

encephalitis and Langat is 88% similar at the amino acid level (Werme et al. 2008). To add to this complexity, neither the entire MTase nor the entire RdRp of the NS5 could be removed without compromising the prevention of STAT1 phosphorylation for Japanese encephalitis virus. As with the Langat virus, the latter residues of the RdRp domain and into the remainder of the NS5 (763-905) could be removed without compromising anti-IFN activity. The authors indicated that there was no interaction between the NS5 with either Jak or Tyk2 via yeast two-hybrid screening; however data was not shown and no other Jak/STAT pathway proteins were evaluated in the article (Lin et al. 2006). It has been speculated that all flaviviruses have developed their own unique methods to accomplish the same goal of undermining the cellular, IFN-mediated signalling responses (Laurent-Rolle et al. 2014). Also synergistic IFN antagonism has recently been proposed as tick-borne encephalitis, Langat and West Nile viruses can suppress IFNAR1 expression through NS5 interacting with a cellular enzyme, Prolidase, thus preventing optimal ISG expression (Lubick et al. 2015). The evidence does seem to support these mechanistic differences of IFN-signalling by flaviviruses, as there is no real consensus between the nature of the NS5 active sites (MTase or RdRp), the amino acids responsible, the mechanisms for targeting Jak/STAT pathway or within flavivirus serocomplex groupings (mosquito-borne or tick-borne virus) (Figure 1.4.).

Figure 1.4. Anti-IFN Activity Of Flaviviruses And The Mechanisms Of Action For NS5. The protein regions of the flavivirus NS5 responsible for interaction with Jak/STAT pathway components and eventual blocking of ISG expression. For each virus depicted, the abbreviations/full names are listed as follows: DENV/dengue virus, JEV/Japanese encephalitis virus, LGTV/Langat virus, TBEV/tick-borne encephalitis virus, WNV/West Nile virus and YFV/yellow fever virus.

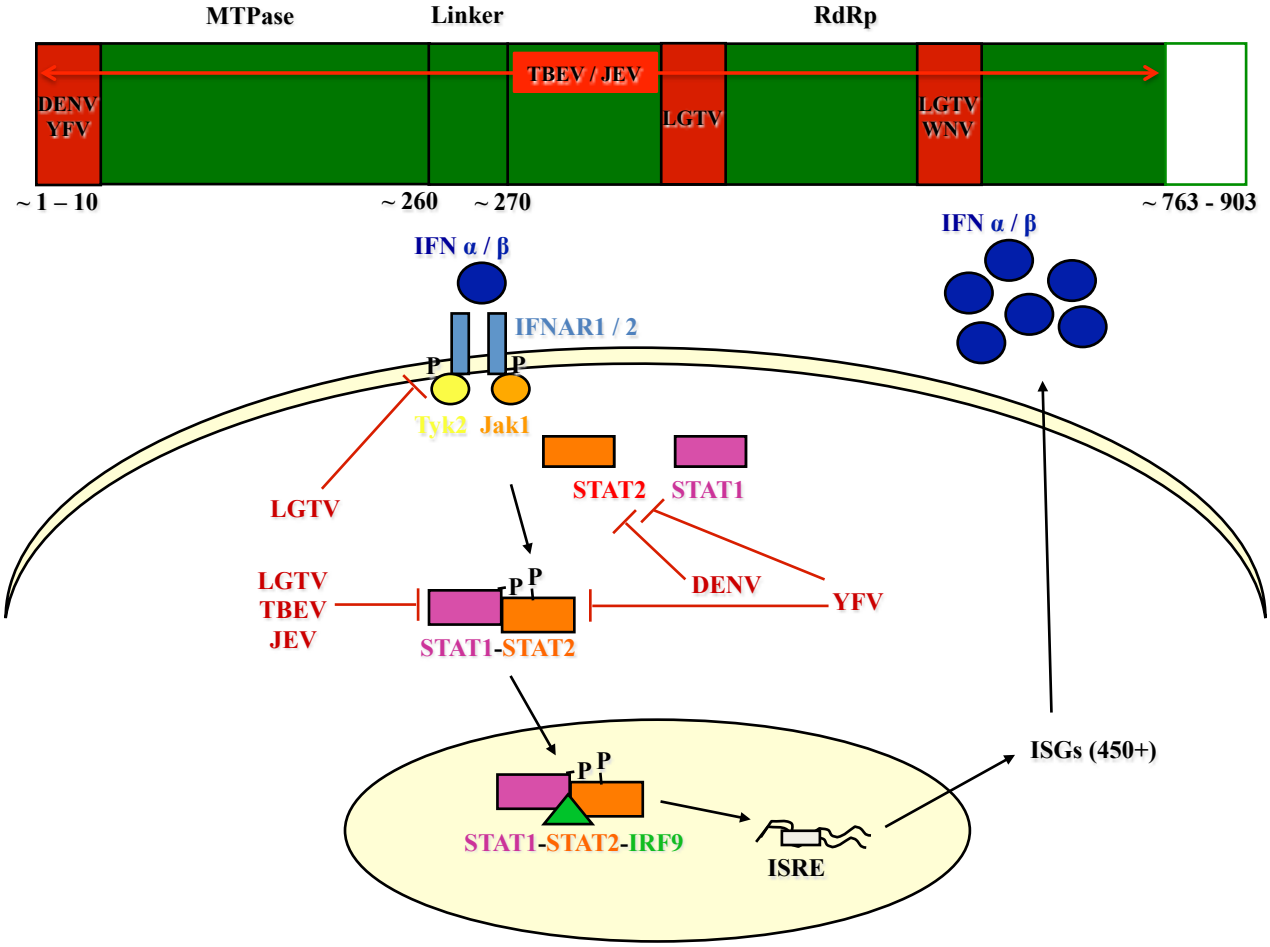

The ramifications of an altered Jak/STAT pathway were demonstrated with IFNAR-double-knockout mice challenged with West Nile virus-New York-2000. Mortality (100% lethality by 5 days and 40% lethality by 11 days post-infection) and clinical disease onset (3 days and 8 days post-infection) was significantly faster in IFNAR-deficient mice than in non-knockout control mice, respectively. Furthermore, the knockout-mice had increased viral load, tissue tropism and infection of immune cells (Samuel & Diamond 2005). An additional study had similar results as IFNAR-knock-out mice challenged with another West Nile virus isolate (New York-1999) demonstrated 100% mortality at 3.4 (+/- 0.5) days post-infection, compared to ~40% lethality by 10-12 days post-infection in control mice (Daffis et al. 2011).

The major aim of IFN potency and the ability of KFDV to avoid IFN signalling, particularly through the Jak/STAT pathway was analyzed in this thesis. The NS proteins required for KFDV were evaluated for anti-IFN signalling inhibition by genetic and viral assays. Moreover, the protein domains and their potential mechanisms of action were explored using co-immunoprecipitation and the activation of Jak/STAT signalling.

1.5. Antigenome And Subgenomic Clone Systems For KFDV

After a flavivirus enters the cell, fusion with the endosome releases the RNA genome into the cytoplasm. Translation of the single open reading frame results in a polyprotein that is subsequently cleaved by the viral serine protease complex (NS2B-NS3) into the individual proteins needed for virion assembly (C, prM and E) and genome replication (NS1, NS2A, NS2B, NS3, NS4A, NS4B and NS5) (Chambers et al. 1990). Translation is thought to occur within

invaginations of the rough endoplasmic reticulum (ER), called convoluted membranes (CM) and paracrystalline (PC) membranes (Westaway et al. 1997) and then replication occurs in spherical-smooth membrane structures called, vesicle packets (VP) adjacent to the CM/PC membrane invaginations (Westaway et al. 1997). As a precursor for replication, the genome circularizes via the RNA-RNA interactions of the cyclization sequences within the 5′ and 3′ untranslated (UTR) regions and the C gene (Villordo & Gamarnik 2009). It is thought that the genome switches between being linear and circular to allow for translation and replication to occur simultaneously (Brinton 2014). A gap in our knowledge of the replication of flaviviruses is the exact role of each NS protein with respect to their composition and role within the replication complex (RC); it is believed that all seven NS proteins are part of RC and are involved in replication, even if it is a minor part (Brinton 2014). Regardless of the circularized or switching models, once assembled the RC drives both stages of genomic replication: positive strand genome conversion into the antigenome, then the reverse copying of the antigenome to the nascent positive strand in an asymmetric manner. The newly synthesized positive strands serve as templates for further translation, replication and as genomes for progeny virions (Howley & Knipe 2007). The RC, while still undefined, involves at the very least, the NS3 and NS5 proteins that interact with one another and are primary players (Kapoor et al. 1995). During replication of the nascent genomes from the antigenome, the NS3 functions as a helicase to unwind the positive RNA-antigenomic RNA (RNA intermediate), allowing the RC to bind and synthesize more positive strand genomes (Villordo & Gamarnik 2009). Secondly, the NS3 removes the three phosphates from the final nucleoside added to the synthesized, positive-strand genome. This RNA-stimulated nucleoside triphosphatase (NTPase) is a precursor for cap addition by NS5 (Li et al. 1999). The NS5

finishes the process by adding the cap, which is a guanosine mono-phosphate (GMP) from a guanosine tri-phosphate (GTP) nucleotide. Finally, the NS5 performs methylation of the guanine cap and the first base (Adenine) (Ray et al. 2006; Issur et al. 2009). Even though all of the NS proteins are thought to compose the RC complex, only the NS1, NS2A, NS3, NS4A and NS5 have been found inside of the VP structures through electron microscopy and immuno-fluorescence (Mackenzie et al. 1998). Additionally, the deletion of NS1 of West Nile virus, resulted in drastically limited antigenome and nascent genome production (Youn et al. 2013). However, interactions of each of these proteins together were assayed *in vitro*, which has led to different and rather confusing findings. Recently, protein interactions within the RC *in vivo* have been described. The authors hypothesize that VP membrane invaginations of the ER are caused by NS2A, NS2B, NS4A and NS4B (all four appeared to interact with each other). The NS3 and NS5 only interacted with each other and are tethered to the VP via the association of NS2B with NS3 (serine protease complex). The NS1, however, is thought to become anchored to the VP, as it may not be cleaved yet from NS2A (Yu et al. 2013). Of course in terms of replication, it is still unclear which proteins are needed and what role each protein plays in the process.

Figure 1.5. Flavivirus Genome, Antigenome And Subgenomic Clone System Schematics. The Flavivirus genome is shown the native positive-sensed orientation. The **Minigenome/Antigenome System** represents a modified negative strand genome and the helper plasmids (non-structural proteins) required to drive replication. The **Subgenomic Clone System** describes the flavivirus genome altered to include a reporter and protease cassette and the non-structural proteins supplied *in cis*.

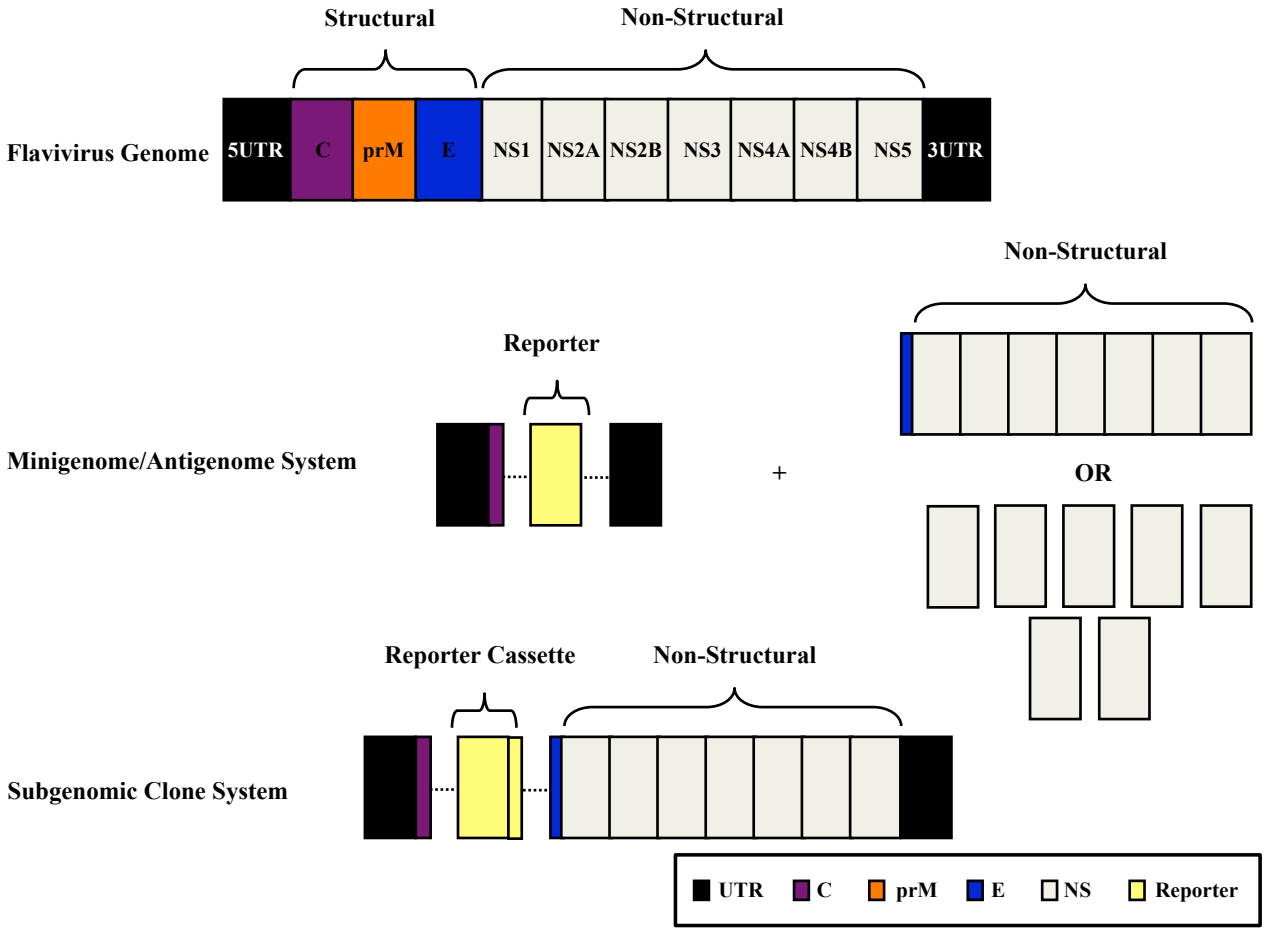

Replication-based reporter systems have been developed for both negative strand viruses (minigenome systems) and positive strand viruses (subgenomic systems) (Figure 1.5.). Two independent systems were attempted to mimic KFDV genome replication: the antigenome system follows the conversion of the antigenome into the positive strand genome (Figure 1.5.) and the subgenomic clone system which requires both steps of the replication cycle for reporter gene expression (Figure 1.5.).

The antigenome system is composed of an antisense reporter gene, flanked by the KFDV untranslated regions (UTR) also in antisense orientation. The signal can only become expressed once the transfected plasmid (negative strand genome) is copied by the RC which will be supplemented, *in trans*. Upon replication, the newly synthesized positive-sensed genome will allow for translation of the reporter signal, providing a detectable measure of virus replication. This strategy is similar to the negative-stranded viruses "minigenome systems" (Kawaoka 2004). The second methodology will feature the KFDV genome with a reporter gene/protease cassette in place of the majority of the structural genes, while remaining in the same genomic reading frame of the following genes for non-structural proteins expression. This reporter cassette and NS protein fusion remains in agreement with the natural flavivirus polyprotein's open reading frame and is flanked by the 5′ and 3′ UTR regions to ensure genomic cyclization for proper replication. Upon transfection, translation of the polyprotein will enable the RC complex to assemble and drive replication of both, antigenome (replication intermediate) and nascent genomes. The newly synthesized positive-strand genomes will be translated and the reporter protein can then be quantified. However, despite being capable of replication, virion production

would not be possible, since the structural genes have been removed. Virion assembly into virus-like particles (VLP) is possible, if the structural genes are supplemented, *in trans*.

The "sub-genomic replicon systems" have been generated for many flaviviruses including dengue virus (Leardkamolkarn et al. 2012; Massé et al. 2010; Ng et al. 2007), Japanese encephalitis virus (Yu et al. 2013), West Nile virus (Moritoh et al. 2011), yellow fever virus (Jones et al. 2005), Omsk hemorrhagic fever virus (Yoshii & Holbrook 2009), tick-borne encephalitis virus (Hayasaka et al. 2004) and Alkhumra hemorrhagic fever virus (Flint et al. 2014). In order for the reporter gene to be expressed efficiently, there appear to be two preconditions: the presence of the first 60-120 bases of the capsid (C) gene fused on the 5′ end of the reporter gene and at minimum, the last 9-75 bases of the envelope (E) protein fused to the 3′ end of the protease gene. The necessity of the C addition is because the start codon at the beginning of the C is often skipped by the ribosome, leading to a truncated version of the polyprotein (Clyde & Harris 2006). To remedy this, flaviviruses contain a RNA-based hairpin immediately downstream of the start sequence, forcing the ribosome to "pause" on the proper start codon, the ribosome will continue with synthesis once the hairpin is unwound by the translational machinery (Clyde & Harris 2006). Trafficking of the polyprotein and efficient cleavage of the NS1 at the ER, requires the C-terminal residues of the E protein (Yu et al. 2013; Alcaraz-Estrada et al. 2010). Thus, after translation of the subgenomic RNA, the polyprotein undergoes normal post-translational cleavage and the 2A protease liberates the reporter for quantification. The RC proteins can then assemble and begin replication into the antigenome, followed by synthesis of the nascent genomes. Without the 2A protease, the reporter gene seemed to hamper efficient genome replication and subsequent reporter gene expression (Jones

et al. 2005). Since the majority of the C, all of the prM and the majority of the E are not included in the subgenomic systems, virus particles cannot be assembled, making the system safe for use under containment level-2 (CL-2) conditions (Yoshii & Holbrook 2009; Moritoh et al. 2011).

The generation of VLPs is possible with this system but only when the structural genes are supplied *in trans* to the subgenomic RNA-transfected cells. These VLPs contain the intact mature flavivirus particle without the full complement of genetic information needed to assemble a second round of infectious particles. This is due to the fact that the particles only contain the subgenomic RNA without the structural genes (C, prM and E). The benefits of the subgenomic clone and VLP generation include: mutational analysis with respect to replication and the requirements for packing into VLPs, as deletions in the NS1 and portions of the NS3 were complemented, *in trans* (Jones et al. 2005; Yoshii et al. 2005; Velado Fernández et al. 2014), a platform for antiviral screening (Flint et al. 2014; Massé et al. 2010; Ng et al. 2007), VLP-based vaccine strategies and virus neutralization assays. This may be very beneficial when working with viruses that require high containment laboratories, as virus may be replaced by VLPs for antibody detection-based diagnostics (Yoshii & Holbrook 2009).

A component of this thesis was the development of two replication-competent, non-infectious KFDV systems, the antigenome and subgenomic systems expressing a foreign reporter gene. The major application of either of these systems is to be a tool to measure anti-replicative substances against KFDV and assessed by the prevention of reporter gene expression. Regardless if IFN is effective at diminishing KFDV replication, these systems can find antivirals to replace or act in concert with IFN. The antigenome may provide an additional benefit of defining the

composition of the NS proteins which make up the RC, thereby defining which NS proteins allow for efficient replication of KFDV.

1.6. Hypothesis, Research Goals And Objectives

The purpose of this thesis is to advance KFDV research by establishing platforms and tools for post-exposure antiviral treatment options, with interferon (IFN) as the focal point. The central hypothesis, similar to other flaviviruses, KFDV will mitigate the antiviral effects of IFN and genetic-based systems are required to test IFN and other potential antivirals against KFDV infection. To address this hypothesis, five main goals were constructed. 1. Monitoring KFDV infection in tissue culture. The intent was to determine which mammalian cell lines displayed discernable cytopathic effect (CPE) manifestations for virus quantification by the 50% tissue culture infectious dose assay ($TCID_{50}$). This would allow for antiviral testing against the virus. 2. Establishing a reliable reporter system with green fluorescent protein (GFP) for the full-length, infectious KFDV. This has not been published for KFDV and will enable quick identification of virus replication, especially for antiviral assays, thus saving time, labour and potentially, reagent consumption for traditional virus titre determinations by plaque or $TCID_{50}$ assays. 3. Since there are no approved antivirals for KFD, the FDA-approved IFN-α2a, IFN-α2b and the other non-FDA approved species of type I IFNs, were assessed for their ability to limit KFDV propagation in tissue culture. 4. Furthermore, as other flaviviruses have the ability to limit the effectiveness of IFN by preventing IFN-based signalling, it was important to investigate this possibility during KFDV infections. 5. In the event that IFN is not successful against KFDV, two high-throughput

systems were attempted to further judge antiviral compounds as an alternative to IFN treatment. Neither system, antigenome or subgenomic clone has been previously generated for KFDV. Altogether, the work described in this thesis was designed to set a foundation for and to further explore antiviral research of KFDV, with analysis of the effectiveness of IFN.

Chapter 2. Material And Methods

2.1. Cells, Viruses And Interferon

Cells: for all experiments, human embryonic kidney HEK 293T (ATCC from Special Pathogens program at the National Microbiology Laboratory (NML) in Winnipeg, Canada), human lung carcinoma A549 cells (ATCC CCL-185), African green monkey kidney VeroE6 (ATCC CRL-1586 at low passage) and VeroE6 [ATCC from Special Pathogens program (NML) referred to as "lab strain" with an unknown passage history] were propagated in Dulbecco's minimal essential medium (DMEM) (HyClone) supplemented with 10% fetal bovine serum (FBS) (Gibco) and 1% antibiotics (Penicillin-Streptomycin) (Gibco). Baby hamster kidney BHK-21 (ATCC CCL-10 at low passage) and BHK-21 [ATCC from Hepatitis program (NML) referred to as "lab strain" with an unknown passage history] were grown in Eagle's minimal essential medium (EMEM) (HyClone) supplemented with 10% FBS and 1% antibiotics. Madin-Darby Canine kidney MDCK [ATCC from Special Pathogens program (NML) with unknown passage history] cells were cultured in minimal essential medium (MEM) (HyClone) with 10% FBS and 1% antibiotics. All virus infections were performed in maintenance medium which

included each cell type's respective growth medium with 2% FBS and 1% antibiotics at 37°C/5% CO_2 unless stated otherwise.

Viruses: KFDV (P9605 strain, GenBank accession number: HM055369) stocks were propagated in VeroE6 (ATCC) cells in containment level 4 (CL-4) at the NML. Infected cells were harvested at 96 hours post-infection. Stocks of vesicular stomatitis virus, genetically manipulated to express green fluorescent protein during replication (VSV-GFP) [kindly provided by Dr. Gary Kobinger of the Special Pathogens program (NML)] were propagated in VeroE6 (ATCC) cells and harvested at 72 hours post-infection.

Interferon: Human type I interferon (α-1 through 14 and β-1) (PBL Assay Science) and a recombinant IFN species (αA/D) (PBL Assay Science) was diluted into 50, 000 U/mL stocks and stored at -80°C. According to the manufacturer, Universal IFN was formulated to minimize cross-species specificity and is active on many mammalian cell types including from hamsters.

2.2. Appropriate Cell Lines For KFDV Propagation And 50% Tissue Culture Infectious Dose ($TCID_{50}$) Determination

Cells: BHK-21 (ATCC and lab strain), VeroE6 (ATCC and lab strain) and MDCK (ATCC) were prepared for 80-90% confluency in 12-well plates. KFDV inoculum at a multiplicity of infection (MOI) of 0.1 adsorbed (incubated) for 1 hour, followed by inoculum removal, addition of fresh virus maintenance medium and incubated. Pictures of infected monolayers and supernatants samples were obtained daily, until monolayers demonstrated near 100% CPE. Supernatants were frozen at -80°C until titration.

2.3. Virus Quantification For KFDV And VSV-GFP

BHK-21 (ATCC) cells were seeded into 96-well plates for 80-90% confluency. Virus-containing supernantants (KFDV or VSV-GFP) were serially diluted 10-fold, 50 µl of from each dilution was added to triplicate wells and incubated for 1 hour. Then 150 µl of virus maintenance medium was added and cells were incubated for 5 days post-infection (KFDV) or 3 days post-infection (VSV-GFP). The 50% tissue culture infectious ($TCID_{50}$) dose was calculated following the Reed and Muench formula (Reed & Muench 1938).

2.4. KFDV-GFP Cloning And Rescues

Three separate clones were produced using polymerase chain reaction (PCR) to insert GFP into the KFDV genome at different sites taking advantage of unique restriction sites within the genome regions. In preparation for site-directed mutagenesis steps, the latter portion of the KFDV reverse genetics system (RGS-ribo) which enables recovery of infectious KFDV particles from cloned cDNA when supplied with a T7 RNA polymerase-expression vector (T7-pCAGGS) (Cook et al. 2012), was digested with *Xma*I (NEB) and *Pac*I (NEB), subcloned into pUC19 vector (Life Technologies) and transformed into Top10 chemically competent *E. coli* (Life Technologies) following standard cloning procedures outlined in Chapter 2.8. All fusions of GFP [pAc-GFP-C1 (ClonTech) template] and parts of the KFDV genome were amplified using the specific primer sets for each clone (described in the subsequent sections and sequence

information is on Table A.1.) by touchdown PCR (68^{o}C annealing with -0.5^{o}C per cycle, over 28 cycles). Chimeric touchdown PCR (using 5 µl of each PCR product described below for the KFDV-RGS-ribo-NS5-GFP and KDFV-RGS-ribo-ENS1-GFP clones) without primer sets was amplified over 6 cycles at 60^{o}C annealing, followed by the addition of their respective primer sets for full length amplification under touchdown annealing conditions for 30 cycles using iProof DNA polymerase (Bio-Rad) following the manufacturer's recommendations. All PCR fragments were separated on agarose gels and were extracted using PCR Gel Extraction kits (Qiagen). All Primers were synthesized from DNA Core Department (NML). Three in-frame GFP-based clones obtained from synthesis of GFP gene from pAc-GFP-C1 (ClonTech) were generated as represented in figure 1.2.2. **Construction of the KFDV-RGS-ribo-NSGFP clone:** the RGS-ribo-subclone had an *Age*I site introduced by site-directed mutagenesis PCR (genome site bases: 7670-7671; NS4B/NS5 protein junction) with primer set E1/E2 (Table A1). On the GFP gene, a NS5 cleavage site (7671-7685 bases; encoding amino acids: GGAEG) was added on the 5′ end and the NS4B cleavage site (7656-7670 bases; corresponding to amino acids: TGTRR) was added to the 3′ end. Both cleavage sites were flanked with *Age*I sites (primer set E3/E4) and the 756 bp amplicon was cloned into the subclone by use of *Age*I restriction digest sites. Site-directed mutagenesis was used to eliminate both *Age*I sites on either side of the GFP insert with primer sets: E5/E6 and E7/E8. The subclone was digested and inserted into the RGS-ribo backbone with *Xma*I/*Pac*I (NEB), transformed into XL-10 Gold *E. coli* (Agilent Technologies) and, verified by sequencing by DNA Core department (NML) and restriction enzyme digestion pattern. Thus, the final clone was: T7 promoter-5′ UTR-C-prM-E-NS1-NS2A-NS2B-NS3-NS4A-NS4B-$_{\text{NS5 cleavage site}}$GFP $_{\text{NS4B cleavage site}}$-NS5-3′ UTR (Figure 1.2.a.). **Construction of the**

KFDV-RGS-ribo-NS5-GFP: Three overlapping touchdown PCR reactions were performed to generate the NS4B/NS5 cleavage site (bases 7653-7685; corresponding to amino acids: TGTRR/GGAEG)-GFP followed by the 3′UTR with primer sets (Table A1): A13/E9 (1.6 kb), E10/E11 (753 bp) and E12/A31 (363 bp in length). Chimeric touchdown PCR (as explained above) was used to amplify to entire insert using primer set A13/A31, the 2.7 kb PCR product was cloned into the RGS-ribo backbone with *EcoRI*/*PacI* (NEB), transformed into XL-10 Gold *E.coli* (Agilent Technologies) and, verified by sequencing (NML) and restriction enzyme digestion pattern. The final clone was a T7 promoter-5′ UTR-C-prM-E-NS1-NS2A-NS2B-NS3-NS4A-NS4B-NS5-$_{\text{NS4B/NS5 cleavage site}}$ GFP-3′ UTR$_{10546\text{-}10774}$ (Figure 1.2.b.). **Construction of the KFDV-RGS-ribo-ENS1-GFP:** PCR amplification of GFP flanked by a portion of NS1 (genome bases: 2462-2463 and a segment of E (genome bases: 2175-2462) was performed in three overlapping reactions with primer sets (Table A1): A1/E13, E14/E15, E16/A21 generating 2.3 kb, 744 bp and 1.7 kb PCR products, respectively. The final chimeric touchdown PCR insert (4.7 kb) was amplified with primer set A1/A21 and cloned into the RGS-ribo backbone with *Nhe*I/*Sgr*AI (NEB), transformed into XL-10 Gold *E.coli* (Agilent Technologies) and, confirmed by sequencing (NML) and restriction enzyme digestion pattern. The final construct has a T7 promoter-5′ UTR-C-prM-E-NS1$_{2463\text{-}2489}$ GFP-E $_{2175\text{-}2462}$-NS1-NS2A-NS2B-NS3-NS4A-NS4B-NS5-3′ UTR (Figure 1.3.c.).

Rescues of each KFDV-GFP RGS clone were performed and compared with the virus rescue from the KFDV-RGS-ribo clone for control purposes, beginning with transfection of BHK-21 cells (ATCC) prepared in 6 well plates. Volume (µl) ratios of 3:1, 3:2 and 6:1 of transfection reagent [FuGene 6 (Promega)] to plasmid DNA (each GFP clone and pCAGGS

vector expressing T7 DNA-dependent RNA polymerase) and transferred into the CL-4 suite (NML). Following incubation for 3 days, supernatants were transferred to fresh BHK-21 (ATCC) cells in T25 flasks and allowed to incubate up to 14 days or until GFP was visualized with a fluorescent microscope.

2.5. Virus Clearance By IFN-α2a Treatment

A549 and BHK (ATCC) cells were seeded in 6-well plates for 80-90% confluency at time of infection. The cells were infected with MOI of 0.00001 (11 $TCID_{50}$ units) of (KFDV or VSV-GFP) for 1 hour; then, virus maintenance medium supplemented with or without 2000 U/mL of IFN-α2a was applied (passage 0). Cells were incubated for 96 hours post-infection (KFDV) or 48 hours post-infection (VSV-GFP). The condition of the cells was recorded photographically and 1 mL of supernatant was removed, stored at -80^{o}C for virus quantification and sequencing. Cells were passaged in paired-wells: one continued 2000 U/mL of IFN-α2a treatment and the other did not. Passaging occurred every 72 hours post-infection for KFDV or 48 hours post-infection for VSV-GFP; images were obtained and supernatants were harvested prior to passaging. Statistical significance was determined using one-tailed Student's t-test.

2.6. Screening Of IFN-α/β Species Against KFDV

A549 cells were prepared in 24-well plates with DMEM growth medium for 80-90% confluency at time of infection. In pre-infection treatment scenario, fresh virus maintenance

medium supplemented with or without 1000 U/mL of the selected IFN-α/β species was added and incubated 24 hours prior to infection. In post-infection treatment, KFDV at a MOI of 1 was adsorbed for 1 hour, inoculum was removed, monolayers were washed, and then fresh virus maintenance medium supplemented with or without 1000 U/mL of the selected IFN α/β species was added. Supernatants from two-independent, biological replicates (pre-infection treatment) and three-independent, biological replicates (post-infection treatment) were harvested and stored in -80^{o}C for virus quantification after an incubation period of 72 hours. Statistical significance was determined using One-way Anova analysis followed by Tukey's post-test.

2.7. Dose-dependent Antiviral Activity Of IFN-αWA, IFN-αK And IFN-α2a Against KFDV And VSV-GFP

A549 (ATCC) and BHK-21 (ATCC) cell cultures were prepared in 96-well plates for 80-90% confluence. Cells were infected with 50 µl/well of KFDV or VSV-GFP at MOI of 0.0003 (11 $TCID_{50}$ units) in three independent experiments performed with triplicate samples. Following an adsorption period of 1 hour, 150 µl of fresh virus maintenance medium was added with or without select concentrations of IFN-α2a or αWA prepared in a two-fold dilution scheme (4,000 U/mL-3.9 U/mL). After incubation for 96 hours post-infection (KFDV) or 48 hours post-infection (VSV-GFP) when mock-treated controls reached near 100% CPE, cell monolayers were fixed in 10% buffered formalin. The cells were subsequently washed with PBS and stained with crystal violet: 0.5 % (wt/vol) crystal violet (Fisher Scientific) dissolved in a solution of 70% methanol/30% phosphate-buffered saline (PBS) (vol/vol). After incubation for 30 minutes at

room temperature, the excess dye was removed with tap water. Once air-dried, crystal violet dye was eluted in 100 µl of 95% ethanol and scanned with a MultiSkan Accent microplate reader at 570 nm (Thermo Scientific). The inhibitory concentration is the amount of IFN (αWA and α2a) needed to protect 50% (IC_{50}) and 90% (IC_{90}) of tissue culture cells from virus-induced CPE (KFDV and VSV-GFP). These values were compared to the un-infected controls representing the full protection from CPE (100%) and to the infected controls, defined as full CPE (0%). Supernatants for concentrations of 2000, 500, 62.5, 7.8 U/mL with controls were harvested titrated for virus reduction. The un-infected controls represent a lack of virus production and full virus infection titres were defined by the infected/mock-treated controls. **Cellular cytotoxicity:** A549 and BHK-21 cells cell cultures were prepared in 96 well plates for 80-90% confluence and final concentrations of IFN-αWA and α2a were added following a two-fold dilution scheme of 16, 000-3.9 U/mL. Control samples included mock-treated and 10% Triton X-100 (Sigma, Oakville, Ontario, Canada) treated. After incubation for 96 hours, monolayers were prepared and subjected to crystal violet staining as described above. The concentration of IFN that causes 50% cell death is defined as the cytotoxicity concentration (CC_{50}). IC_{50}, IC_{90} and CC_{50} were calculated with curve fitting using GraphPad software (Prism 5).

2.8. Polyprotein-Encoding Nucleotide Sequencing

KFDV was inactivated and removed from the CL-4 suite using our institution's approved protocol. RNA extraction using the Viral RNA Mini Prep kit (Qiagen) occurred under CL-2 conditions. Complementary DNA (cDNA) was generated with an antisense primer (Primer B4)

from two independent replicates using Superscript II Reverse Transcription kit (Invitrogen) following the manufacturer's protocol. The polyprotein-encoding region of KFDV (bases 132-10379) was amplified using iProof high-fidelity DNA polymerase (Bio-Rad) according to the manufacturer's protocol with touchdown polymerase chain reaction (PCR) conditions: primer annealing (Primer set: A32/B4 (Table A1)) and extension times of 68^{o}C (-0.5^{o}C per cycle) and 72^{o}C for 5.5 minutes, respectively over 30 cycles. Products from PCR were extracted from agarose gel (Qiagen) following electrophoresis and sequenced by the Genomics Core Department (NML) using primer sets A (A1 to A49) and B (B3 and B4) (Table A1).

2.9. KFDV IFN Antagonism Assays

Cloning: KFDV NS proteins were cloned into pCAGGS expression vectors, as described previously (Cook 2010). The NS5 mutants were prepared to corresponding to the published polyprotein sequence [AY323490/AAQ91607] which indicated the MTase and RdRp regions (Grard et al. 2007). The mutants are numbered in accordance with the full-length sequenced genome (GenBank accession number: HM055369). The mutants are named based on the site of amino acid deletion. Site-directed mutagenesis was performed from the subclone of KFDV RGS-ribo digested with *Xma*I and *Pac*I as described in chapter 2.4. Site directed mutagenesis of the NS5 gene was completed by touchdown PCR with a 4.0-minute extension time for all clones (please see Table A.1. for corresponding primer sequences), PCR product ligation with T4 ligase (NEB), transformation and sequencing was achieved as outlined in Chapter 2.8. The clones are as follows: mutant 6 (primer set C: C1/C2) maintained the native viral serine protease cut site,

then the coding region for amino acids 6-54 of the NS5 open reading frame (7686-7832 base pairs) was deleted while maintaining the reading frame with the NS5. Mutant 55 (Primer set C: C3/C4) carries a MTase region deletion corresponding to amino acids 55-222 (7833-8336); mutant 223 (Primer set C: C5/C6) lacks the sequence encoding the amino acid region of 223-431, which is in between MTase and the RdRp (8337-8963). Mutant 432 (Primer set C: C7/C8) lacks the RdRp coding region (amino acids 432-742) (8964-9896) and for mutant 743 (Primer set C: C9/C10), the coding sequence for the 743-903 amino acid region following the RdRp and before the stop codon was deleted (9897-10379). Table 3.4.2. provides a summary of each mutant with respect to the amino acid deletions of the NS5 protein and their genome positions. Once deletions were confirmed by sequencing, touchdown PCR with an extension time 1.5 minutes off of the pUC19 sub-clone templates (mutants 55, 223 and 432 with primer set B3/B4, mutant 6 with primer set C11/B4 and mutant 743 with primer set B3/C12), digestion with *Cla*I (NEB) and *Kpn*I (NEB) for PCR mutants and pCAGGS-MCS vector, ligation, transformation into Top10 *E. coli* (Life Technologies) and sequencing was completed, as described in Chapter 2.8. The final mutant clones had start and stop codons inserted during the PCR reaction thus, creating an open reading frame. The *Zaire ebolavirus* VP24 was amplified from the Ebola virus RGS system template (Theriault et al. 2004) by touchdown PCR with an extension time of 0.5 minutes using primer set B1/B2 and cloned into pCAGGS-MCS using *Cla*I and *Sph*I, as described in Chapter 2.8 and transformed into Top10 *E. coli* (Life Technologies).

Measuring The Anti-IFN Activity of KFDV NS Proteins With Luciferase Assay:

HEK 293T cells were passaged into 24-well tissue culture plates for 80% confluency, 24 hours prior to the transfections. The transfections using Attractine transfection reagent (Qiagen) were

performed according to the manufacturer's protocols using 0.6 µg of each plasmid (KFDV NS proteins, NS5 mutations, *Zaire ebolavirus* VP24 and Interferon-stimulated response element (ISRE)-luciferase reporter construct set (SA Biosciences)) with 1.8 µl FuGene 6 (Promega) into 500 µl Opti-MEM serum-free medium (Gibco). Each of the KFDV NS proteins including NS4B-2k and full-length NS5 were previously cloned into pCAGGS-MCS (Cook 2010). The clones were assessed individually and in combination with the ISRE enhancer-luciferase fusion gene system. After an incubation period of 24 hours, transfection mixtures were removed, cells were washed with PBS and growth medium with or without 1, 000 U/mL of Universal IFN-α. The cells were washed with PBS, lysed and harvested following the 18-hour incubation using the Dual-Luciferase Reporter assay system (DLR) (Promega). Activity was quantified with a luminometer (Tecan Group Ltd.) using 96-well white flat-bottom plates (Fisher Scientific) and normalized with internal *Renilla* luciferase control.

Measuring The Anti-IFN Activity of KFDV NS Proteins With VSV-GFP Infection Assay: VeroE6 (ATCC) cells were transfected with each KFDV NS protein, VP24 or NS5 mutations with pAcGFP1-C1 (ClonTech) transfection control, then treated with 1000 U/mL of Universal IFN-α under the same conditions described above. Following the 24-hour incubation with IFN, medium was removed and the cells were infected with VSV-GFP (MOI of 2) in 500 µl of virus maintenance medium for an hour. Virus inoculum was removed and monolayers were washed once with virus maintenance medium and fresh maintenance medium was added. After an incubation period of 24 hours, supernatants were harvested and stored for quantification. The cells monolayers were fixed in 10% buffered formalin overnight at 4^{o}C. The formalin was

discarded and, cells were washed with PBS and viewed under light and fluorescent microscopy with Axiovert 40 CFL (Carl Zeiss).

2.10. Immunoprecipitation And Western Blotting For Mechanism Of Jak/STAT Pathway Inhibition By KFDV NS5

Cloning: The full-length KFDV NS5 (bases 7671-10379 or 903 amino acids) gene and NS5 mutations (6 and 743) were amplified with primer sets (Table A1): B3/B5, C11/B5 and B3/C13 by touchdown PCR, under the same conditions as described in Chapter 2.8 and cloned into pCAGGS with *Cla*I and *Kpn*I restriction digest sites, forming NS5-HA-pCAGGS. The other NS5 mutations (55, 223 and 432) were sub-cloned from their respective NS5 mutation-pCAGGS vectors into using *Cla*I and *Bst*XI into NS5-HA-pCAGGS. Thus, the full-length and mutated NS5 genes had an open reading frame fused to a hemagglutinin (HA) tag on the C-terminus of the NS5 gene and were transformed into Top10 *E. coli* (Life Technologies). Thus, the sizes for each NS5 truncation are: 98.3 kDa (864 amino acids) for 6-HA, 85.3 kDa (745 amino acids) for 55-HA, 80.6 kDa (704 amino acids) for 223-HA, 68.6 kDa (602 amino acids) for 432-HA, 85.3 kDa (752 amino acids) for 743-HA and 104.1 kDa (913 amino acids) for NS5-HA. These are summarized in Table 3.4.2.

NS5 Immunoprecipitation And Western Blotting: The NS5-HA clone (2.5 µg) was transfected into 6 well plates of HEK 239T cells at 80% confluency with 6 µl of FuGene 6 following the manufacturer's protocol and incubated for 24 hours. Tissue culture medium was discarded and replaced with growth medium containing or without 1000 U/mL of Universal IFN

and incubated for 8 or 24 hours. Medium was removed and cells were washed once with PBS, then lysed for 30 minutes on ice while rocking with lysis buffer, containing 0.5% Triton X-100, 120 mM NaCl, 25 mM Tris (pH 7.2), 1 mM ethylene-diamine-tetra-acetic acid (EDTA) and 50 µg/mL phenyl-methane-sulfonyl-fluoride (PMSF) cocktail. Cell debris was removed by centrifugation at 20, 000xg for 10 minutes at 4^{o}C and, clarified lysates were incubated with 6 µg of an anti-HA primary antibody of mouse origin (CedarLane) then incubated overnight at 4^{o}C. The protein-protein-antibody complexes were added to 100 µl of proteinA/G (Thermo Scientific) slurry and incubated for 2 hours at room temperature. Complexes were washed and centrifuged three times in lysis buffer and eluted in 50 µl of 0.1 M glycine-HCl elution buffer. Immunoprecipiated samples were loaded into NuPAGE Bis-Tris polyacrylamide gels (Life Technologies) under denaturating conditions following the manufacturer's recommendations with Magic Mark XP protein ladder as a reference for protein sizes (Life Technologies). Gels were stained and de-stained using the Coomassie Brilliant Blue staining kit (Bio-Rad). Bands from the 24 hour-interferon sample were excised, digested and sequenced by the Proteomics Core Department (NML). Gels were also transferred to Amersham-HyBond nitrocellulose membranes (GE Life Sciences) with the XCell II Blot semi-wet transfer module (Life Technologies) and, probed with 1:500 mouse-derived, anti-HA primary (CedarLane) and 1:2000 goat-derived, anti-mouse horse-radish peroxidase (HRP) conjugated secondary antibody. Then, the TMB-1 peroxidase substrate (Mandel Scientific Company) was incubated with the membranes, until desired band intensity was achieved.

Western Blotting Of Jak/STAT Pathway Activation:

Phosphorylated STAT1 And STAT2: HEK 293T cells were cultured in 6-well plates for 80% confluency. The NS5-HA clone (2.5 µg) was transfected into the cells with 6 µl of FuGene 6 following the manufacturer's protocol and cells were incubated for 24 hours. Tissue culture medium were discarded and replaced with and without 1000 U/mL of Universal IFN and was incubated for another 24 hours. Medium was removed and cells were washed once with PBS, lysed for 30 minutes on ice while rocking with lysis buffer, consisting of 0.1 M Tris-HCl (pH 7.5), 35% glycerol, 0.5% (w/v) bromophenol blue, 2% beta-mercaptoethanol and 2% SDS. Samples were processed (SDS-PAGE and transfer) as described in previous section for HEK 293T cells, except that blots were probed with 1:500 rabbit-derived, anti-STAT1 (Phospho Y701) (AbCam) or anti-STAT2 (Phospho Y690) (AbCam) with anti-actin (AbCam) as primary antibodies. The secondary was a 1:2000 sheep-derived, anti-rabbit horse-radish peroxidase (HRP) conjugated antibody.

NS5 Mutations: VeroE6 (ATCC) cells were passaged into 12-well tissue culture plates for 80% confluency prepared 24 hours prior to transfections. The NS5-HA clones at 0.8 µg (full-length, 6, 55, 223, 432 and 743) were transfected using 3.6 µl FuGene 6 transfection reagent (Promega) as per the manufacturer's protocol, into 1 mL of maintenance medium. After incubation for 72 hours, the medium was removed and discarded and, cells were washed once with PBS. Then cells were lysed for 30 minutes on ice while rocking using SDS-lysis buffer as described above. Samples were similarly processed (SDS-PAGE and transfer) as described in previous sections for HEK 293T cells with the exception that membranes were probed with 1:250 of anti-HA (mouse-origin) (AbCam) primary antibody and 1:3000 goat-derived, anti-

mouse horse-radish peroxidase (HRP) conjugated (AbCam) secondary antibody. Additionally, blots were probed with 1:4000 of mouse-origin, anti-beta Actin, horse-radish peroxidase (HRP) conjugated (AbCam) primary antibody.

2.11. Antigenome And Subgenomic Clone Generation

Antigenome: The GFP and luciferase genes used for these clones were obtained from the pAcGFP1-C1 (bases 613-1329) vector (ClonTech) and the ISRE-luciferase vector (SA Biosciences), respectively. Touchdown PCR with iProof DNA polymerase (Bio-Rad) as described in Chapter 2.8., was used to amplify all of the individual PCR fragments in antisense orientation for the pPOL vector backbones. Each PCR product was generated to have overlapping homology with the next product in succession. Sequences for all primers are listed on Table A.1. Primer set D1/D3 generated a 437 bp PCR product containing, pPOL vector-KFDV 3′ UTR (genome bases: 10383 to 10774)-GFP. The next PCR fragment was amplified using primer set D4/D5, this synthesized a 751 bp amplicon containing, 3′ UTR-GFP ORF-KFDV 5′ UTR. The last PCR reaction amplified a 291 bp fragment with primer set D2/D6 that contained, GFP-KFDV 5′ UTR fused to a portion of the C gene (genome bases 1-131 and 132-248, respectively). All three PCR products and the pPOL linearized with *Bsm*BI (NEB) were separated on and purified (Qiagen) from 1% agarose gels and prepared for In-Fusion HD cloning (ClonTech) following the manufacturer's recommendations. Luciferase reporter gene inclusion was performed following the same method as the GFP clone using primer sets: D1/D7 (435 bp), D8/D9 (~ 1.7 kb) and D2/D10 (288 bp). Thus generating AG-GFP-pPOL and AG-Luciferase-

pPOL clones under the human polymerase I promoter control (Flick & Pettersson 2001). For the construction of pTM1 [T7 promoter control (Moss et al. 1990)] clones, amplification of the entire antigenome from both AG-GFP and AG-luciferase-pPOL clones (primer set D11/D12) and cloning into pTM1 with *Nco*I/*Pac*I (NEB) restriction digest sites and, transformation into Top10 *E.coli* (Life Technologies) was used. These clones were named AG-GFP-pTM1 and AG-Luciferase-pTM1. All four antigenome constructs (Figure 1.5.) were confirmed by sequencing (NML) and restriction enzyme digestion pattern.

Antigenome helper plasmids: The NS proteins (NS1, NS2A, NS2B, NS3, NS4A, NS4B and NS5) were individually amplified and cloned into pCAGGS mammalian expression vectors previously (Cook 2010). The KFDV NS polyprotein (E_{23}-NS1-NS2A-NS2B-NS3-NS4A-NS4B-NS5) (Figure 1.5.) was generated following identical touchdown PCR annealing conditions with iPoof (Bio-Rad) with D13/B4 (Table A1) (Genome bases 2394-10379 to express amino acids 755-3416), from the KFDV RGS-ribo as a template (Cook et al. 2012). Standard cloning techniques were used to assemble the construct in XL-10 Gold chemically competent *E.coli* cells (Agilent).

Subgenomic Clone: Two sets of sequence overlapping PCR products were amplified using iProof under the manufacturer's reaction volumes under touchdown conditions. The primer sets are listed on Table A.1. The insert PCR of 2.0 kb was amplified from the AG-Luciferase-pPOL clone with primer set D14/D15 to include the T7 promoter, 5′ UTR (genome bases 1-131), a portion of the C gene (genome bases 132-248 encoding amino acids 1-39), luciferase (~ 1.7 kb), and 2A protease (48 bases). The vector (RGS-ribo) was amplified with primer set D16/D17 to include 2A protease (48 bases), a segment of the E gene (bases 2394-2462 for expression of

amino acids 755-777), the remainder of the KFDV genome (genome bases 2463-10774), pTM1 vector backbone. This 13.2 kb fragment was combined with the 2.0 kb insert for In-Fusion HD cloning (Clontech) following the manufacturer's recommendations, transformed into XL-10 Gold *E.coli* cells (Agilent). The subsequent, SG-Luciferase-pTM1 (T7 promoter-5′ UTR-$C_{117\ bases}$-luciferase-2A protease-$E_{69\ bases}$-NS1-NS2A-NS2B-NS3-NS4A-NS4B-NS5-3′ UTR-HDV ribozyme-pTM1 backbone) (Figure 1.5.) construct was verified by sequencing (NML) and restriction enzyme digestion pattern. Similarly, a control subgenomic clone was generated with a frame-shift mutation at the start of the NS5 gene following the NS4B/NS5 cleavage site (missing genome bases 7686-7710), the entire NS5 is out of frame and is replication-incompetent.

2.12. Antigenome And Subgenomic Clone Assays

Antigenome Transfection And Reporter Assays: Each antigenomic clone (AG-Luciferase or GFP-pTM1 or AG-Luciferase or GFP-pPOL) at various concentrations (2.0, 1.0, 0.5 and 0.2 μg) along with either individual clones expressing the KFDV NS proteins (500 μg) or the clone expressing the NS proteins as a polyprotein (500 μg) and, 10 ng of *Renilla* internal control construct and T7-RNA polymerase-pCAGGS (only for pTM1-based expression) were transfected with FuGene 6 (Promega) following the manufacturer's conditions in 12-well plates of HEK 293T (ATCC), BHK-21 (ATCC) or VeroE6 cells (ATCC). After incubation periods of 24 or 48 hours at 37^{o}C/5%CO_2, the cells were either viewed for GFP presence using a fluorescent microscope or the supernatant was discarded and the cells were assayed for luciferase

activity (as explained in Chapter 2. 9.) using a Veritas GloMax-96 microplate reader (Promega) in opaque-white microplates (Fisher Scientific).

Antigenome Verification Of Replication: Additional transfections of AG-Luciferase-pTM1 with the clones expressing all NS proteins individually and T7 RNA polymerase were performed (as described above in BHK-21 cells). RNA extractions were performed at 48 hours post-transfection using the RNeasy kit with QIAshredder columns (Qiagen) followed by DNase I (RNAse free) (NEB) treatment for 10 minutes at 37^{o}C and heat inactivation for 15 minutes at 75^{o}C. The cDNA was generated using OmniScript II (Qiagen) and a 3′ UTR antisense-orientation primer (A31) (Table A1), incubated for 60 minutes at 37^{o}C for positive-strand genome detection (RNase H activity is part of the OmniScript reaction). PCR amplification was performed using iProof (Bio-Rad) at 58^{o}C and 72^{o}C extension for 1.5 minutes (28 cycles) and a primer set for both luciferase (D18: LucSeq1s) and the KFDV genome (A18: KFDSeq3as) (Table A1). The AG-Luciferase-pTM1 plasmid was used as a positive control for PCR amplification. Expected PCR products of ~ 1.2 kb were separated by agarose gel electrophoresis and the 1 kb Plus DNA ladder (Life Technologies) was used as a reference. Assessing KFDV virus recognition and activation of the antigenome system was performed in 6-well plates of either BHK-21 or VeroE6 cells. Briefly, 1.0 and 2.0 µg of either AG-Luciferase and AG-GFP-pPOL or AG-Luciferase and AG-GFP-pTM1 clones with 500 µg of T7-pCAGGS were transfected with FuGene 6 (Promega) and incubated for 24 hours. Plates were transferred into the CL-4 suite, transfection medium was removed and cells were infected with KFDV at MOIs of 1 and 0.1 for 1 hour. Inoculum was removed and an appropriate volume of virus maintenance medium was added to wells and re-incubated. After 24 and 48 hours of incubation, the

monolayers were either viewed for the presence of GFP using a fluorescent microscope or the supernatant was discarded and prepared for luciferase activity as outlined in Chapter 2.9., using a Turner Designs-TD20/20 single-tube luminometer (Promega).

Subgenomic Clone Transfection And Reporter Assay: The SG-Luciferase-pTM1 clone (2.5 µg) was digested with *Pac*I and the linear DNA was subjected to *in vitro* transcription using the T7-mMessage/mMachine kit (Life Technologies) following the manufacturer's recommendations with the addition of 1 µl of GTP for 5′ RNA capping. Nascent RNA was subjected to DNase I (RNase free) (NEB) digestion for 10 minutes at 37^{o}C and stocks were stored at -80^{o}C until needed. Control RNA was similarly linearized and *in vitro* transcribed, the RNA stocks were stored at -80^{o}C. For time course experiments: BHK-21 (ATCC) cells were prepared in 12-well plates for 80-90% confluence. Subgenomic RNA of 2.5 or 5 µg was transfected with TransIT-mRNA reagent (CedarLane Laboratories) following the manufacturer's recommendations and incubated. Control RNA (frame-shift mutation of subgenomic clone) was transfected and assayed for comparison. Subgenomic and control RNA were harvested at 12-hour intervals by lysis for the DLR luciferase assay (Promega) and measured with Veritas GloMax-96 microplate reader (Promega)

Subgenomic Verification Of Replication: Additional RNA transfected (as described above) was performed (as described above in BHK-21 cells) and was harvested for RNA extraction at 2 hours and 6 hours post-transfection with RNeasy kit/QIAshredder columns (Qiagen) followed by DNase I (RNAse free) (NEB) treatment for 10 minutes at 37^{o}C and heat inactivated for 15 minutes at 75^{o}C. The cDNA was generated using SuperScript II (Invitrogen) using a sense-orientation C gene primer (A32: VirCs) (Table A1) and incubated for 50 minutes

at 42°C for antigenome and genome. After digestion of RNA with RNase H (NEB), touchdown PCR amplification was performed using iProof (Bio-Rad) as explained in Chapter 2.8., with an extension time of 1.5 minutes (30 cycles) and a primer set for both the KFDV genome (A1: KFDSeq1s) and luciferase gene (D19: LucSeq3as) (Table A1). The SG-Luciferase-pTM1 plasmid was used as a positive control for PCR amplification. Expected PCR products of ~ 1.5 kb were separated by agarose gel electrophoresis.

Chapter 3. Results

3.1. Monitoring Kyasanur Forest Disease Virus Infection In Tissue Culture

Kyasanur Forest disease virus (KFDV) has been propagated by different research groups in many cell lines: chick embryo (Mansharamani et al. 1967; Mansharamani & Dandawate 1967), VeroE6 (Dodd et al. 2011; Dodd et al. 2014), Vero, LLC-MK2, Porcine Stable (PS) kidney (Calisher et al. 1989) and A549 cells (Flint et al. 2014). However BHK-21 cells have been used in the cultivation and titrations of other tick-borne flaviviruses (Madani et al. 2014; Yoshii et al. 2014). It is unclear which cell lines may work best for KFDV propagation and developing the cytopathic effects (CPE) required for $TCID_{50}$ titrations; thus, the replication kinetics and CPE production of KFDV were evaluated using common laboratory cell lines used in our facility (NML). Cell cultures of VeroE6 (ATCC CRL-1586), VeroE6 (a long-term NML lab strain with unknown passage history), BHK-21 (ATCC CCL-10), BHK-21 (a long-term NML lab strain with unknown passage history) and MDCK (a long-term NML lab strain with

unknown passage history) were infected with KFDV at MOI of 0.1, monitored daily for CPE production and supernatants were harvested for virus quantification.

The manifestations of CPE were apparent in all cell lines tested when compared to mock-infected controls. Generally, CPE was pronounced between 3 and 4 days post-infection with the appearance of nearly 90-100% infection (Figure 3.1.a.); thus 3 days post-infection was used for visual CPE assessment for each cell line. For MDCK cells, the mock-infected controls displayed cell death and this made KFDV-induced CPE difficult to visually contrast. The BHK-21 lab strain and ATCC cell lines demonstrated clear CPE that was distinguishable from mock-infected controls; however the mock-infected lab strain controls began to display cytotoxicity at day 3 but became pronounced by day 4. The lab and ATCC VeroE6 cell lines showed CPE at 3 days post-infection when compared to mock-infected controls. However the CPE never appeared to affect greater than 70% of the cells beyond days 3-4 or even up to 21 days after infection. In fact, it was apparent that the cells began to propagate, despite the presence of high concentrations of virus. Despite the fact that the VeroE6 (ATCC and lab strain) and BHK-21 (ATCC and lab strain) cell lines demonstrated clear manifestations of CPE, the cytotoxicity of BHK-21 lab strain and the 70% infection ceiling of the VeroE6 cells suggest that the BHK-21 ATCC cells would be best for titration experiments.

In terms of virion production, supernatants from the KFDV-infected cell lines were quantified by $TCID_{50}$ on BHK-21 (ATCC) cells. Peak virus amounts in MDCK and BHK-21 (lab strain) were at 3 days and 2 days post-infection respectively, followed by sharp declines in titres (Figure 3.1.b.). The VeroE6 (lab strain) had its highest titres at day 3 post-infection and only trailed off slightly in subsequent time points until 21 days post-infection. The BHK-21 (ATCC)

and VeroE6 (ATCC) cells demonstrated the largest amounts of virus at days 3 and 4 post-infection followed by slight declines (Figure 3.1.b.). In summary from both CPE and titration experiments, BHK-21 (ATCC) and VeroE6 (ATCC) were the clear choices for propagation of our KFDV (P9605) isolate. The BHK-21 (ATCC) cell line demonstrated near 100% infection and thus was chosen for use in virus titrations.

Figure 3.1. KFDV Tissue Culture Infection Characteristics. (a) BHK-21 (ATCC) and (lab strain), VeroE6 (ATCC) and (lab strain) and MDCK (ATCC) were infected with KFDV at a MOI of 0.1 and harvested daily for titrations, until 100% CPE was observed. Pictures of cell monolayers were taken at 3 days post-infection at 4x magnification **(b)**. Supernatants were quantified by the 50% tissue culture infectious dose assay and are expressed in $\log_{10}$ scale. The VeroE6 cell culture supernatants were not harvested on day 7, but rather extended to day 21. Two technical replicates from one biological replicate were assayed ($TCID_{50}$) in duplicate. Averages with standard deviation are presented.

(a)

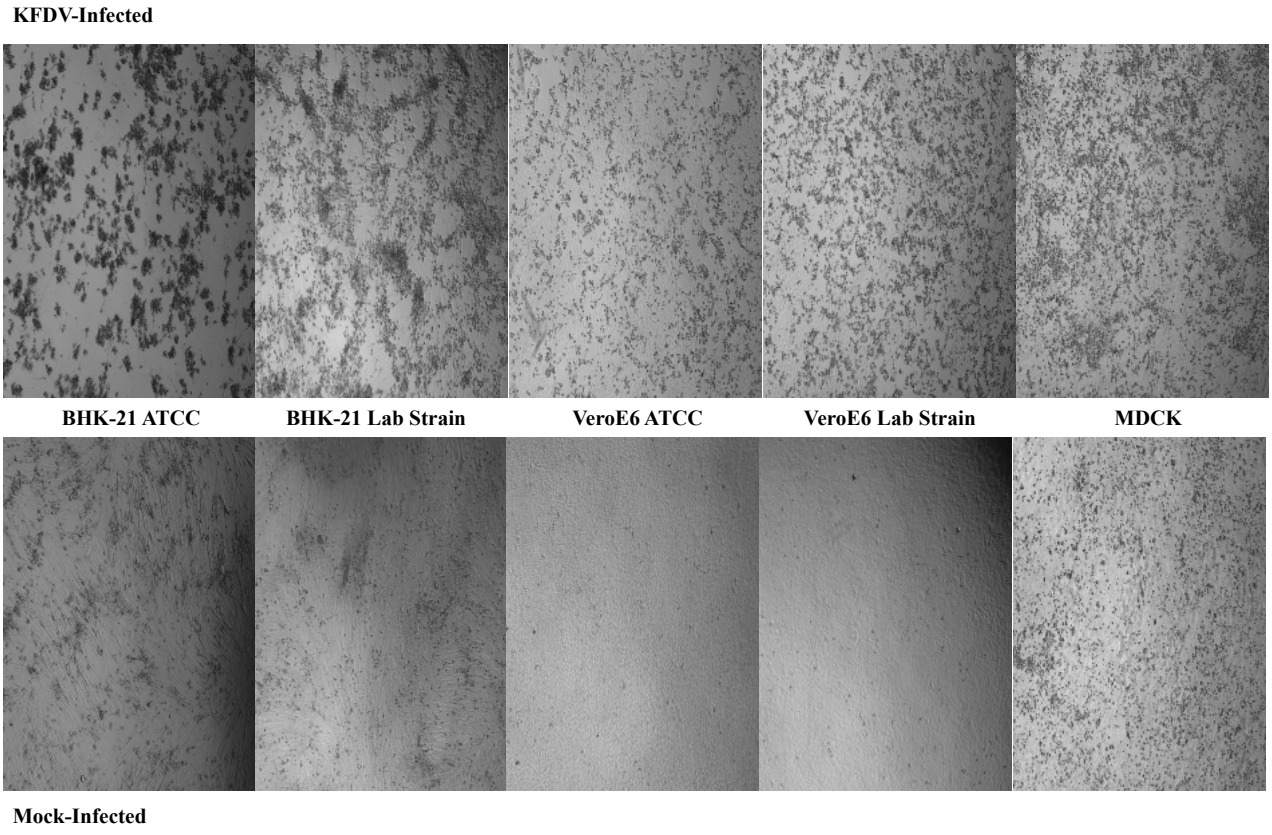
KFDV-Infected
BHK-21 ATCC
BHK-21 Lab Strain
VeroE6 ATCC
VeroE6 Lab Strain
MDCK
Mock-Infected

(b)

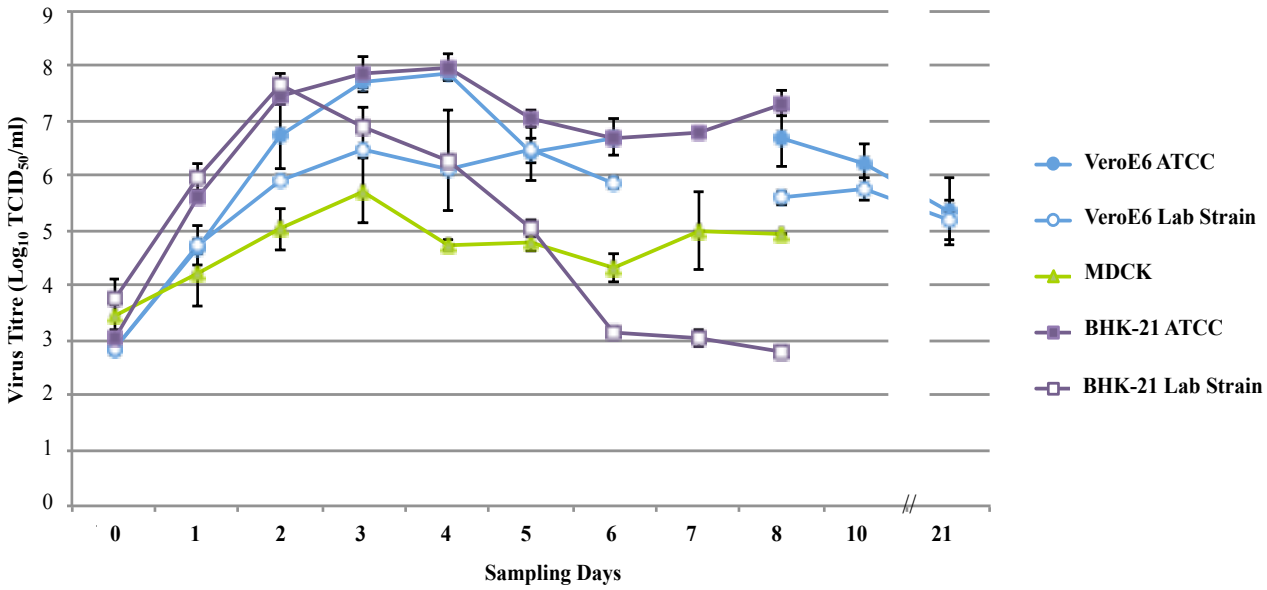
Virus Titre (Log10 TCID50/ml)
9
8
7
6
5
4
3
2
1
0
0
1
2
3
4
5
6
7
8
10
21
Sampling Days
VeroE6 ATCC
VeroE6 Lab Strain
MDCK
BHK-21 ATCC
BHK-21 Lab Strain

3.2. Developing A Reporter System With The Green Fluorescent Protein (GFP) Coding Sequence Inserted Into The Full-Length, Infectious KFDV Genome

A reporter gene construct for KFDV has never been published. The KFDV-GFP-tagged virus would be beneficial in allowing for visual virus replication identification before pronounced CPE is produced and signal quantification with fluorescence-activated cell sorting (FACS) and spectrophotometric methods. This would reduce time, labour and consumables used in virus titrations by plaque assay or $TCID_{50}$ assays. Integrating reporter systems into the full-length genomes in other flaviviruses has been problematic, with delayed virus replication and reporter instability occurring within very few passages (Pierson et al. 2005; McGee et al. 2010; Zou et al. 2011), with the exception of a more stable GFP in yellow fever virus (Bonaldo et al. 2007). Building on the information obtained from the previously unsuccessful attempts at stable GFP insertion into full-length flavivirus genomes, three KFDV genomes were constructed with an in-frame GFP ORF (see Figure 1.2.2.): i) KFDV-RGS-ribo-NSGFP, in which the GFP ORF is incorporated into the polyprotein flanked by duplicated NS4B and NS5 cleavage sites, to be cleaved by the natural KFDV protease. ii) KFDV-RGS-ribo-NS5-GFP, the NS4B/NS5 cleavage site fused to the GFP ORF immediately following the NS5. This included removal of a portion of the 3′ UTR (bases 10380-10545), but did include the proposed cyclization sequences. iii) KFDV-RGS-ribo-ENS1-GFP clone has the GFP ORF at the junction of the structural and non-structural genes with small duplications of the E and NS1 protein coding sequence flanking the ORF (Bonaldo et al. 2007). Rescue of the GFP-expressing KFDV was compared to the rescue of KFDV (from the KFDV-RGS-ribo clone) to assess CPE. The GFP clones were judged for GFP

production by fluorescence microscopy and by CPE development. Unfortunately, none of the clones assayed in three technical samples of three biological replicates, demonstrated any observable GFP expression or CPE at any point during the 14-day post-infection period. This result was unchanged regardless of alterations of transfection conditions (ratios of transfection reagent and plasmid concentrations).

3.3. Analyzing The Capabilities Of IFN-α2a And Other IFN-α/β Species To Restrict KFDV Propagation

3.3.1. IFN-α2a Treatment Does Not Clear KFDV Infection *In Vitro*

IFN-α2a has been used for treatment of patients with flavivirus-diseases with limited success, as summarised in Chapter 1.3. In tissue culture IFN was able to inhibit two members of the TBE serocomplex Langat and tick-borne encephalitis viruses, in a time-dependent manner (Best et al. 2005; Taylor et al. 2011). This aim attempted to determine if IFN-α2a could eliminate KFDV from infected cells. The KFDV data were compared to those obtained with VSV-GFP for control purposes, through virus clearance and rebound assays (Rocha-Pereira et al. 2013; Lin et al. 2004). The sensitivity of KFDV and VSV-GFP was assessed as 2000 U/mL of IFN-α2a was added immediately following virus adsorption on A549 and BHK-21 (ATCC) cells, referred to as passage 0. Virus supernatants were harvested and, infected-cells were then passaged into two wells and another 2000 U/mL of IFN-α2a was or was not added (passage 1). The IFN-treated

cells were subcultured again into two wells and either re-treated with IFN or un-treated (passage 2).

During the initial infection (passage 0), the IFN treatment of infected cells caused declines in virus titres when compared to the mock-treated controls for KFDV in A549 cells (reduction of $10^{0.8}$ $TCID_{50}$/mL, $P< 0.1$) and BHK-21 cells (reduction of $10^{0.4}$ $TCID_{50}$/mL, $P< 0.1$). The decreases were more striking for VSV-GFP in A549 cells (reduction of $10^{5.2}$ $TCID_{50}$/mL, $P< 0.01$) and in BHK-21 cells (reduction of $10^{6.5}$ $TCID_{50}$/mL, $P< 0.01$) (Figure 3.3.1. a and b). When passage 0 IFN-treated cells were subcultured and re-treated with another 2000 U/mL of IFN, there were marked differences in titres of KFDV and VSV-GFP. In spite of IFN addition, KFDV titres did not appreciably decrease following successive passages in both A549 cells (decrease of $10^{0.1}$ $TCID_{50}$/mL, not significant and increase of $10^{0.7}$ $TCID_{50}$/mL, $P< 0.1$) and BHK-21 cells (increase of $10^{0.6}$ $TCID_{50}$/mL, not significant and a decrease of $10^{0.3}$ $TCID_{50}$/mL, not significant) for passages 1 and 2, respectively (Figure 3.3.1. a). In contrast, VSV-GFP demonstrated more substantial declines in titre from the passage 0-treated A549 cells ($10^{1.6}$ $TCID_{50}$/mL, $P< 0.1$ and $10^{1.7}$ $TCID_{50}$/mL, $P< 0.01$) over passages 1 and 2, respectively (Figure 3.3.1. b). In the IFN-treated BHK-21 cells in passage 1, no virus was detected by the $TCID_{50}$ assay. Thus, this represents a decrease from passage 0 to passage 1 of $10^{2.9}$ $TCID_{50}$/mL, $P< 0.01$. As anticipated, passage 2-treated IFN cells also had un-detectable levels of VSV-GFP (Figure 3.3.1. b).

When IFN-treated cells from passage 0 were subcultured without IFN re-treatment, the titres for both viruses rebounded and displayed significant CPE to near mock-treated passage 0 values. Interestingly, despite IFN treatment and high KFDV infectious virion production, A549

and BHK-21 cells displayed limited CPE (Figure 3.2.1. c and d). Thus, unlike the IFN-sensitive VSV-GFP, KFDV infection of tissue culture cannot be eliminated by repeated IFN-α2a additions.

To determine if the limited antiviral effects of IFN are in fact a natural feature of KFDV and not due to IFN-induced alterations in viral genotype from passage 0 to passage 2, RNA obtained from virus-containing supernatants was sequenced for mutational changes in the polyprotein region. When using passage 0 (mock-treated) RNA of both A549 and BHK-21 cell-derived virus controls, no nucleotide changes within the polyprotein-encoding region of the genome were observed for any of the passage 2-IFN treated virus samples. Thus, the nature of the avoidance of IFN-α2a from passage 0 to 2 does not appear to due to a selection of variants.

Figure 3.3.1. IFN-α2a Does Not Clear KFDV Infection. (a and c) A549 and **(b and d)** BHK-21 cells were infected with an MOI of 0.00001 (11 $TCID_{50}$ units) of the indicated virus, and either treated or mock-treated with 2000 U/mL of IFN-α2a (designated as P0). Monolayers were passaged when untreated controls reached CPE of nearly 90%. 2000 U/mL of IFN-α2a was either added or omitted (P1) and after 3 days post-infection, this procedure was repeated again (P2). Before each passage, supernatants were harvested for titration by $TCID_{50}$ assay determination on BHK-21 cells. The averages and standard deviation from three biological replicates are shown graphically and expressed in $\log_{10}$ scale $TCID_{50}$/mL. Statistical significance is denoted as * $P < 0.1$, ** $P < 0.05$, *** $P < 0.01$ for **(a)** A549 cells and **(b)** BHK-21 cells. Pictures of cell monolayers were taken for **(c)** A549 cells and **(d)** BHK-21 cells. Mock, Non-IFN treated, infected controls. UI, Un-infected controls.

(a)

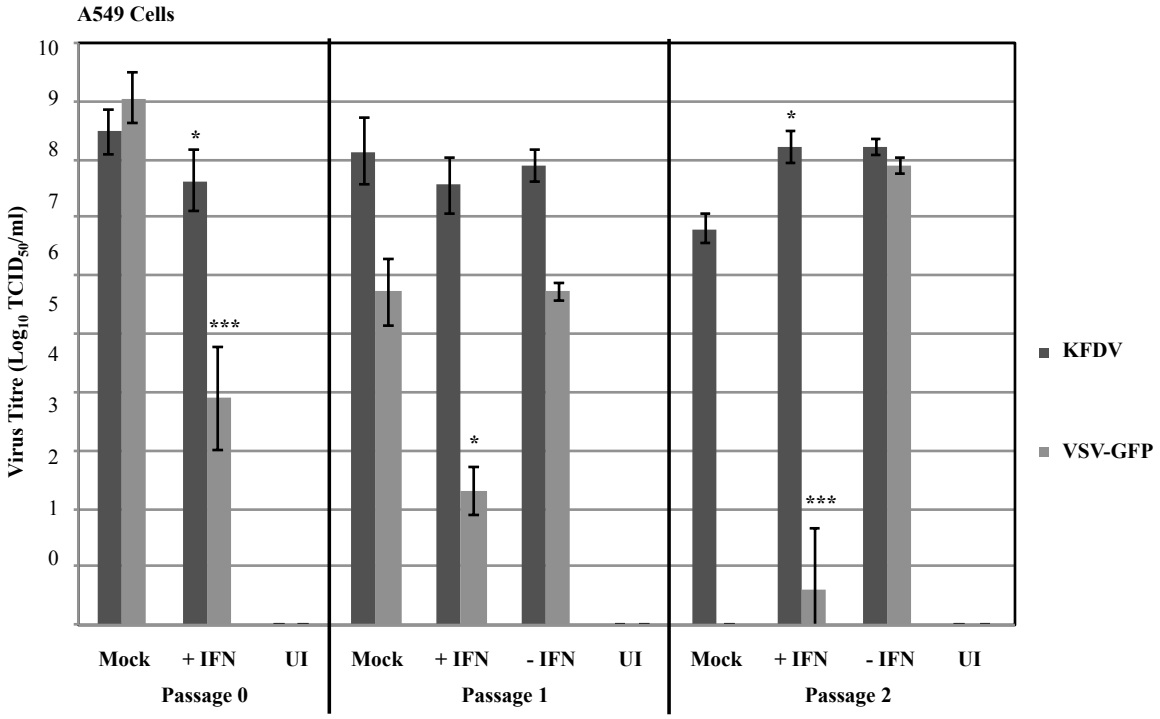
A549 Cells
Virus Titre (Log10 TCID50/ml)
10
9
8
7
6
5
4
3
2
1
0
*
***
*
*
***
Mock
+ IFN
UI
Mock
+ IFN
- IFN
UI
Mock
+ IFN
- IFN
UI
Passage 0
Passage 1
Passage 2
KFDV
VSV-GFP

(b)

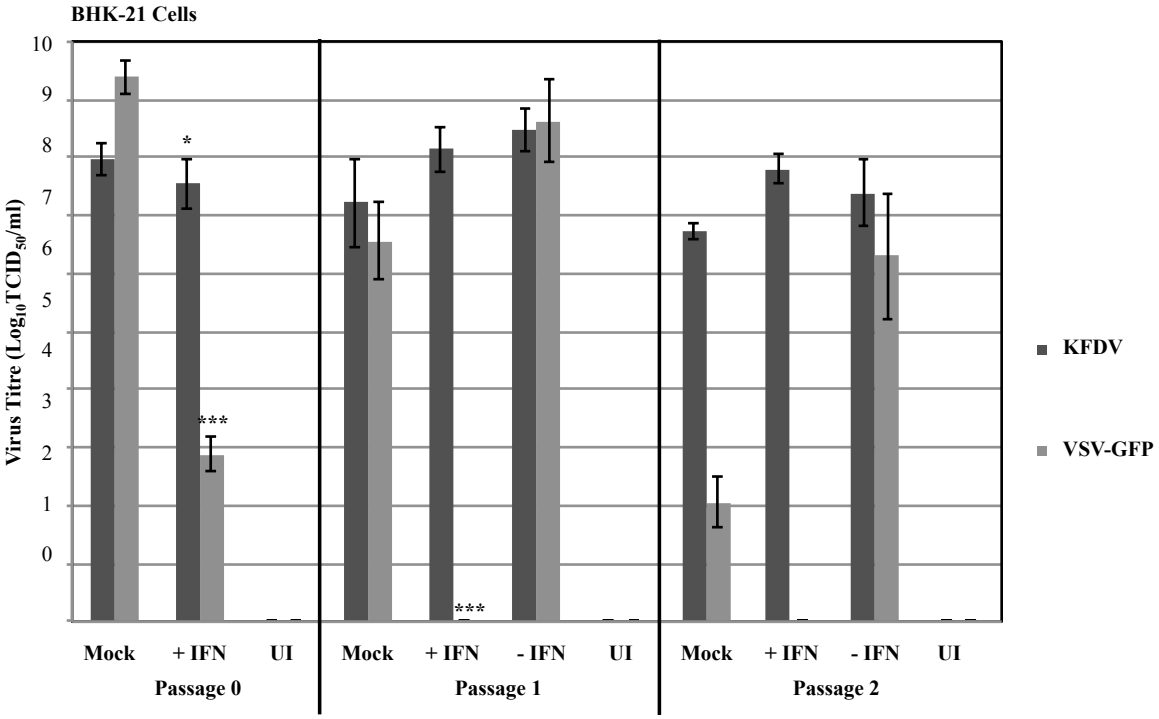
BHK-21 Cells
Virus Titre (Log10TCID50/ml)
10
9
8
7
6
5
4
3
2
1
0
*
***
***
Mock
+ IFN
UI
Mock
+ IFN
- IFN
UI
Mock
+ IFN
- IFN
UI
Passage 0
Passage 1
Passage 2
KFDV
VSV-GFP

(c)

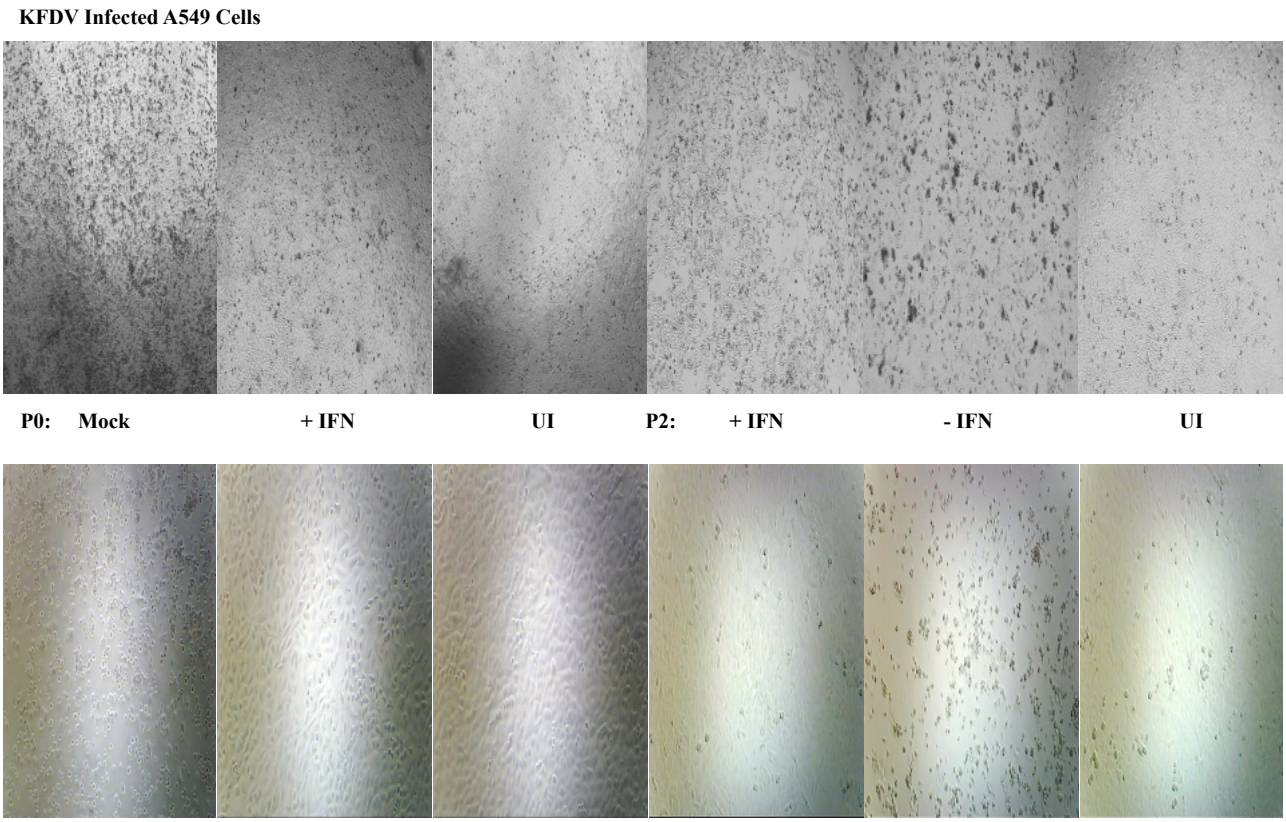
KFDV Infected A549 Cells
P0: Mock
+ IFN
UI
P2: + IFN
- IFN
UI
VSV-GFP Infected A549 Cells

(d)

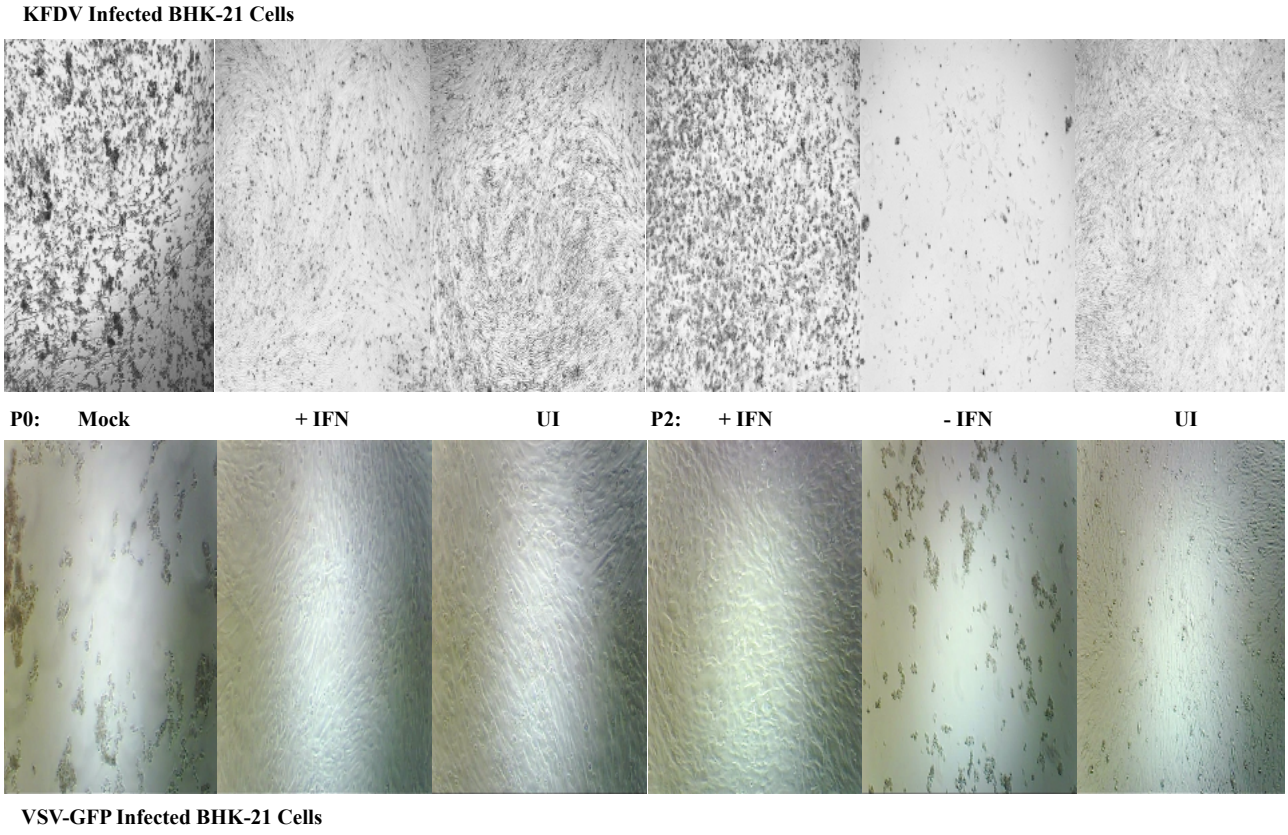
KFDV Infected BHK-21 Cells
P0: Mock
+ IFN
UI
P2: + IFN
- IFN
UI
VSV-GFP Infected BHK-21 Cells

3.3.2. Assessing The Inhibition Of KFDV Replication By Interferon α/β Species

From the results of aim 3.3.1., it is apparent that IFN-α2a is unable to successfully eliminate KFDV from cell culture when added post-virus adsorption (post-infection treatment). Previous studies with flaviviruses have indicated that IFN is more effective when added before cells are infected and wanes over time of addition in post-infection scenarios (Best et al. 2005; Diamond et al. 2000; Samuel & Diamond 2005; Samuel et al. 2006). In addition, the range of antiviral potency of the different IFN-α/β species could uncover a stronger repressor of KFDV replication than IFN-α2a. Thus, the activity of a single dose of IFN in both pre and post-infection treatment scenarios was evaluated for their ability to curtail KFDV replication in A549 cells.

To screen for the IFN candidates that were able to limit KFDV replication to the greatest degree, A549 cells were infected (MOI of 1) and 1000 U/mL of each IFN-α/β was added either before or after infection. Supernatants were harvested when mock-treated controls cells demonstrated 90-100% CPE. In pre-infection treatment conditions, IFN-αK and IFN-αWA demonstrated the strongest antiviral activity leading to 16- and 14-fold decreases in virus titre when compared to the mock-treated control. IFN-α2a was considerably less effective, demonstrating a 3-fold reduction in titre versus the mock-treated samples (Figure 3.3.2., gray bars). In post-infection treatment settings, IFN-αK and IFN-αWA again demonstrated the more significant reductions in KFDV propagation, as 132- ($P<0.01$) and 37-fold ($P<0.01$) reductions compared to mock-treated controls were observed, respectively. This is in contrast to IFN-α2a, which resulted in 6-fold ($P<0.1$) reduction in titre. IFN-α2b was not associated with a significant decrease in KFDV titre (Figure 3.3.2., black bars). These data suggest that IFN-αK and IFN-

αWA may be better able to restrict KFDV infection than IFN-α2a or IFN-α2b, regardless of their delivery time.

Figure 3.3.2. Interferon-α/β Species Screening Against KFDV. Cultures of A549 cells individually, were pre-treated (grey bars) or post-treated (black bars) with 1000 U/mL of each IFN-α (B2, C, D, F, G, H2, I, J1, K, WA, 2a, 2b and 4b), IFN-β (Beta-1) and a recombinant IFN-α (Universal) species and infected with KFDV at a MOI of 1. Supernatants were harvested for each treatment after 3 days of incubation and quantified (expressed in $\log_{10}$ scale $TCID_{50}$/mL) on BHK-21 (ATCC) when the mock-treated control cells displayed CPE near 100%. Pre-infection treatment experiments were assayed in two biological replicates and post-infection treatment experiments were assayed in three biological replicates; the resulting averages and standard deviations are presented. Mock, Mock-treated with IFN. UI, Un-infected control. IFN-α2b was excluded from 24-hour pre-infection treatment. * Significant compared to mock-treated samples ($P < 0.1$). *** Significant compared to mock-treated samples ($P < 0.01$).

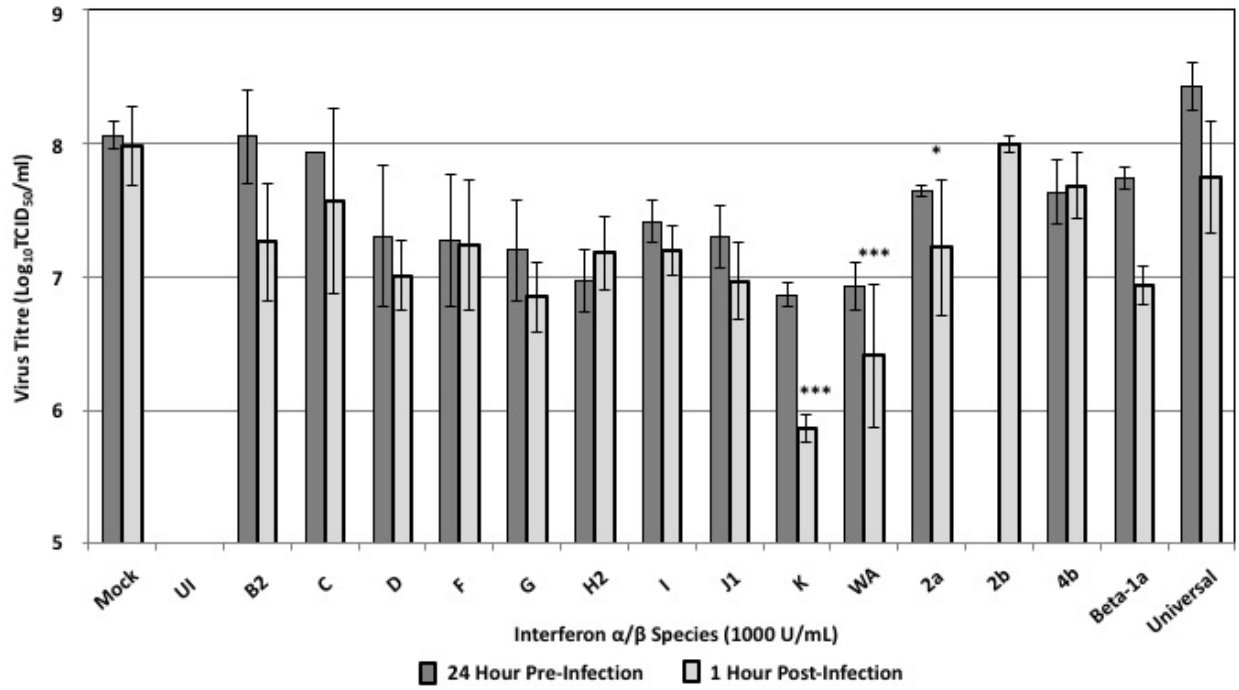
9
8
7
6
5
Virus Titre (Log10TCID50/ml)
*
***
***
Mock
UI
B2
C
D
F
G
H2
I
J1
K
WA
2a
2b
4b
Beta-1a
Universal
Interferon α/β Species (1000 U/mL)
24 Hour Pre-Infection
1 Hour Post-Infection

3.3.3. Dose-dependent Antiviral Activity Of IFN-αK, IFN-αWA And IFN-α2a

The two candidate IFNs, IFN-αK and IFN-αWA, appeared to have the greatest ability to restrict KFDV replication in both pre- and post-infection scenarios (Figure 3.3.2.). Dose-range series experiments were conducted to determine if the potency of IFN-αWA (as a representative of the more potent IFN-α species) was more significant than IFN-α2a by protecting cells from the cytopathology of KFDV. CPE reduction, reported as IC_{50} and IC_{90}, was determined using monolayer staining which was measured with a spectrophotometer rather than a potentially subjective visual CPE determination (Meager 2002; Armstrong 1981; Berger Rentsch & Zimmer 2011; Morrey et al. 2002; Voigt et al. 2013). Furthermore, some of these IFN concentrations were assessed by $TCID_{50}$ assays for their antiviral activity. Once again, VSV-GFP was used to serve as a control for IFN-sensitivity. A549 cells and BHK-21 cells were infected with KFDV or VSV-GFP [MOI of 0.0003 (11 $TCID_{50}$ units)] and treated with two-fold dilutions of each IFN and monolayers were fixed and stained when the infected controls displayed near 100% CPE (defined as 0% protection). For calculation purposes, 100% protection is defined by the un-infected cell controls. Beginning with KFDV, IC_{50} values of 5.2 and 7.4 U/mL in A549 cells; and, 23.3 and 6.9 U/mL in BHK-21 cells (Table 3.3.3.a.) for IFN-αWA and IFN-α2a respectively, were calculated. It would appear that low concentrations of IFN were sufficient to protect A549 and BHK-21 cells from KFDV-induced cytopathology. This is comparable to the IC_{50} values obtained when A549 cells were infected with the IFN-sensitive control virus (VSV-GFP); IC_{50} values are 5.1 and 5.6 U/mL for IFN-αWA and IFN-α2a, respectively (Table 3.3.3.a.). However, this was not the case for BHK-21 cells, as IC_{50} could not be determined (ND)

for IFN-αWA and were very high for IFN-α2a (988.1 U/mL). Furthermore, the respective IFN-αWA and IFN-α2a IC_{90} values are: 406.8 and 125.4 U/mL in A549 cells and, 23711.0 and 2048.0 U/mL in BHK-21 cells (Table 3.3.3.a). The values obtained with KFDV contrast those with VSV-GFP for both IFN-αWA and IFN-α2a, as the IC_{90} values are 48.5 and 50.0 U/mL in A549 cells and 3808.0 and 56.2 U/mL in BHK-21 cells (Table 3.3.3.a.) respectively.

CC_{50} values could not be determined for either IFN tested, as 16, 000 U/mL, which was far more than that used for experiments, led to only 25% and 11% cell death in A549 cells and in BHK-21 cells. As expected, the un-treated control did not show cytotoxicity and the 10% Triton X-100-treated control showed 100% cytotoxicity (Table 3.3.3.a.).

The data from the previous experiment (Table 3.3.3.a.), were used to determined the concentration of IFN needed to protect cells from infection (IC_{50} and IC_{90} values). In addition, it is important to understand the effect of the IFN not only on CPE reductions, but virus titres. Therefore, four concentrations of IFN-α2a and IFN-αWA, and two concentrations of IFN-αK were tested to determine if the response to these cytokines is dose-dependent (Table 3.3.3.b.). Given the range of IC_{50} values (Table 3.3.3.a.), it was decided that concentrations of 2000, 500, 62.5 and 7.8 U/ml would be used. As a control, VSV-GFP virus production was measured under the same conditions. In A549 cells, the reductions in VSV-GFP titres were similar for IFN concentrations of 2000 and 500 U/mL ($10^{6.9}$ and $10^{7.5}$ $TCID_{50}$/mL reductions for IFN-α2a, $10^{7.9}$ and $10^{7.0}$ $TCID^{50}$/mL reductions for IFN-αWA). At lower concentrations, the response was dose-dependent, and reductions in titre of $10^{3.5}$ and $10^{3.6}$ $TCID_{50}$/mL were seen at the lowest concentrations of the IFN (7.8 U/mL).

In stark contrast, the reductions in viral titre following KFDV infection ranged between

$10^{0.2}$ and $10^{1.1}$ $TCID_{50}$/mL (Table 3.3.3.b.). Additionally, there was less than $10^{0.4}$ $TCID_{50}$/mL difference between the titres produced from A549 cells in the presence of 2000 and 7.8 U/ml IFN. In BHK-21 cells, there was evidence of a weak, dose-dependent effect of IFN-α2a; there was a $10^{0.8}$ $TCID_{50}$/mL difference between the titres produced in 2000 and 7.8 U/ml of this cytokine. IFN-αWA had a negligible effect on viral titre in BHK-21 cells infected with KFDV.

Unfortunately, due to time constraints and shifted priorities, IFN-αK was not fully examined for its effect on KFDV and VSV-GFP viruses; however preliminary data (duplicate biological replicates assayed in triplicate) indicates that IC_{50} and IC_{90} values for IFN-αK treated, KFDV-infected A549 cells were: 18.7 U/mL and 108.0 U/mL, respectively. KFDV titre reductions for A549 cells treated with 2000 and 7.8 U/mL IFN-αK resulted in decreases of $10^{0.6}$ and $10^{0.2}$ $TCID_{50}$/mL, respectively.

In summary it would appear that IFN is ineffective at reducing KFDV infection as the dose-dependent relationship seen with VSV-GFP does not occur with KFDV. Thus, KFDV is insensitive to the effects of IFN.

Table 3.3.3.a: Antiviral Activity Of Interferon-α/β Against Cytopathology Of KFDV And VSV-GFP.

Interferon (IFN) species	KFDV IC_{50} (U/mL)	VSV-GFP IC_{50} (U/mL)	KFDV IC_{90} (U/mL)	VSV-GFP IC_{90} (U/mL)	CC_{50} (U/mL)
A549[a]					
WA	**5.2**	**5.1**	**406.8**	**48.5**	**> 16, 000.0**
2a	**7.4**	**5.6**	**125.4**	**50.0**	
K	**18.8**	**ND[c]**	**108.0**	**ND**	
BHK-21[b]					
WA	**23.3**	**ND**	**23711.0**	**3808**	**> 16, 000.0**
2a	**6.9**	**988.1**	**2048.0**	**56.2**	

[a] IC_{50}, CC_{50} and IC_{90} values from three technical replicates of each of three biological replicates in A549 cells

[b] IC_{50}, CC_{50} and IC_{90} values from three technical replicates of each of one biological replicates in BHK-21 cells

[c] ND = Not Determined.

Table 3.3.3.b: Antiviral Activity Of Interferon-α/β Against KFDV And VSV-GFP Virion Production.

Interferon (IFN) Species	Concentration (U/mL)	Virus Titre Reduction From Mock-Treated [c]	Virus Titre Reduction From Mock-Treated [c]
A549		KFDV	VSV-GFP
2a	2000.0	0.5	6.9
	500.0	0.7	7.5
	62.5	0.7	4.7
	7.8	0.4	3.5
WA	2000.0	0.7	7.9
	500.0	0.6	7.0
	62.5	1.1	6.2
	7.8	0.5	3.6
K	2000.0	0.6	ND
	7.8	0.2	ND
Mock-Treated [a]	0.0	0.0	0.0
BHK-21		KFDV	VSV-GFP
2a	2000.0	0.9	4.4
	500.0	0.5	1.2
	62.5	0.1	0.7
	7.8	0.1	1.5
WA	2000.0	0.0	1.8
	500.0	0.1	-0.4
	62.5	0.2	0.1
	7.8	0.0	0.3
Mock-Treated [b]	0.0	0.0	0.0

[a] Titre reduction of mock-treated samples were calculated from original titres in A549 cells of 8.2 and 9.5$\log_{10}$ $TCID_{50}$/mL for KFDV and VSV-GFP, respectively.

[b] Titre reduction of mock-treated samples were calculated from original titres in BHK-21 cells of 7.2 and 9.1 $\log_{10}$ $TCID_{50}$/mL for KFDV and VSV-GFP, respectively.

[c] Titre reduction expressed in $\log_{10}$ scale $TCID_{50}$/mL.

3.4. Investigation Of The Anti-Interferon Activity Of KFDV

The work in this chapter was published in the following reference: Cook, B. W. M., Cutts, T. A., Court, D. A., Theriault, S. (2012) The generation of a reverse genetics system for Kyasanur Forest disease virus and the ability to antagonize the induction of the antiviral state. Virus Research 163:2. BC performed the majority of the experiments and had input in experimental design, TC and ST conducted experiments and aided in experimental design, DC provided critical review and editing.

3.4.1. Discovering The Proteins Responsible For Anti-Interferon Activity

Flaviviruses have been reported to inhibit the hosts' type I IFN response via their non structural (NS) proteins, thereby halting the cellular antiviral state (Laurent-Rolle et al. 2010; Robertson et al. 2009). The major proteins involved are: the NS5 for dengue, yellow fever, Langat, West Nile, tick-borne encephalitis and Japanese encephalitis viruses (Best et al. 2005; Laurent-Rolle et al. 2010; Ashour et al. 2009; Laurent-Rolle et al. 2014), and NS4B-2k as seen with dengue, West Nile and yellow fever viruses (Laurent-Rolle et al. 2010; Liu et al. 2006; Munoz-Jordan et al. 2005). The NS proteins of KFDV have not been investigated in the same context.

The cellular response to IFN can be evaluated by measuring the activity of the Jak/STAT pathway. Two assays were utilized to address the NS protein interference of IFN signalling by KFDV. The first utilizes luciferase-induction from a plasmid designed to mimic interferon-

stimulated gene (ISG) expression by the Jak/STAT pathways' end product, Interferon-stimulated growth factor complex (ISGF3). The other assay allows for exogenous IFN to elicit the antiviral state to block subsequent infection by vesicular stomatitis virus (VSV). Thus, interruption of the Jak/STAT signalling cascade by KFDV NS proteins would prevent luciferase expression and allow for virus infection, despite IFN addition.

Based on the luciferase assay, the NS5 protein of KFDV appears to act as the strongest repressor of the Jak/STAT cascade and subsequent ISG expression. The presence of NS5 caused a decline of 98% in luciferase activity, compared to the total amount IFN induction (100% induction). This was comparable to the 97% value obtained from a known Jak/STAT inhibitor, VP24 of *Zaire ebolavirus* (Reid et al. 2006). The other NS proteins may play secondary roles in inhibition; NS4B and NS4B-2k, while combined with NS2A and NS4A, caused less severe declines of 83% and 75%, respectively, as seen in Figure 3.4.1.a. Additionally, the NS2A protein demonstrated stronger reductions, as represented by a 77% reduction in luciferase activity, compared to NS4B (60%) and NS4B-2k (67%). The E protein of KFDV was included as a negative control because there has been no reported anti-IFN activity associated with the structural proteins of flaviviruses (Figure 3.4.1.a.).

In the VSV-GFP-based assay, only NS5 enabled VSV to establish an infection in cell culture, even in the presence of any of the type I IFNs (Figure 3.4.1.b.). The mock-treated cell culture had significant infection as visualized by CPE and the GFP signal. The control experiments comprised of IFN-treated cells and cells that were transfected with an empty vector (pCAGGS) and infected in the presence of IFN, did not display any observable CPE or GFP fluorescence. As expected, cells transfected with NS5 but not NS4B-2k protein-expressing

plasmids, produced CPE and GFP signal, albeit at lower levels than the mock-treated controls. The ability of NS5 to disrupt the antiviral effects of IFN appeared to be comparable to that of VP24 (Figure 3.4.1.b.). When virion assembly and release were analyzed by titration ($TCID_{50}$/mL), the cells expressing NS5 regardless of the IFN-α/β species used, were susceptible to VSV-GFP ($P < 0.01$) (Figure 3.4.1.c.).

The expression of NS5 did not negatively impact the propagation of VSV-GFP in mock-treated cells controls, as a $TCID_{50}$ of $10^{9.5}$ was detected in both NS5 transfected cells and non-transfected cells. Due to the presence of NS5, cellular protection provided by IFN against VSV-GFP was reversed as indicated by log changes in titres ($TCID_{50}$). Comparing the NS5-transfected cells (light grey bars) to the control un-transfected cells (dark grey bars) titres increased by: $10^{1.3}$ (IFN-α species, B2), $10^{1.3}$ (C), $10^{1.7}$ (D), $10^{1.3}$ (F), $10^{1.1}$ (G), $10^{2.3}$ (H2), $10^{1.4}$ (I), $10^{1.6}$ (J1), $10^{1.4}$ (K), $10^{2.8}$ (WA), $10^{1.3}$ (2a), $10^{1.3}$ (2b), $10^{1.4}$ (4b), $10^{3.2}$ (IFN-β species, beta-1), $10^{1.8}$ $TCID_{50}$/mL (recombinant IFN-α species, Universal), suggesting that NS5 can alleviate the antiviral effects of IFN (Figure 3.4.1.c.). Interestingly, the extent of NS5's disruption appeared to be stronger than VP24, by nearly $10^{1.4}$ $TCID_{50}$/mL, for Universal-IFN ($P < 0.01$) (Figure 3.4.1.c.). Thus, the NS5 of KFDV appears to be a potent inhibitor of the antiviral state induced by IFN.

Figure 3.4.1. KFDV NS5 Impedes The Cellular Antiviral State. (a) HEK 293T cells were transfected with DNA constructs expressing KFDV NS proteins, Zaire ebolavirus VP24 and ISRE-luciferase reporter, and 1000 U/mL of Universal IFN-α added 24 hours post-transfection. Cells were lysed and analyzed for luciferase activity, 18 hours post-IFN treatment. Average raw light units (RLU) units and standard deviations were determined from normalized luciferase activity in triplicate from each of three biological experiments and was converted to a percentage of induced luciferase activity compared to mock control. Mock control is background levels of luciferase activity from mock-transfected cells. Positive control is a constitutively expressing luciferase gene under CMV promoter control. Induction control refers to background luciferase expression without exogenous IFN added. This is in contrast to the IFN-induction control where exogenous IFN was added. Black and grey bars are designed to visually separate control and experimental parameters respectively. **(b)** VeroE6 (ATCC) cells were transfected with plasmid encoding KFDV NS proteins and Zaire ebolavirus VP24 and treated with 1000 U/mL of Universal IFN, 24 hours post-transfection. After a 24-hour incubation period, cells were infected with VSV-GFP (MOI of 2) and, pictures were taken with light and fluorescent microscopy 24 hours later. **(c)** VeroE6 (ATCC) cells were transfected with KFDV NS5-pCAGGS and treated with 1000 U/mL of commercially available type I IFNs, 24 hours post-transfection. After a 24-hour incubation period, cells were infected with VSV-GFP (MOI of 2) and, 24 hours later, the virus-containing supernatants were harvested for virus quantification. Dark grey bars indicate experiments in which cells were un-transfected. Light grey bars indicate that NS5-expressing cells. Mock indicates no IFN treatment of cells lacking (dark gray bar) and expressing (light gray bar) NS5; UI represents uninfected and un-treated cells. Universal IFN controls included VP24-

pCAGGS as anti-IFN control. The graph represents the $\log_{10}$ scale $TCID_{50}$/mL averages and standard deviations from three biological repetitions. ***, Significant difference of NS5-expressing cells compared to VP24-expressing cells ($P < 0.01$).

(a)

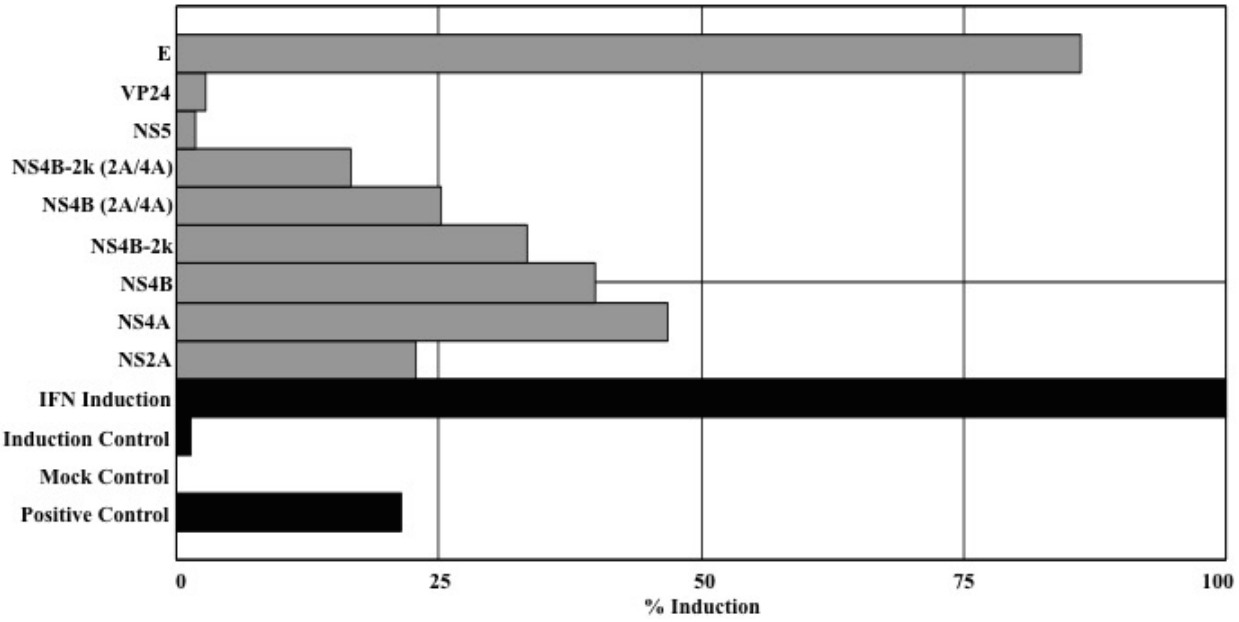
E
VP24
NS5
NS4B-2k (2A/4A)
NS4B (2A/4A)
NS4B-2k
NS4B
NS4A
NS2A
IFN Induction
Induction Control
Mock Control
Positive Control
0
25
50
75
100
% Induction

(b)

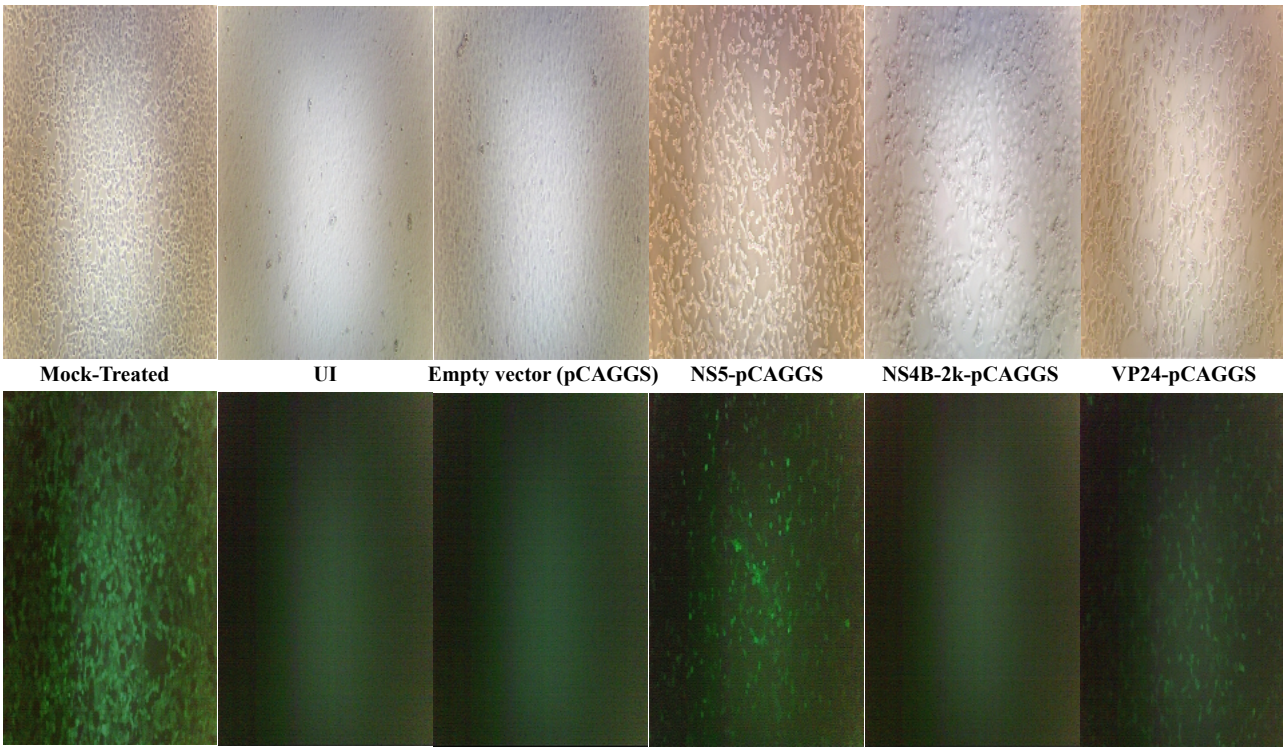
Mock-Treated
UI
Empty vector (pCAGGS)
NS5-pCAGGS
NS4B-2k-pCAGGS
VP24-pCAGGS

(c)

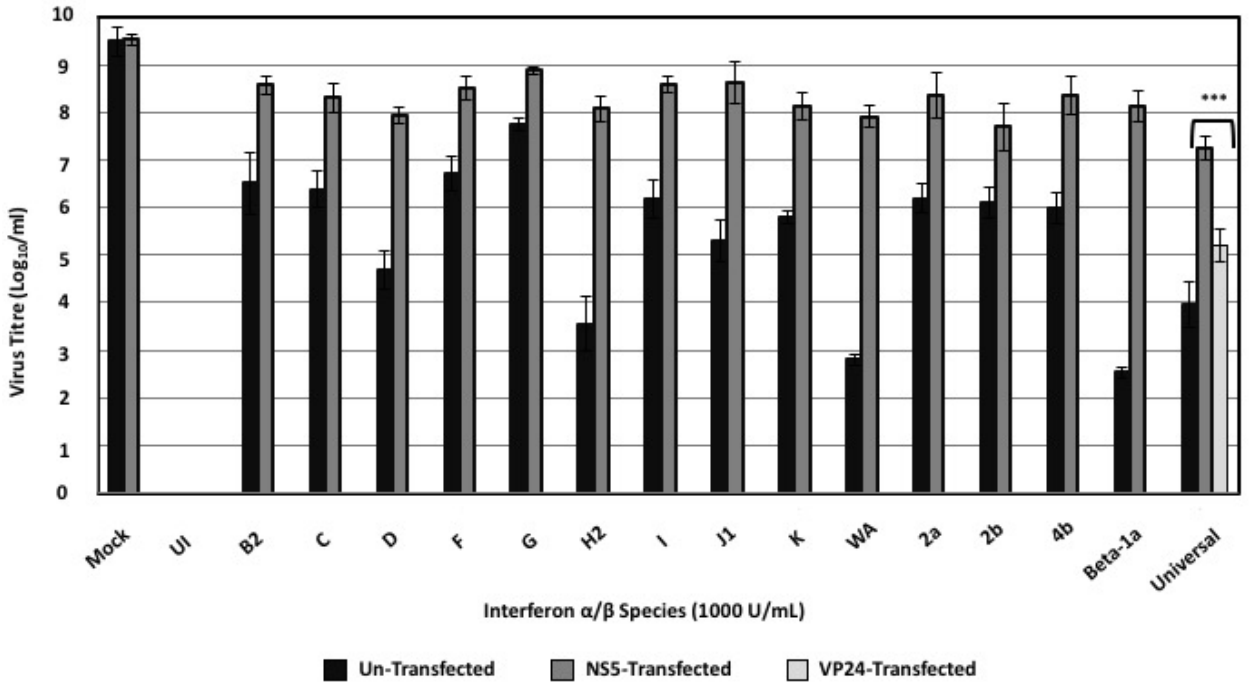
Virus Titre (Log10/ml)
10
9
8
7
6
5
4
3
2
1
0
***
Mock
UI
B2
C
D
F
G
H2
I
J1
K
WA
2a
2b
4b
Beta-1a
Universal
Interferon α/β Species (1000 U/mL)
Un-Transfected
NS5-Transfected
VP24-Transfected

3.4.2. Mutational Analysis And Mechanism Of Antagonism Of The Jak/STAT Pathway Activity Of NS5

The work in this chapter was published in the following reference: Cook, B. W. M., Cutts, T. A., Court, D. A., Theriault, S. (2012) The generation of a reverse genetics system for Kyasanur Forest disease virus and the ability to antagonize the induction of the antiviral state. Virus Research 163:2. BC performed the majority of the experiments and had input in experimental design, TC and ST conducted experiments and aided in experimental design, DC provided critical review and editing.

The NS5 protein is associated with two main functions during replication. The amino terminus has the methyltransferase (MTase) activity, which is responsible for capping and methylation of nascent genomes, and the carboxyl terminus is necessary for the RNA-dependent RNA polymerase (RdRp) activity. However, it is not entirely clear where such regions are precisely defined at the amino acid level. For Japanese encephalitis and dengue viruses respectively, the MTase may span residues 1-266 and 1-296 and, the RdRp may be from residues 276-905 and 273-900. These regions are not believed to overlap, as a 10 amino acid long linker domain is sandwiched in between both domains (Lu & Gong 2013; Davidson 2009). Mutational analysis and protein-interaction studies have revealed that Jak/STAT pathway interference caused by NS5 may be unique for each virus. These abilities can be attributed to either MTase and/or the RdRp but seem to use different mechanisms. These modes of action can include physical interaction with IFN receptors, interaction with host membrane proteins (scribble) and

blocking/degrading STAT protein signalling. These observations highlight the uniqueness of these functions among the flaviviruses.

In an attempt to narrow-down the region of the KFDV NS5 protein that is responsible, in-frame deletions within the NS5 coding sequence were constructed and the impact of the resulting NS5 variant was assessed via co-immunoprecipitation and separately for the prevention of Jak/STAT pathway from being activated by IFN. HEK 293T cells were chosen over A549 cells for possible human Jak/STAT pathway binding partners with NS5 due to their higher transfection capability (Caignard et al. 2009) and to represent the human IFN signalling cascade. The mutants are numbered in accordance with the full-length sequenced genome (GenBank accession number: HM055369) and are summarized in Table 3.4.2. The NS5 protein variants are as follows: the protein encoded by mutant 6 maintained the cut site of the KFDV viral serine protease (residues 1-5), then had amino acids 6-54 of the MTase region removed; mutant 55 encodes a variant with amino acids 55-222 deleted; the protein resulting from mutant 223 had the amino acid region of 223-431 withdrawn, which spans the MTase-linker-RdRp; the region absent from variant 432 was within the RdRp region (amino acids 432-742) and in variant 743, the 743-903 amino acid region is the C-terminal end of the RdRp was removed. These NS5 deletion clones were assayed for their ability to interrupt the signalling of the Jak/STAT pathway using the same luciferase bioassay and VSV-GFP recovery conditions mentioned previously (Section 3.4.1.).

Table 3.4.2. NS5 Mutants.

Mutant	Deletion	
	Amino Acid Position Of NS5	Genomic Base Position
6	6-54	7686-7832
55	55-222	7833-8336
223	223-431	8337-8963
432	432-742	8964-9896
743	743-903	9897-10379

Expression of the wild type NS5 and each NS5 variant was confirmed using HA-tagged fusions, as there was not an anti-NS5 antibody for KFDV available. Western blotting detected the NS5-HA (104.1 kDa) and the NS5-HA tagged variants 6-HA (98.3 kDa), 223-HA (80.6 kDa), 432-HA (68.6 kDa) and 743-HA (85.3 kDa), indicating that each protein was successfully expressed, albeit at different levels. The exception was 55-HA (85.3 kDa), which was not detected on the membrane (Figure 3.4.2.1.a.).

In order to determine the ability of each variant to interfere with Jak/STAT signalling, the luciferase assay described in section 2.9 and sections 3.4.1., was used. Results of this assay suggest that the regions of NS5 that are responsible for Jak/STAT pathway inhibition are in the latter portion of the MTase (variant 223) and the majority of the RdRp (variant 432) as luciferase induction values were nearly 100% in comparison to the induction control (Figure 3.4.2.1.b.). Alternatively, the remaining NS5 truncations (variants 6, 55 and 743) still enabled reductions in luciferase-induction by 90, 88 and 99%, respectively. This suggests that the regions responsible for the interference of Jak/STAT signalling caused by the NS5 protein can be primarily attributed to the amino acid regions deleted in the 223 and 432 variants with secondary effects in the 6 and 55 variants and that 743 does not play a significant role.

In order to examine the biological function of the NS5 variants further, their effects on the IFN-response was assayed using VSV-GFP infection assay, as described in sections 2.9 and 3.4.1. The lack of IFN-treated VeroE6 cell susceptibility to VSV-GFP infection indicated that the 223 and 432 variants of NS5 did not enable infection. The visual CPE and GFP signals representative of VSV-GFP infection via disruption of the antiviral effects of IFN was also seen with the other NS5 truncations, albeit to a lesser extent. The disruption was highest for variants

743 and lower for variants 6 and 55. Transfection control experiments using pAcGFP1-C1 and anti-IFN activity by NS5-pCAGGS served as references for the mutants (Figure 3.4.2.1.c.). Virus titres reflected the trend visually observed with CPE and GFP fluorescence. When compared to the full-length NS5 protein that blocked the effects of IFN, the VSV-GFP titre reductions were the largest for variants 223 and 432 with $10^{4.8}$ and $10^{4.3}$ $TCID_{50}$/mL respectively, indicating that these regions were more important for NS5's anti-IFN activity (Figure 3.4.2.1.d.). The other deletions resulted in virus titre reductions of $10^{3.4}$ and $10^{2.1}$ $TCID_{50}$/mL for 6 and 55 variants, respectively, meaning that NS5's anti-IFN activity was relatively restored compared to variants 223 and 432. Finally, mutant 743 displayed a 1.5-fold decrease in $TCID_{50}$/mL compared to NS5 indicating that this region of NS5 may be required for full anti-IFN activity, but it may not be critical for the majority of the activity. Consequently, it would appear as though the entire NS5 protein may be required for full repression of the antiviral state induction by IFN. However the latter residues of the MTase-linker and most of the RdRp (represented by their absence in variants 223 and 432) seem to be predominantly responsible for this action and the other regions may have some minor activity (Figure 3.4.2.1.d.).

In an attempt to uncover a mechanism of antagonism of the Jak/STAT pathway by the KFDV NS5 protein, full length NS5 fused to a HA tag was expressed in HEK 293T cells, which were treated 24 hours later either with or without Universal IFN for 8 hours and 24 hours. Post-lysis, NS5-HA was immuno-precipitated and the protein complexes obtained were subjected to SDS-PAGE to determine a Jak/STAT pathway-binding partner for NS5. The predicted weight of NS5-HA is estimated at ~ 104.1 kDa with the HA peptide contributing 1.1 kDa. Probing with a murine-derived anti-HA monoclonal antibody indicated that the NS5-HA was expressed in the

HEK 293T cell line and was immuno-precipitated (Figure 3.4.2.1.e.). Due to the denaturing conditions, the other bands observed at 25 and 50 kDa were assumed to be antibody light and heavy chains, respectively. This was confirmed by extraction of these peptides from the gel, followed by digestion and sequencing by mass spectrometry. The antibody light chain, antibody heavy chain and NS5 were confirmed at 25, 50 and 104.1 kDa, respectively. Degraded or truncated NS5 products are present in between the NS5-HA (~ 104.1 kDa) and the heavy chain of the antibody (~ 50 kDa) (Figure 3.4.2.1.e.). In an attempt to visualize NS5-HA binding partners, gel electrophoresis was repeated, followed by Coomassie staining of the gel. The absence of bands in addition to those corresponding to NS5-HA and the antibody chains indicates that NS5-HA did not have a strong binding partner, as only the NS5-HA (~ 104.1 kDa) and anti-HA antibody portions were visualized (Figure 3.4.2.1.f.). Furthermore, there were no apparent differences between the banding patterns of the IFN-treated and the non-IFN-treated samples (Figure 3.4.2.1.e. and f.). The absence of NS5 was confirmed in the non-transfected controls (Figure 3.4.2.1.e. and f.). Minor binding partners cannot be ruled out, as they might be in amounts that are too low to be detected by Coomassie staining.

One possible explanation for the lack of binding partners would be that the IFN-response was not activated under the experimental conditions used. To test this possibility, extracts of infected cells were probed by western blotting for the presence of phosphorylated (activated) STAT1 and STAT2. The presence of NS5-HA did not inhibit the activation of either STAT1 or STAT2 (Figure 3.4.2.2.). The data in summation indicate that a binding partner for NS5 could not be detected, and the activation of the Jak/STAT pathway (IFN binding and signalling up until STAT1 and STAT2 activation) does not appear to be prevented by NS5. This result is

unexpected, as it was shown that the expression of NS5-HA reduces the titre of the reporter virus (VSV-GFP).

Figure 3.4.2.1. Mutational Analysis Of NS5 To Define Jak/STAT Pathway Antagonism. (a) VeroE6 cells were transfected with NS5-HA and NS5-HA tagged mutant clones and after an incubation period of 72 hours, cells were lysed and subjected to western blotting and probed with 1:250 of anti-HA (mouse-origin) primary antibody and 1:3000 goat-derived, anti-mouse horse-radish peroxidase (HRP) conjugated secondary antibody (**upper panel**) or probed with 1:4000 of mouse-origin, anti-beta Actin, horse-radish peroxidase (HRP) conjugated primary antibody (**lower panel**). **(b)** HEK 293T cells were transfected with plasmids encoding KFDV NS5 truncations (6, 55, 223, 432 and 743) and control plasmids (empty pCAGGS vector and pAc-GFP-C1). The transfected cells were then treated with 1000 U/mL of Universal IFN for 18 hours and cells were then lysed and analyzed for luciferase activity. Average RLU units and standard deviation were determined from normalized luciferase activity in triplicate repetitions of triplicate experiments and was converted to a percentage of induced luciferase activity compared to mock control. Mock control is background levels of luciferase activity from mock-transfected cells. Positive control is a constitutively expressing luciferase gene under CMV promoter control. Induction control refers to background luciferase expression without exogenous IFN added. This is in contrast to the IFN-induction control where exogenous IFN was added. Black and grey bars are designed to visually separate control and experimental parameters respectively. **(c)** and **(d)** VeroE6 (ATCC) cells were transfected with plasmids encoding KFDV NS5, NS4B-2k, NS5 truncations and, control plasmids (empty vector and pAc-GFP-C1) and, treated with 1000 U/mL of Universal IFN, 24 hours post-transfection. After an 18-hour incubation period, cells were infected with VSV-GFP (MOI of 2) and, 24 hours post-infection treatment, pictures were taken under fluorescence **(c)** and virus supernatants were harvested for virus quantification

(d). The $\log_{10}$ scale $TCID_{50}$/mL averages and standard deviations from three biological replicates are presented. **(e)** and **(f)** HEK 293T cells were transfected with KFDV NS5-HA-pCAGGS and 1000 U/mL of Universal IFN was added 24 hours post-transfection. At specified time points, cells were lysed and, immune-precipitated with an anti-HA monoclonal antibody and protein A/G agarose beads. The immune-precipitated protein were separated on denaturing PAGE gels, which were transferred to nitrocellulose membranes and, probed with primary (mouse anti-HA) and secondary (goat anti-mouse HRP-conjugated) antibodies and assayed for HRP activity **(e)** or stained with Coomassie Brilliant Blue **(f)**. In **(e)** and **(f)**, antibody light chain (*), antibody heavy chain (**) and NS5-HA (***) are indicated.

(a)

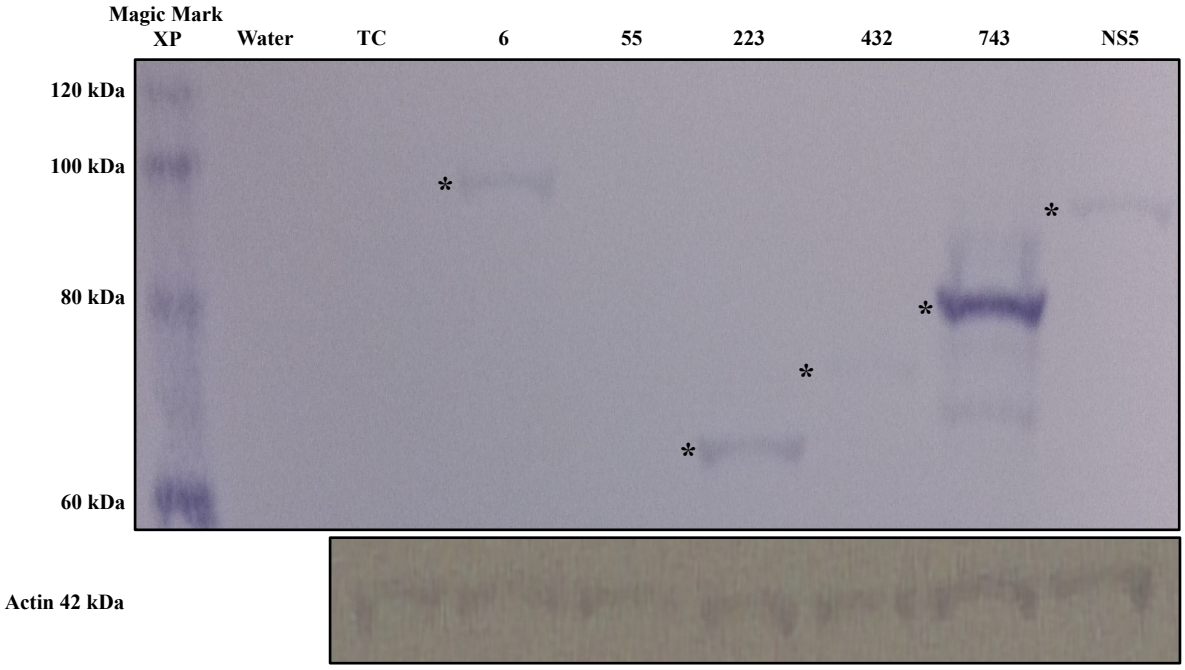
Magic Mark XP
Water
TC
6
55
223
432
743
NS5
120 kDa
100 kDa
80 kDa
60 kDa
Actin 42 kDa

(b)

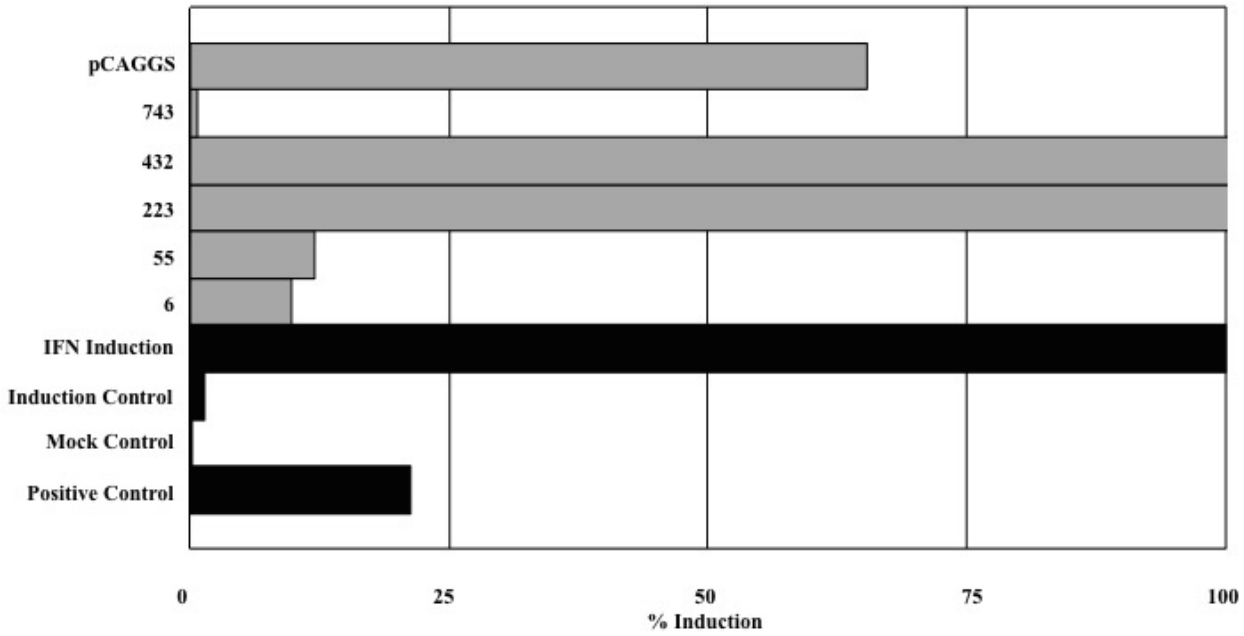
pCAGGS
743
432
223
55
6
IFN Induction
Induction Control
Mock Control
Positive Control
0
25
50
75
100
% Induction

(c)

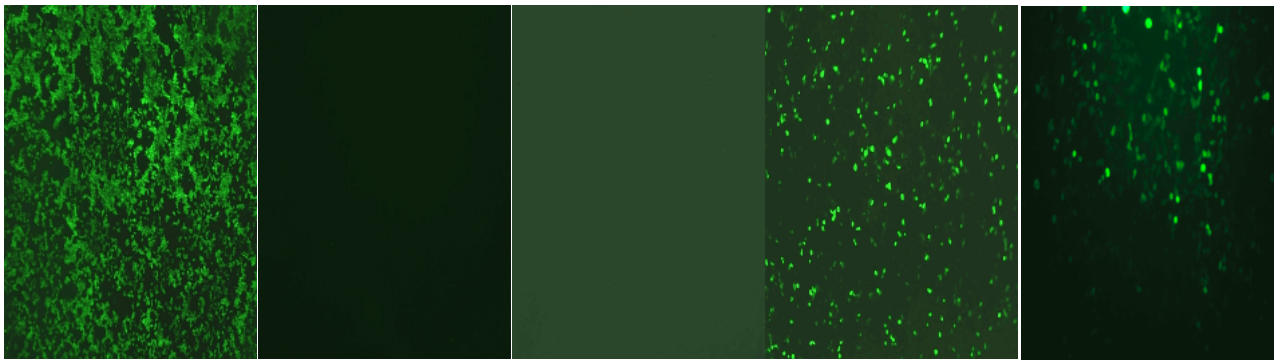

Mock-treated **UI** **Empty vector (pCAGGS)** **pAcGFP-c1** **NS5-pCAGGS**

6 **55** **223** **432** **743**

(d)

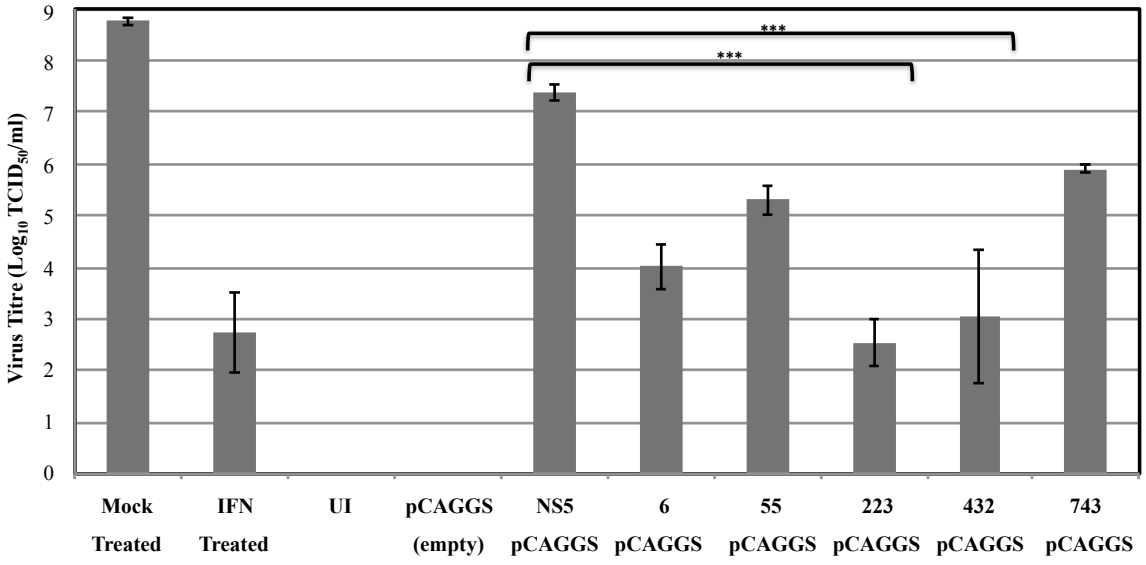
Virus Titre (Log10 TCID50/ml)
9
8
7
6
5
4
3
2
1
0
***
***
Mock Treated
IFN Treated
UI
pCAGGS (empty)
NS5 pCAGGS
6 pCAGGS
55 pCAGGS
223 pCAGGS
432 pCAGGS
743 pCAGGS

(e)

	Condition					
	NS5-HA	+	+	+	+	-
	Universal Interferon (1000 U/ml)	-	+	-	+	+
MagicMark XP	Hours Post-Transfection	8	8	24	24	24

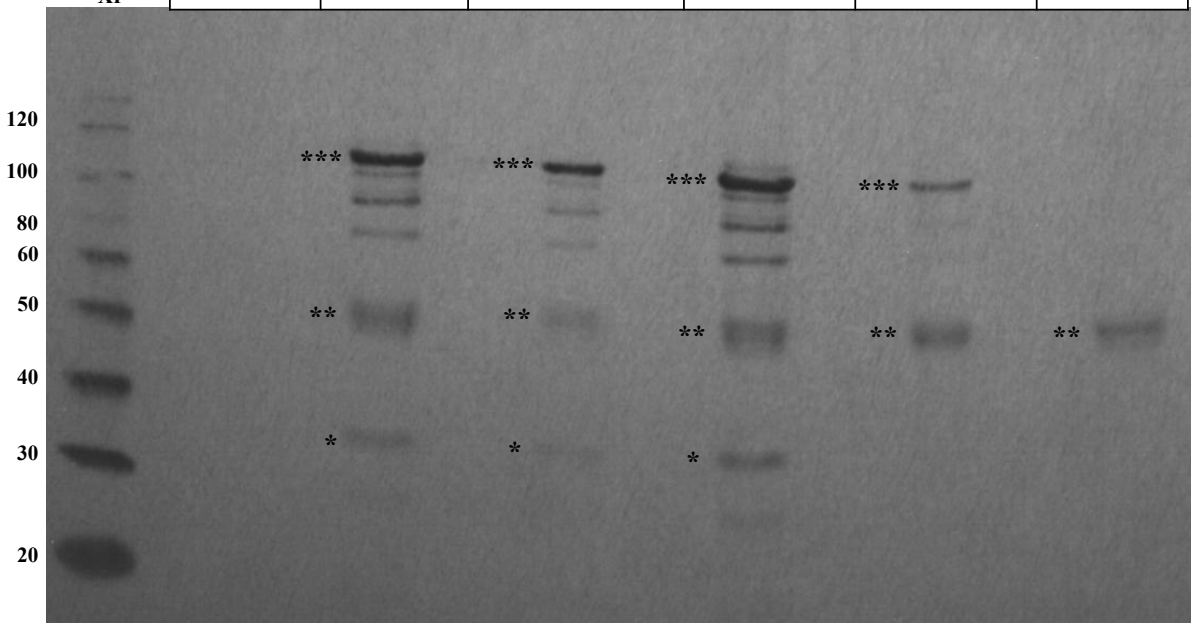

(f)

	Condition					
	NS5-HA	+	+	+	+	-
	Universal Interferon (1000 U/ml)	-	+	-	+	+
MagicMark XP	**Hours Post-Transfection**	**8**	**8**	**24**	**24**	**24**

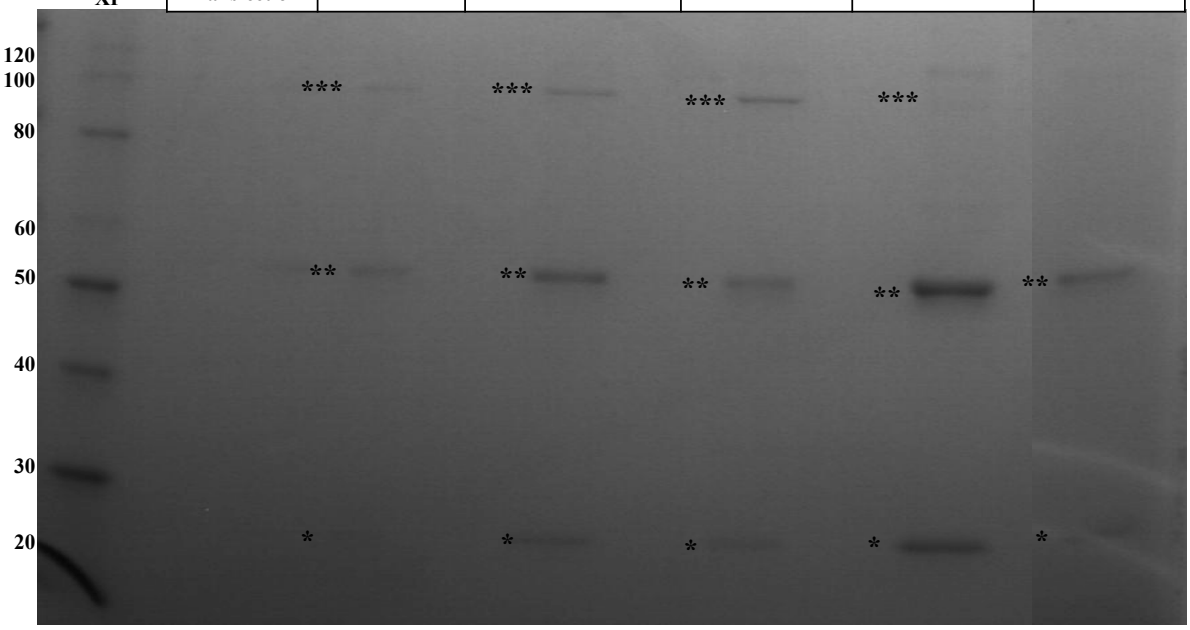

Figure 3.4.2.2. Jak/STAT Pathway Initiation Despite The Presence Of NS5. HEK 293T cells were transfected with KFDV NS5-HA and treated with Universal IFN for 24 hours. Post lysis, lysates were separated by SDS-PAGE, transferred to nitrocellulose membrane, probed with primary (rabbit anti-STAT1 (Phosphorylated) or rabbit anti-STAT2 (phosphorylated)) and secondary (HRP-conjugated, sheep anti-rabbit) antibodies and assayed for HRP activity. Rabbit anti-Actin served as a loading control. Weak bands are indicated (*).

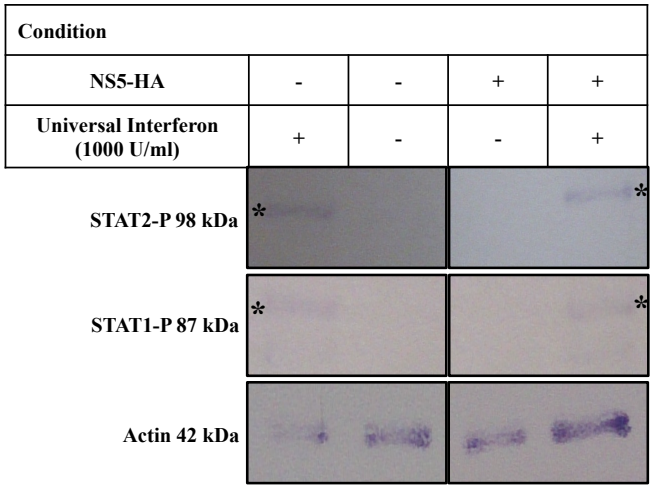

3.5. Developing Antigenome And Subgenomic Clone Systems For High-Throughput Screening Of Antiviral Compounds

Subgenomic clone systems have been created for many flaviviruses; such systems allow study of the replication and packaging aspects of the viral life cycle, along with the testing of antivirals and/or small molecules to inhibit those steps. Subgenomic constructs are unable to form virions as the structural genes have been replaced with a reporter gene cassette. However, structural genes can be supplemented *in trans*, thereby generating particles capable of single-round infection. One facet of the replication cycle that cannot be addressed by the subgenomic system is the non-structural (NS) protein composition of the replication complex (RC). In an attempt to define the RC, an antigenome system, similar to the negative-stranded virus minigenome system was developed for KFDV.

As determined in chapter 3.1., VeroE6 (ATCC), BHK-21 (ATCC) cells allowed for efficient KFDV replication, so these cells were selected for antigenome assays. HEK 293T (ATCC) cells were also included because of their high transfection efficiency (Gaynor et al. 1984). Each cell line used was transfected with the plasmids to transcribe the antigenome (3′ UTR-GFP-5′ UTR), under either the T7 RNA polymerase (pTM1 backbone) or human polymerase I (pPOL backbone) promoters. Along with both antigenome clones, all seven NS proteins from individually-expressed plasmids (NS1, NS2A, NS2B, NS3, NS4A, NS4B and NS5) or all seven NS proteins, expressed as a polyprotein (E_{23}-NS1-NS2A-NS2B-NS3-NS4A-NS4B-NS5) were also transfected, thus mimicking a natural infection or life cycle step. There was no GFP production after incubation at 37^{o}C/5% CO_2 for 24 or 48 hours. The same

experiments were performed with the luciferase reporter antigenome constructs (3′ UTR-Luciferase-5′ UTR), which did not give readings above background levels (Table 3.5.1). Since this system follows the negative-stranded minigenome system, virus infection can replace the need for transfection of the genes for the proteins needed for RC, driving replication and ultimately expression of reporter genes (Feldmann et al. 2004; Brown et al. 2012; Groseth et al. 2005). The transfections of both KFDV antigenome-promoter clones with GFP and luciferase were repeated, and 24 hours post-transfection, the cells were infected with KFDV at different MOIs and evaluated for reporter expression at 24, 48 and 72 hours post-infection. Regardless of virus infection, GFP expression was not detected and the luciferase signal did not exceed background levels (Table 3.5.1). In order to address if antigenome replication into positive/nascent genomes with all seven NS proteins was indeed occurring, RNA was extracted and two-step RT-PCR was performed in search of the positive-stranded genome RNA, 48 hours post-transfection of BHK-21 cells. Positive-stranded RNA was detected, as indicated by the PCR product of ~ 1.2 kb which was similar to the AG-luciferase-pTM1 PCR-positive control. The samples without the transfected NS proteins did not display a band, indicating that antigenome replication had not occurred (Figure 3.5.1.).

A second assay uses *in vitro* T7-driven transcription of the subgenomic RNA, this was then transfected at 2.5 µg and 5 µg into BHK-21 (ATCC) cells and evaluated for luciferase enzyme activity. Spanning the collection time points of 12, 24, 36 and 48 hours post-transfection, cells that were transfected with the subgenomic RNA (2.5 µg) gave a gradual increase in luciferase values, reported as raw light units (RLU) in $\log_{10}$ scale. Light production at intensities of 3.5 and 3.9 RLU were observed at 12 and 48 hours, followed by a peak of 4.8 RLU at 36

hours, then a decline (4.2 RLU) at the termination point of 48 hours post-transfection. The single-peaked trend was not seen in transfection experiments using 5 μg of RNA. In this case, values fluctuated between 4.7 and 5.7 RLU (Figure 3.5.2.a.). The in-frame NS5 deletion subgenomic control RNA demonstrated initial luciferase values at 12 hours of 3.0 and 2.4 RLU for cells transfected with 2.5 and 5 μg of RNA respectively, followed by decreases of nearly a log until the end of the study (48 hours) (Figure 3.5.2.a.). Thus the expression of the genes on the transfected RNA was optimal with the full-length NS5, as expected.

An RT-PCR based study was used to verify that the subgenomic RNA (positive-sensed) was being replicated into its antigenome-counterpart. The results indicated that replication had occurred by 2 and 6 hours post-transfection, but only in one of the duplicate samples as indicated by the 1.5-kb band (Figure 3.5.2.b.). The mock-transfected controls and the NS5 frame-shift mutated subgenomic RNA did not display the 1.5-kb band at either 2 or 6 hours in either of the duplicate samples. Taken together, the data suggest that the subgenomic RNA becomes replicated by the RC proteins and this may happen within 2-6 hours post-transfection.

Table 3.5. Antigenome Assay Summary.

Antigenome Plasmid	Promoter Type	Reporter Gene	Rescue From Replication Complex Delivered By Plasmid		Rescue From Replication Complex Delivered By Virus	
			Individual (NS Proteins)	Polyprotein (NS Proteins)	MOI 1	MOI 0.1
AG-GFP-pTM1	T7	GFP	-	-	-	-
AG-GFP-pPOL	RNA Polymerase I	GFP	-	-	-	-
AG-Luciferase-pTM1	T7	Luciferase	-	-	-	-
AG-Luciferase-pPOL	RNA Polymerase I	Luciferase	-	-	-	-

Figure 3.5.1. Antigenome System Verification Of Replication. AG-Luciferase-pTM1 was transfected in duplicate samples along with seven individual plasmids, each encoding one of the NS proteins in pCAGGS expression plasmids and the T7-RNA polymerase-pCAGGS plasmid in BHK-21 cells. Cells were lysed after incubation for 48 hours and extracted RNA was subjected to two-step RT-PCR. The AG-Luciferase-pTM1 DNA plasmid was used as a control for second step PCR. Lane 1: 1 kb Plus DNA ladder, Lane 2: water control, Lanes 3 and 4: duplicate antigenome samples without RC complex, Lane 5: DNA plasmid positive control, Lane 6: mock-transfected cells, Lane 7: space, Lane 8: 1 kb Plus DNA ladder, Lane 9: water control and Lanes 10 and 11: duplicate antigenome samples with RC complex. The flavivirus genome replication scheme is depicted and includes the transfected "input" genome and the subsequently replicated genome "detected" marked accordingly.

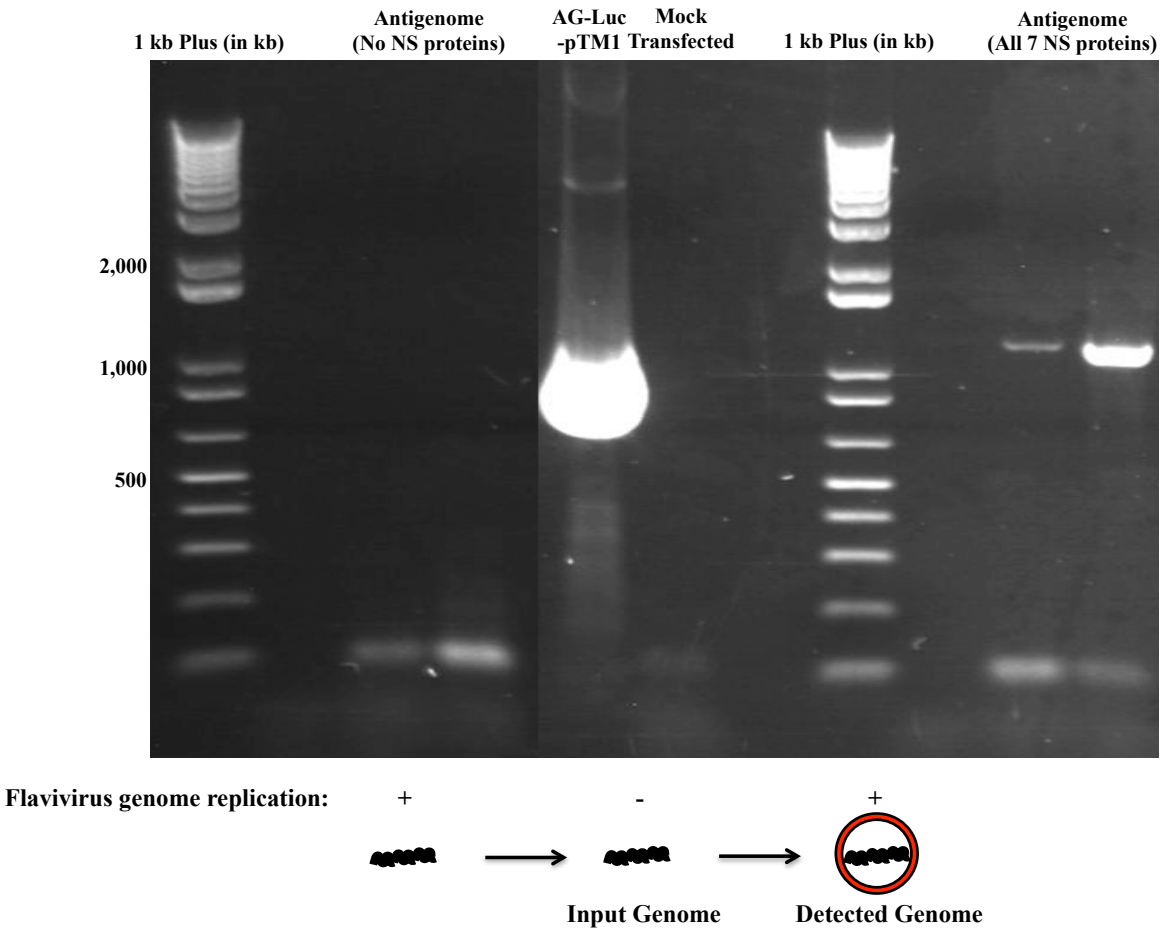
1 kb Plus (in kb)
Antigenome
(No NS proteins)
AG-Luc
-pTM1
Mock
Transfected
1 kb Plus (in kb)
Antigenome
(All 7 NS proteins)
2,000
1,000
500
Flavivirus genome replication:
+
-
+
Input Genome
Detected Genome

Figure 3.5.2. Subgenomic Clone Assay And Verification Of Replication. (a) RNA generated from *in vitro* transcription of SG-Luciferase-pTM1 clone and the control RNA from the truncated NS5 version of the SG-Luciferase-pTM1 clone, were transfected at 2.5 µg and 5 µg into BHK-21 (ATCC) cells. Monolayers were lysed, and luciferase assays were performed at 12-hour intervals. The averages and standard deviations from the mean are presented from three technical replicates of each of three biological replicates for 2.5 µg, and one biological replicate with luciferase assayed in triplicate for 5 µg samples. **(b)** Monolayer lysis, RNA extraction and two-step RT-PCR for detection of replicated antigenome of KFDV at 2 and 6 hours post-transfection. The KFDV subgenomic clone (SG-Luciferase-pTM1 DNA plasmid) was used as a control for second step PCR. Lanes 1 and 6: duplicate 6 hour subgenomic RNA, Lanes 2 and 10: duplicate 2 hour subgenomic RNA, Lanes 3 and 7: duplicate NS5 deletion (Δ) RNA, Lanes 4 and 8: duplicate 2 hour NS5 deletion (Δ) RNA, Lane 5: 6 hour mock-transfected RNA, Lane 9: 2 hour mock-transfected RNA, Lane 11: water control, Lane 12: DNA plasmid positive control, Lane 13: space and Lane 14: 1 kb Plus DNA ladder. The flavivirus genome replication scheme is depicted and includes the transfected "input" genome and the subsequently replicated genome "detected" marked accordingly.

(a)

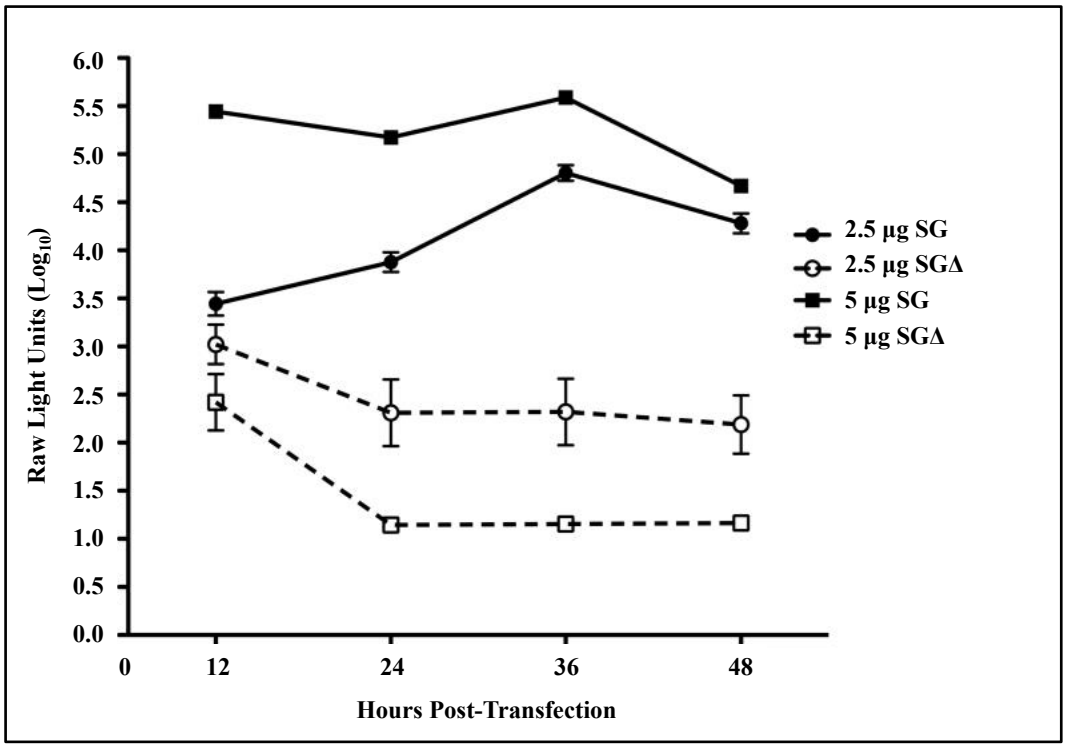
6.0
5.5
5.0
4.5
4.0
3.5
3.0
2.5
2.0
1.5
1.0
0.5
0.0
Raw Light Units (Log10)
0
12
24
36
48
Hours Post-Transfection
2.5 µg SG
2.5 µg SGΔ
5 µg SG
5 µg SGΔ

(b)

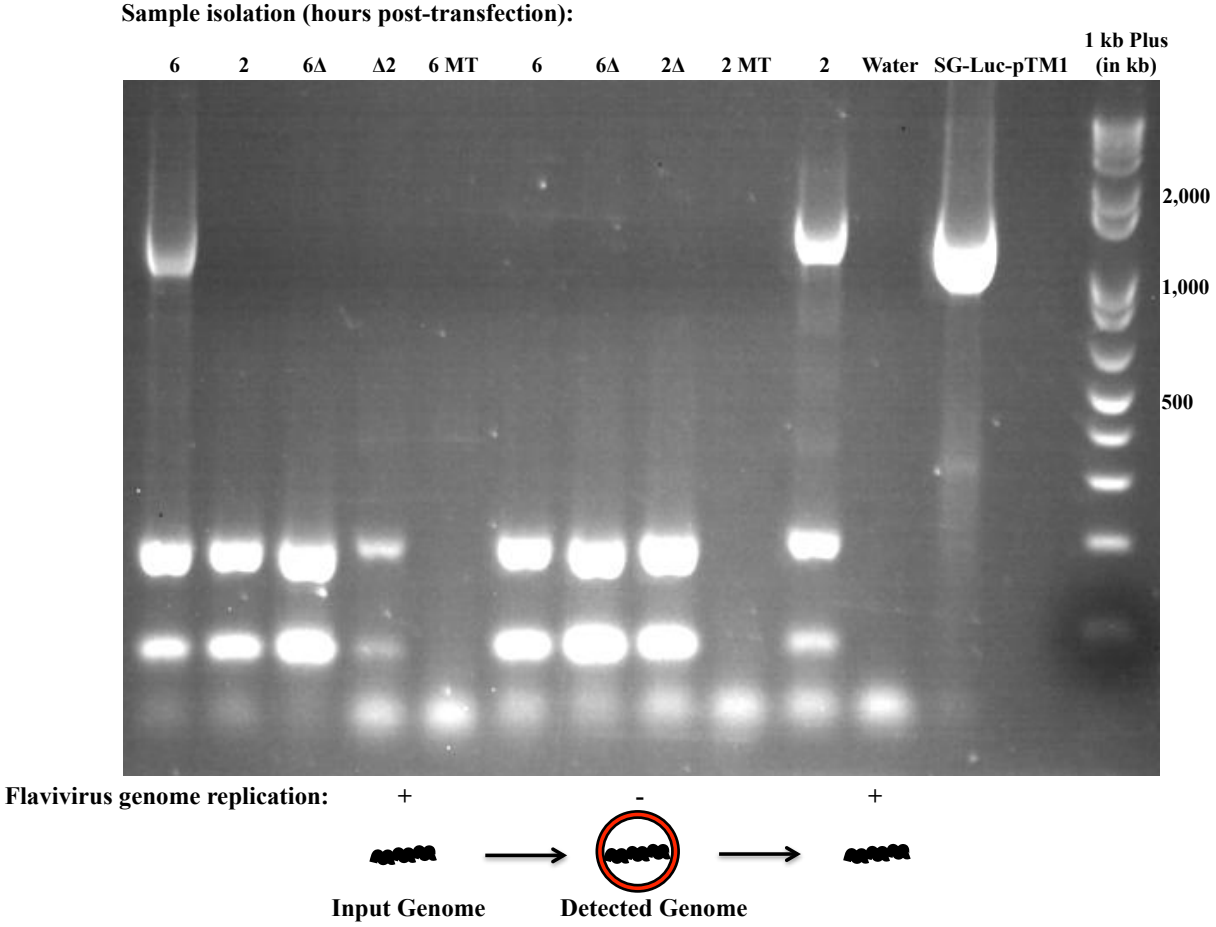
Sample isolation (hours post-transfection):
6
2
6Δ
Δ2
6 MT
6
6Δ
2Δ
2 MT
2
Water
SG-Luc-pTM1
1 kb Plus (in kb)
2,000
1,000
500
Flavivirus genome replication:
+
-
+
Input Genome
Detected Genome

Chapter 4. Discussion

4.1. Monitoring Kyasanur Forest Disease Virus Infection In Tissue Culture

Since various cell lines have been used for KFDV research, we sought to determine which mammalian cell lines are suitable for CPE development and virus propagation. The experiments were not fully inclusive of all of the previously tested cell lines (described in chapter 1.1); however, we discovered that VeroE6 (ATCC) and BHK-21 (ATCC) were adequate for our research endeavours. The possibility remains that the other cell lines previously reported in KFDV research may be just as capable of producing high virus titres and clear CPE manifestations, such as those we have observed in our experiments with A549 cells (chapter 3.3.). Hopefully other cell lines can be evaluated in this same context, including A549 in future studies. Additionally, we were unsuccessful at obtaining a kidney cell line (MRK-90) from the red-faced bonnet (*Macaca radiata*) monkey (Gogate et al. 1996). It would have been interesting to see how the cell line responded to KFDV infection, as the red-bonnet monkey is naturally and experimentally susceptible and, succumbs to KFDV disease (Webb & Chaterjea 1962; Shah et al. 2012).

The commercially obtained cell lines VeroE6 (ATCC) and BHK-21 (ATCC), behaved differently when compared to the VeroE6 and BHK-21 laboratory strains for KFDV-induced CPE. It is unclear why such pronounced differences existed since the same medium formulations and same passaging procedures were used in all. This is especially true with the BHK-21 lab strain, which generated very acidic medium throughout the infection study, most notably by 4

days post-infection. It may be possible that the lab stock of BHK-21 cells may be contaminated with mycoplasma, resulting in delayed or poor growth. There are a few methods to determine if mycoplasma is the culprit, such as Hoechst DNA staining, culturing on solid agar plates and genetic-based (PCR) methods (Chernov et al. 2014). For our purposes, we opted not to complete the diagnostic testing and to proceed with the commercial BHK-21 (ATCC) stock for KFDV propagation and for $TCID_{50}$ assays for the antiviral properties of IFN (section 3.3.) and prospective antiviral trials.

4.2. Developing A Reporter System With Green Fluorescent Protein (GFP) Inserted Into The Full-Length, Infectious KFDV Genome

The attempts to use three independent methods to utilize GFP as a reporter embedded into the full-length genome of KFDV were unsuccessful. There are many reasons as to why this may have failed. The inability to rescue the recombinant-reporter flaviviruses, such as with our case, has been seen before with dengue virus. However, the authors were able to detect GFP and virus proteins, but with no virion release (Leardkamolkarn et al. 2012). During KFDV-GFP rescue attempts, there were no indications of either GFP fluorescence or CPE in our experiments; however replication and translation of viral proteins/GFP were not assessed because the final, detectable output of the system was the critical component. The GFP appears to be the cause of the failure because all three full-length KFDV-GFP clones were generated using the same plasmid construct as the RGS system, which is the only system to genetically manipulate and successfully recover KFDV (Cook et al. 2012). The assumption here for KFDV-GFP is that

expression of both viral protein and GFP are negatively impacted, especially since the GFP protein would be translated as part of the polyprotein and would need to be subsequently cleaved by the viral protease. It cannot be excluded that transcription from the T7 promoter on the reverse genetics system/GFP fusion backbones did not occur, or that premature termination occurred in or near the GFP coding sequence, or that the resulting RNA was less stable. Interestingly, it has been proposed that GFP-encoding RNA region may have secondary structures which may be problematic for proper or efficient translation from the full-length dengue virus polyprotein resulting in delayed virus production and GFP mutations (Zou et al. 2011). These possibilities were not investigated further, because even if transcription and translation of viral proteins occurred, the lack of GFP and CPE would still represent a lack of success, as the goal was to have infectious virus with a stable GFP reporter. It is interesting that many flavivirus GFP reporter clones, despite using different methodologies, did generate recombinant virus, even though the virus was attenuated and the reporters eventually became unstable (McGee et al. 2010; Pierson et al. 2005; Bonaldo et al. 2007; Zou et al. 2011). These observations may justify the examination of other reporter genes that may have less problematic secondary RNA structures, such as firefly or *Renilla* luciferases and chloramphenicol-acetyl-transferase (CAT), rather than new GFP inclusion strategies.

An alternative to using any of these reporter genes in flavivirus genomes could be the stable transfection of the GFP reporter gene into cells, in which case KFDV replication can still be determined empirically, as reporter expression would decrease as CPE and cellular destruction proceeds. This may be the more ideal option, as all reporter genes regardless of

cloning methodology attenuated the flaviviruses in cell culture and reporters were not permanently maintained.

A reporter-expressing KFDV would have aided in the IFN assays and for future antiviral testing. Without this reporter, subsequent IFN experiments (section 3.3.) utilized classical CPE and virus titre production.

4.3. Analyzing The Capabilities Of IFN-α2a And Other IFN-α/β Species To Restrict KFDV Propagation

Interferons, specifically IFN-α2a and IFN-α2b, have been used as treatments for many different viral diseases, most notably those caused by hepatitis B and C viruses (Pestka 2007). The use of IFN as a treatment against numerous flaviviruses in clinical settings has had variable success and some patients still developed long-term sequelae from the central nervous system involvement of these encephalitic viruses (Solomon et al. 2003). The antiviral nature of each IFN-α/β species was pursued in the hope of finding a strong repressor of KFDV virion production.

The application of 2000 U/mL, more than double the reported IC_{50} of IFN-α2a (863 +/- 450 U/mL) against KFDV (Flint et al. 2014) was unable to clear KFDV infection in either A549 or BHK-21 cells. This was in contrast to the situation observed with cells that were infected with IFN-sensitive VSV-GFP. The lack of impact on virus production during IFN treatment led us to believe that the KFDV isolate used was inherently able to overcome the IFN effects. Since nucleotide polymorphisms were not observed through Sanger sequencing of the IFN-insensitive

virus, it is apparent that no amino acid changes within the polyprotein were needed for this resistance phenotype. In summation, the evidence suggests that KFDV avoidance of the antiviral state induced by IFN is an inherent property of the virus. As described in section 3.4., the NS5 protein provides this ability for KFDV to overcome the antiviral effects of IFN. Much like the antiviral state-induced by IFN, the natural cellular breakdown and nutrient recycling process known as autophagy can be triggered by the Jak/STAT pathway, as Jak/Tyk2 will activate the phosphatidyl-inositol-3-kinase class 3 (PI3K)/Akt/mTORC1 pathway rather than the STAT1/2 proteins (Kaur, Sassano, Joseph, et al. 2008; Kaur, Sassano, Dolniak, et al. 2008). Flaviviruses such as dengue (McLean et al. 2011; Samsa et al. 2009) and Japanese encephalitis (Li et al. 2012) viruses, are thought to take advantage of autophagy compartments, preventing apoptosis and prolonging cell survival for long term virus replication. While it is tempting to speculate that KFDV may be using autophagy when IFN is present and reverting back to virus-induced apoptosis when IFN is absent resulting in CPE development (Figure 3.3.1.c. and d.), further studies are certainly required for confirmation of this speculation.

IFN has been delivered in tissue culture and in pre and post flavivirus-exposure scenarios. In the literature IFN pre-infection treatment of cells (24 to 2 hours before infection) delivers stronger repression against flavivirus challenge than in post-exposure (2-24 hours after infection) IFN treatment (Anderson & Rahal 2002; Best et al. 2005; Daffis et al. 2011; Samuel & Diamond 2005). In contrast to the reports in the literature, our experiments suggest that 1-hour post-exposure IFN treatment was more effective than a 24 hour-pre-infection treatment at repressing KFDV titres. Perhaps this highlights a time-dependence relationship not only for the establishment, but for the duration of the antiviral state and ISG production (Hoffmann et al.

2015). Regardless, the results of chapter 3.3.2., demonstrate that 1 hour post-infection is suitable to eliminate the IFN-sensitive VSV-GFP control virus production from A549 cells. Thus, it is clear that IFN-α2a was not enough to quell KFDV infection. It is apparent that IFN-αWA and IFN-αK were more potent than IFN-α2a and IFN-α2b in post-exposure application. Varied antiviral actions by the IFN-α/β species are not surprising and has been previously described for many viruses (Sperber et al. 1992; Lavoie et al. 2011). The causes for such variation are still unknown, but are thought to be due to binding affinities of IFN to its receptors or the subsequent expression of potentially species-specific antiviral ISGs (Lavoie et al. 2011) or unequal or specific ISG activity on different viruses (Hoffmann et al. 2015). With respect to flaviviruses, such specificity was seen with TRIM79α. This ISG restricted the propagation of tick-borne but not mosquito-borne flaviviruses by targeting NS5 for degradation (Taylor et al. 2011), thereby demonstrating the utility of screening the over 350 known ISGs such as with the many flaviviruses (Schoggins et al. 2011), but looking for KFDV-specific antiviral ISGs. Besides the Jak/STAT pathway, it should be noted that there are other IFN-induced pathways besides Jak/STAT and PI3K, including cGAS/STING (Schoggins et al., 2014) and IRF-1 (Robertson et al. 2014), which may potentially lead to variable antiviral responses to IFN in different cell lines. Paradoxically, certain ISGs appear to promote replication of yellow fever and West Nile viruses (Schoggins et al. 2011). Additionally an ISG, IRF-1 demonstrated specificity to mosquito-borne and tick-borne flaviviruses (Robertson et al. 2014) and is thought to be independent of IFN-based signalling by a "unique antiviral program" (Schoggins et al. 2011). Although ISGs were not addressed in this study, it would be interesting to determine if KFDV replication can be enhanced by certain ISGs, thus curtailing the effects of the inhibitory ISGs.

Since a single dose of IFN was used for the initial experiments described in this thesis, dose-series concentrations of IFN-αWA and IFN-α2a were tested and the results indicated that there were marked differences between cellular protection and the titre of virus production with respect to KFDV. Our methodology for assessing cell protection from CPE by staining may not be entirely reflective of cell viability. However, this approach was chosen over metabolic assays because of a lack of equipment inside of the CL-4 containment facility and because traditionally crystal violet staining has been used for IFN potency assessment through protection from the damage represented by CPE (Meager 2002; Voigt et al. 2013). Recent comparisons of dye-uptake methods for measuring CPE and metabolic assays with reporter gene-expressing viruses have demonstrated that the latter is the better method with respect to ease of use, sensitivity and minimized background signals (Berger Rentsch & Zimmer 2011; Voigt et al. 2013). The crystal violet staining data imply that the higher the IFN dose applied, the less cellular destruction occurs, suggesting that the propagation of KFDV and VSV-GFP was restricted by IFN. However, the lack of CPE observed with IFN treatment did not reflect a repression of KFDV virion release. The toxic effects of IFN were ruled out because at the highest concentrations tested (16, 000 U/mL) very low levels of cytotoxicity were observed. The presumption that the CC_{50} is much greater than 16, 000 U/mL agrees with the literature, as the CC_{50} of IFN in A549 cells was found to be greater than 160, 000 U/mL (Flint et al. 2014). Interestingly, this same report demonstrated a wide range of IC_{50} values for the IFN-α2a treatment for many tick-borne flaviviruses in cell culture. These IC_{50} values were lowest for Powassan virus (7.8 U/mL) and Omsk hemorrhagic fever (135 U/mL) viruses and, highest for Alkhumra hemorrhagic fever (684 U/mL) and KFD (863 U/mL) viruses (Flint et al. 2014), thereby demonstrating the variability

inherent with IFN treatment of tick-borne flaviviruses and lends credence to the KFDV response to IFN in this work. In comparison to the reported IC_{50} for KFDV of 863 U/mL, this thesis (section 3.3.3.) uncovered an IC_{50} of 7.4 U/mL. Flint *et al*. had used a metabolic assay for cell viability for IC_{50} value determination, perhaps that may account for the value differences. Overall, the determination of the titre reduction as a measure of IFN activity is more definitive as a measure of the antiviral impacts of IFN, as virus production is the best measure of IFN potency.

In clinical settings, IFN-α (2a or 2b) is commonly injected via the intravenous route and serum concentrations can vary from 100-750 U/mL (Falzarano et al. 2013). Our experiments suggest that those serum concentrations of IFN may not be high enough to achieve favourable outcomes for patients afflicted with KFDV. Moreover, the high doses needed to maintain these concentrations in the body is between 10-20 Million units per day and this will certainly worsen the side effects of IFN (Pestka 2007; Sleifer et al. 2005), potentially intensifying patients' symptoms. Despite the fact that IFN-α2a and α2b have been used with varying success rates against many flavivirus infections in humans (Chan-Tack & Forrest, 2005; Kalil et al., 2005; Rahal, Anderson, Rosenberg, Reagan, & Thompson, 2004; Solomon et al., 2003), the *in vitro* data obtained in this work for KFDV would indicate that IFN alone may not be adequate as a treatment in human cases.

4.4. Investigation Of The Anti-Interferon Activity Of KFDV

The ability to circumvent the Jak/STAT pathway and prevent the establishment of the cellular antiviral state has been attributed to the NS proteins of flaviviruses. The two major

proteins involved are the cleavage precursor NS4B-2k (Laurent-Rolle et al. 2010; Liu et al. 2006; Munoz-Jordan et al. 2005) and NS5 (Best et al. 2005; Laurent-Rolle et al. 2010; Ashour et al. 2009; Laurent-Rolle et al. 2014). While a few tick-borne flaviviruses have been analyzed in detail, the NS proteins of KFDV and their mechanism have yet to be investigated. The results in section 3.4., would indicate that the NS5 of KFDV is the primary inhibitor of the Jak/STAT signalling cascade in response to IFN treatment (Figure 3.4.1.). Overall, these experiments and the results obtained were similar to those found with dengue, yellow fever, Langat, West Nile, tick-borne encephalitis and Japanese encephalitis viruses (Best et al. 2005; Laurent-Rolle et al. 2010; Ashour et al. 2009; Laurent-Rolle et al. 2014). The potency of NS5's anti-IFN-α/β activity is highlighted by its ability to allow VSV-GFP replication in the presence of IFN, despite the fact that this virus is very sensitive to the effects of IFN. The presumption that this observation is indicative of interference caused by NS5 on the Jak/STAT pathway is primarily due to the fact that the luciferase gene from this assay is driven by the enhancer element (ISGF3) required for Jak/STAT pathway signalling. Therefore, luciferase protein expression cannot occur without the activation, nuclear translocation and promoter enhancement of STAT1/2, again suggesting that NS5 stops this signalling cascade. While it is tempting to speculate that the VSV-GFP assay works solely by Jak/STAT-induced ISG expression to eliminate VSV-GFP propagation, other pathways like the PI3K signalling cascade (autophagy pathway) and IRF-1 can also induce ISG production (Randall & Goodbourn 2008). We have not determined how these pathways may influence KFDV infection or NS5 counteraction; however future studies including genetic-based studies to determine if KFDV can alter Jak/STAT, PI3K and IRF-1 pathways would be very informative. This is because many flaviviruses can take advantage of the PI3K signalling cascade

for enhancing cell survival and promoting their long term replication (Ghosh Roy et al. 2014) and tick-borne flaviviruses (Tick-borne encephalitis and Langat viruses) have been shown to prevent IRF-1 signalling through the NS5 (Robertson et al. 2014).

Aside from the complexity of these signalling cascades and how they can impact flaviviruses, the NS5 protein has been found within the nucleus of infected cells and is thought to aid in virulence (Kapoor et al. 1995; Uchil et al. 2006). It has been speculated that it acts as an enhancer for expression of chemokines such as IL-8, thereby exacerbating vascular leakage during dengue virus hemorrhagic fever manifestations (Medin et al. 2005; Talavera et al. 2004). The potential for KFDV to alter the antiviral properties of IFN and perhaps promote hemorrhaging is a very interesting research avenue.

Further examination of the regions of NS5 that are responsible for Jak/STAT interruption suggested that the MTase (variant 223, deletion of residues 224-431) and the RdRp (variant 431, removal of residues 432-742) domains were important. Minor pathway inhibition was seen with the variants 6 and 55, which had amino acids 1-5 and 6-54 removed respectively. There is a possibility that these actions are due to the alteration to the NS5's overall three-dimensional structure resulting in varied anti-IFN actions or perhaps they are due to the differential expression of the NS5 mutants as seen in western blots (Figure 3.4.2.1.a.). There is evidence that the full-length NS5 protein can be separated into its individual domains; both the MTase (~ 1-296 amino acids) (Egloff et al. 2002) and RdRp (~ 273-900 amino acids) (Yap et al. 2007) have been individually cloned, expressed, crystallized and successfully assayed for their respective enzymatic properties. It should be noted that the amino acids that make up the nuclear localization signal (residues 315-415), occur within a proposed interface between MTase and

RdRp, which contains the hydrophobic interactions necessary for stabilizing the overall NS5 structure (Yap et al. 2007); this may have led to the results seen with variant 223, which lacks amino acids 223-431). If this segment is essential for the generation of the three-dimensional structure of NS5 and the full enzymatic activity of the RdRp, then the apparent inability of variant 223 to display anti-IFN activity as detected by the expression of the luciferase reporter in the presence of variant 223 (Figure 3.4.2.1.) is expected. However, there was a reduction in virus titre, suggesting that the remainder of the protein still retains some anti-IFN activity. Moreover, this would imply that the other mutations including variant 432 (lacking amino acids 432-742), might be legitimate with respect the luciferase and VSV-GFP assays, since the NLS would be intact. The folded state of all of the variants remains to be determined; however the partial anti-IFN activity of some variants implies that some structural elements are correctly folded. However the data from section 3.4., indicate that optimal anti-IFN effects of NS5 require the MTase and RdRp, as only the carboxyl terminal amino acids 743-903 are dispensable. It should be noted, however, that the expression levels of the variants were not uniform (Figure 3.4.2.1.a.). The differences in activity as detected by luciferase induction and VSV-GFP recovery by variants 6, 223 and NS5 perhaps can be compared, as the expressed protein levels appear to be relatively similar.

Immunoprecipitation of the NS5 did not hint at any strong physical interactions with the Jak/STAT proteins or any other cellular proteins. Previously reported NS5 protein-protein interaction studies demonstrated that NS5 with C-terminal HA and V5 tags could interact with the IFNAR and STAT2 (Best et al. 2005; Laurent-Rolle et al. 2014). Therefore it would seem unlikely that this tag would inhibit protein-protein interactions, as this type tag and its location

on the C-terminus of NS5 was similar to that used in previous studies (Laurent-Rolle et al. 2010; Best et al. 2005; Ashour et al. 2009). Cellular lysis and protein binding were carried out under conditions of low salt and in the presence of a non-ionic detergent, which would favour the maintenance of protein-protein interactions. It should be noted that the co-immuno-precipitated STAT2 and IFNAR in the other studies were detected by western blotting; it is likely that Coomassie staining was not sensitive enough for detecting binding partners. As alternatives, the more sensitive silver or fluorescent stains should be considered in future experiments (Andreou 2013) as an addition to western blotting. Improved detection methods might also reveal potential chaperone proteins acting to link NS5 with a Jak/STAT pathway protein. This would be similar to dengue virus' NS5 using UBR4 to bind to and degrade STAT2 (Morrison et al. 2013; Ashour et al. 2009). Ideally, over-expression of Jak/STAT pathway proteins (near levels similar to that of NS5) could lead to ease of resolving by gel staining, since insufficient amounts existed. Furthering this thought, tandem or dual-tagged NS5 and the Jak/STAT pathway proteins would certainly lead to an increased likelihood of co-immunoprecipitation.

The phosphorylation of STAT1/2 (Figure 3.4.2.2.) is indicative of a functioning Jak/STAT pathway. Although the fractions of phosphorylated STAT1 and STAT2 could not be determined from these experiments, it does not appear that NS5 completely inhibits those phosphorylation events. In addition, the interruption of STAT1/2 dimerization and translocation into the nucleus may be occurring. Although binding of NS5 with STAT1 or STAT2 was not observed and the presence of the phosphorylated versions would indicate that neither had become degraded. Another mechanism by which NS5 could block the effects of IFN is by stopping the interaction of IRF-9 with the STAT1-STAT2 dimer or preventing the ISGF3

(STAT1-STAT2-IRF-9 trimer) from binding to the promoter of ISGs. This speculation has potential, since high amounts of NS5 have been shown to be in the nucleus of infected cells (Davidson 2009) and the NS5 of yellow fever virus prevents ISGF3 binding on ISG promoters (Laurent-Rolle et al. 2014). Immunofluorescence microscopy or western blotting of nuclear fractions may aid with investigating this speculation. Additionally, precise deletion of the NLS signals on NS5 could aid in determining whether the blockage of Jak/STAT signalling is in the later, nucleus-associated stages of the pathway.

In summary, the results presented in this thesis indicate that IFN may not be an adequate antiviral for post-exposure treatment of KFDV infections, as evidenced by whole virus infections (section 3.3.) and with NS5 transfections (section 3.4.). Thus, other antivirals should be examined for their ability to treat KFDV infections.

4.5. Developing Antigenome And Subgenomic Clone Systems For High-Throughput Screening Of Antiviral Compounds

Replication-based reporter systems for KFDV were attempted using two designs: an antigenome system based on the negative-stranded RNA virus and a subgenomic clone, which is used for many positive-strand viruses. Unfortunately the antigenome system failed to produce reliable or repeatable reporter gene expression. Many factors could have contributed to this failure. The most obvious is failed or insufficient expression or the assembly a functional RC, since many plasmids were needed for this assay. While antibodies were not available for these proteins, NS5 fused to a C-terminal HA tag was successfully expressed (section 3.4.). Since the

same plasmid and cloning strategies were used for all of the RC complex proteins, it can only be assumed that expression does occur and should be similar to that of NS5-HA. Of course, this assumption should be tested, possibly by adding epitope tags to all of the other proteins. However, it is not known if the tags would impede their RC formation or their replicative activities. Moreover, the system did appear to work with respect to antigenome replication into the positive-stranded nascent genome, again implying that RC expression did occur. However despite this apparent replication, a signal (GFP or luciferase) was not detected. Thus regardless of the reason, the system ultimately failed. Even more striking was that upon KFDV superinfection, above-background signals were still unattainable. Taken together, the data would imply that the system, besides becoming expressed and replicated, either through RC complex added via transfection or by virus superinfection, was unable to express the reporter gene to significant levels. This result is somewhat similar to a recent Andes virus minigenome system in which GFP and luciferase both failed as reporters even with superinfection, however the chloroamphenicol acetlytransferase (CAT) reporter system did succeed (Brown et al. 2012). Another factor could be the size of the KFDV RNA (10.8 kb) versus the smaller length of the antigenome (1.4 kb for GFP and 2.3 kb for luciferase) as it relates to circularization. This is unlikely, since the circularization sequences contained in the RNA of C, 5′ and 3′ UTR regions were included in the antigenome system. In addition, studies have indicated that RdRp activity on similar sized truncated dengue virus genomes is comparable to those of the full-length genomes, as long as the 5′ and 3′ UTRs are present (Filomatori et al. 2006).

The luciferase activity detected from the subgenomic clone system would suggest that the system was successful. It is clear from time course studies that the trends in reporter signals do

vary with the quantity of RNA transfected (Figure 3.5.2.a.). The KFDV subgenomic clone data straddle that of other flavivirus systems. The data obtained using 5 µg of subgenomic RNA resembles that of Japanese encephalitis (Li et al. 2013) and dengue virus (Filomatori et al. 2006) reporter systems in which luciferase was observed in two peaks, at 12/24 hours and from 36/144 hours post-transfection of BHK-21 cells. Interestingly, other flavivirus systems behave differently with a steady and gradual increase to generate a single peak and the maximum peak time post-infection can vary from 36 hours [yellow fever virus (Jones et al. 2005)], 48 hours [West Nile virus (Moritoh et al. 2011)] and 72 hours post-transfection [Omsk hemorrhagic fever virus (Yoshii & Holbrook 2009)]. This result mirrors the data obtained using the 2.5 µg of subgenomic RNA, as a single peak at 36 hours was observed. It stands to reason that two peaks may still be occurring with these systems; perhaps, the lysis and signal detection were assayed after the first peak (before the typical 12 hours post-transfection time point). This is possible since, initial reporter gene expression would begin upon transfection, as translation is the first step of genome replication in flaviviruses (Chambers et al. 1990). The antigenome was detected by 2-6 hours post-transfection suggesting that translation and replication can occur early once the RNA enters the cytoplasm. Although the amount of antigenome generated was never quantified, antigenomes are in very small quantities (ratio of 1 antigenome for every 100 nascent genomes) as they are used as templates for nascent genomes (Davis et al. 2007). The exact time frames for virus binding, replication and virion egress is difficult to fully extrapolate from the literature, but flavivirus binding, fusion and uncoating, are thought to occur within 1 hour post-infection (De Burghgraeve et al. 2012; Ichiyama et al. 2013) with virion release beginning from 8-10 hours post-infection (Brinton 2014). If true, it is therefore conceivable that translation and replication,

albeit at very low levels, can occur within 2-6 hours post-transfection as both processes are thought work in a concerted manner (Harris et al. 2006).

Transfection efficiency may be another concern, as displayed by variable luciferase value per input RNA concentrations and antigenome RNA detection in 1 of 2 replicates for both the 2 and 6 hours post-transfection time points. Indeed electroporation and liposome-mediated transfections with a wide range of subgenomic RNA concentrations have been used in the other flavivirus subgenomic clone systems. These factors can certainly play a role in subgenomic RNA replication and reporter signal production and should be considered for optimization of the subgenomic clone system for KFDV.

Thus, the generation of a subgenomic clone system for KFDV was successful and will permit investigation of antivirals against KFDV without the need for a CL-4 laboratory for initial screening. Any promising antiviral "hits" should be followed up with validation against the virus in high-level containment.

Chapter 5. Overall Conclusions And Future Perspectives

With a devastating and continuing ebola virus outbreak in West Africa, other viral hemorrhagic fever viruses, while being over-shadowed at the present time should not be ignored. Flaviviruses, most of which are arthropod-borne, have a global presence and in some instances have moved from localized-endemic areas into newer locations (Go et al. 2014; Gould et al. 2004). With respect to KFDV, prime examples have already been demonstrated with the movement to new districts within Karnataka state and even further into the neighboring states of

Kerala, Tamil Nandu and Goa (Mourya et al. 2013; Tandale et al. 2015; ProMED-mail 2015). Additionally, KFDV's closest relative, Alkhumra hemorrhagic fever is no longer contained in Saudi Arabia but appears to present in Egypt (Carletti et al. 2010; Ravanini et al. 2011; Musso et al. 2015). The factors that are vital for arthropod-borne viruses to establish and exploit a new naïve region are: arthropod vector competence, vertebrate reservoir susceptibility and being able to survive during winter or dry seasons (Calisher 2000). With regards to India and KFDV issues promoting the merger of forest-dwelling vectors and reservoir animals with human habitats include climate change, deforestation and urbanization and, increased agricultural practices (Singh & Gajadhar 2014; Stone 2014).

The important work presented in this thesis will aid in the pursuit of antiviral research for KFDV. The findings of appropriate cell lines for propagation and infection characteristics and, the subgenomic clone system are major developments to that end. The failure of the KFDV GFP-reporter virus, while disappointing is similar to that reported by others and supports the notion that maintenance of a stable GFP reporter within flavivirus genomes may be futile. Since IFN is a common antiviral and has been successful for combatting flavivirus disease, albeit in a very narrow clinical delivery window, its use for KFDV treatment was a logical pursuit. However, the findings that IFN including the clinically approved species IFN-α2a, cannot clear KFDV in cell culture prompted investigation into other IFN-α/β species. The comparisons between IFN-αWA and IFN-αK with IFN-α2a demonstrated that the two former IFN species may be better suited for treating KFDV infection. This perhaps should be evaluated further in animal models to determine if there are any clinical benefits. However the finding that the NS5 of KFDV can weaken the antiviral properties of any of the IFNα/β species against KFDV via the Jak/STAT

pathway is important, as this may explain, IFN treatment may fail. Since there are no effective treatments, this highlights the relevance of these research tools for the evaluation of other antiviral treatment options for KFDV infection. Future examinations to further the research objectives of this dissertation would be of great benefit to KFDV research, specifically the hunt for successful antivirals. Future work should begin with examination of the replication capabilities of KFDV using more cell lines including primary cells. These cell lines may provide more insight into mechanisms of pathology in local Indian monkey populations and perhaps suspected but yet unproven reservoir animals. Another long-term aim is the generation of a reporter gene-expressing KFDV other than GFP as the reporter; alternatively stable GFP-transfected cell culture could be used. Further insight into the role of NS5 in encouraging replication and pathology perhaps by autophagy and ISG production should be explored. Re-examination of NS5 and its mechanism of Jak-STAT pathway interference should be undertaken and should include the investigation of other IFN-induced pathways like the utilization of IRF-1 and PI3K. Finally, comparing electroporation and liposome-mediated transfection of the subgenomic system will enable optimization and better reliability. The work presented in this thesis will help direct these important future studies by providing a foundation for working on this neglected tropical pathogen.

Appendix.

Table A.1. The Primer Sequences Used For The Molecular Biology Of KFDV. Colored font indicates non-KFDV sequence primer additions.

KFDV Sequencing					
Set A	**Primer Name**	**Sequence**	**Tm (^{o}C)**	**Additions (colored font)**	**Deleted Region**
A1	**KFDseq1s**	**GCGGTCCCCCTAGGCGAGTGC**	**66.9**	**N/A**	**N/A**
A2	**KFDseq2s**	**CCCTTTGCCTGGCTCCTACATA**	**58.6**	**N/A**	**N/A**
A3	**KFDseq3s**	**ACCTGCGATGTGGGCCTTGAAAA**	**64.3**	**N/A**	**N/A**
A4	**KFDseq3.5s**	**ATCATCAGTGGGGAAGGCTCTACA CAC**	**61.5**	**N/A**	**N/A**
A5	**KFDseq4s**	**TCTGTCCTTGCGGCATCTCTAAAA**	**60.3**	**N/A**	**N/A**
A6	**KFDseq5s**	**CCTGGGACTGCGGTTAAGATTGAC**	**61.5**	**N/A**	**N/A**
A7	**KFDseq6s**	**TTGGAGGCGAGGGAGTGGGTCTTA**	**64.5**	**N/A**	**N/A**
A8	**KFDseq7s**	**GGGGTATGGAGCCAAGGGAGTTC**	**62.4**	**N/A**	**N/A**
A9	**KFDseq8s**	**CGGAGAGTGGAGAGTGGGCTTTGA**	**63.5**	**N/A**	**N/A**
A10	**KFDseq9s**	**TTGCAGCCGGTGTGGAAGGACT**	**64.4**	**N/A**	**N/A**
A11	**KFDseq10s**	**GCAGAGGGCGCACAGGGTAT**	**61.1**	**N/A**	**N/A**
A12	**KFDseq11s**	**GCAGAGGCGGGTGGTCATACTACG**	**64.0**	**N/A**	**N/A**
A13	**KFDseq12s**	**TGCGGGAAAGAAAACACCACGACT**	**64.3**	**N/A**	**N/A**
A14	**KFDseq13s**	**AAATGACATGGCCAAGGTGAGAAA**	**59.9**	**N/A**	**N/A**
A15	**KFDseq14s**	**GGCCCCGAGAGGTATGCTGATTAT**	**60.3**	**N/A**	**N/A**

A16	KFDseq1as	GTTTCCCACACCTTCCGTATTCCAGTG	64.7	N/A	N/A
A17	KFDseq2as	CTCGGACTGCGTTGTGAAAGAT	58.4	N/A	N/A
A18	KFDseq3as	ATGCCGCCTACCGAACCGAAGTC	65.4	N/A	N/A
A19	KFDseq3.5as	CCCTCACCACATCGTAGCTCCATCC	64.9	N/A	N/A
A20	KFDseq4as	CACTCCCGTTGCATTCCTGT	57.7	N/A	N/A
A21	KFDseq5as	CCAGCACGAGGAGCAAGAAATAGG	61.7	N/A	N/A
A22	KFDseq6as	ACCAACCCTGCAAGAAGCCATAAC	61.1	N/A	N/A
A23	KFDseq7as	ATGCCCTCTTGCCGCGATACTGTG	66.1	N/A	N/A
A24	KFDseq8as	AGGTCCAGCTCCGATCCAACACAT	63.6	N/A	N/A
A25	KFDseq9as	CACCACTTGCCACTGAACTG	54.1	N/A	N/A
A26	KFDseq10as	ATGGCCTTTCCCTCCTATCGTGTA	60.2	N/A	N/A
A27	KFDseq11as	AAAGGCCGTTGTGTCCGTCAT	60.4	N/A	N/A
A28	KFDseq12as	GTTCGGTGTTCGCCTTCCAGATAA	61.4	N/A	N/A
A29	KFDseq13as	CCTGCGGGACCCAATCAAT	59.5	N/A	N/A
A30	KFD 5UTR-pTM1	GTACACCGGTAGATTTTTTTGCACGTGAGTGCTCTC	70.5	Add AgeI	N/A
A31	KFD 3UTR-pTM1	GTACGGCGCCAGCGGATGTTTTTTCCGAAAC	74.2	Add KasI	N/A

A32	KFDvpVirCs	GTACGAGCTCATGGCCAAAGGAGC	63.5	Add SacI-start codon	N/A
A33	KFDvpVirCas	GTACGGTACCTTACCTTCTCTTCCCTCTTC	61.8	Add KpnI-stop codon	N/A
A34	KFDvpprMs	GTACGAGCTCATGGCGACAGTTCGCAGAGAGAGAACAGG	76.6	Add SacI-start codon	N/A
A35	KFDvpprMas	GTACGGTACCTTAGGCATATGTAGGAGCCAGGCAAAGGG	73.4	Add KpnI-stop codon	N/A
A36	KFDvpEs	GTACGAGCTCATGACACGATGCACACACCTG	70.2	Add SacI-start codon	N/A
A37	KFDvpEas	GTACGGTACCTTAAGCACCAACCCCCAGTGTCATTGTC	73.4	Add KpnI-stop codon	N/A
A38	KFDvpNS1s	GTACGAGCTCATGGATATGGGCTGTGCAATTGATGCTAACAGGATG	78.2	Add SacI-start codon	N/A
A39	KFDvpNS1as	GTACGGTACCTTAGTCAGCCAGCACCATCGACCTCACCAGA	76.6	Add KpnI-stop codon	N/A
A40	KFDvpNS2As	GTACATCGATATGAACGGAGCCATGCTAAGTGAAGGTGGAGTC	75.0	Add ClaI-start	N/A

				codon	
A41	KFDvpNS2 Aas	GTACGGTACCTTACCGTCTGTTCCT TCGCTCGGCAAGCT	76.4	Add KpnI-stop codon	N/A
A42	KFDvpNS2 Bs	GTACGAGCTCATGTCTTTCAGTGAA CCACTGACGGTGGTG	75.7	Add SacI-start codon	N/A
A43	KFDvpNS2 Bas	GTACGGTACCTTACCTTCGCCCCGA GCCCAGC	74.8	Add KpnI-stop codon	N/A
A44	KFDvpNS3 s	GTACGAGCTCATGTCTGAACTTGTC TTCTCTGGA	66.8	Add SacI-start codon	N/A
A45	KFDvpNS3 as	GTACGGTACCTTAGCGACGCCC	60.5	Add KpnI-stop codon	N/A
A46	KFDvpNS4 As	GTACGAGCTCATGAGTGTTGGTGA TGTTTTGGGTGGTCTGGC	78.1	Add SacI-start codon	N/A
A47	KFDvpNS4 Aas	GTACGGTACCTTATCGCTGTTTTCC CGGCTCTGGCTG	75.6	Add KpnI-stop codon	N/A
A48	KFDvpNS4 Bs	GTACGAGCTCATGAACGAAATGGG CATGTTGGACAAGACAA	76.3	Add SacI-start codon	N/A
A49	KFDvpNS4	GTACGGTACCTTATCTGCGTGTTCC	73.6	Add	N/A

	Bas	AGTTGTCCTAAGCCAC		KpnI-stop codon	
Anti-IFN Activity					
Set B	Primer Name	Sequence	Tm (°C)	Additions	Deleted Region
B1	ZEBOV VP24s	GTACATCGATATGGCTAAAGCTACGGG	60.9	Add ClaI-start codon	N/A
B2	ZEBOV VP24as	GTACGCATGCTTAGATAGCAAGAGAGCTATTAAA	62.5	Add SphI-stop codon	N/A
B3	KFDvpNS5s	GTACATCGATATGGGAGGTGCCGAGGGAGAGACTCTTGG	75.9	Add ClaI-start codon	N/A
B4	KFDvpNS5as	GTACGGTACCTTAGATGATATTGCTTTCCAACTTCAGGTCCCAG	72.9	Add KpnI-stop codon	N/A
B5	KFDvpNS5HAas	GTACGGTACCTTAGGCATAATCTGGGACATCATAAGGGTAGATGATATTGCTTTC	64.6	Add KpnI-HA tag-stop codon	N/A
B6	KFD2kNS4Bs	GTACGAGCTCATGAGTAGCGATGACAACAGACTG	68.1	Add SacI-start codon	N/A
B7	KFD2kNS4Bas	GTACGCATGCTTATCTGCGTGTTCCAGTTGTC	69.1	Add SphI-stop codon	N/A

Anti-IFN NS5 Mutants					
Set C	Primer Name	Sequence	Tm (^{o}C)	Additions	Deleted Region
C1	NS5Δ7686(6)s	GTCTCTCGAGGGACGGCTAAGCTGGCATGGCTAGAAGAACG	78.3	Add Phosphate	Δ 7686-7832 (6-54)
C2	NS5Δ7686(6)as	TCCCTCGGCACCTCCTCTGCGTGTTCCAGTTGTCCTAAG	79.0	Add Phosphate	Δ 7686-7832 (6-54)
C3	NS5Δ7833(55)s	TCCACTGCGATCAGTGGTAACATTATCAACTCAGTGAAC	71.3	Add Phosphate	Δ 7833-8336 (55-222)
C4	NS5Δ7833(55)as	AGCCAGTCCCATGTTTGTCTCACCTCTCTTCAGAAG	71.5	Add Phosphate	Δ 7833-8336 (55-222)
C5	NS5Δ8337(223)s	TTTTGGAGGCTCGTTGATGAGGAAAGAGAGAGACATC	71.8	Add Phosphate	Δ 8337-8963 (223-431)
C6	NS5Δ8337(223)as	GAAGTACATCTCATGCGTGGAATTGCGGGAGAAAG	72.4	Add Phosphate	Δ 8337-8963 (223-431)
C7	NS5Δ8964(432)s	CCTGGGTGTGGCTGGAGCGTTAGGGAAACAG	73.7	Add Phosphate	Δ 8964-9896 (432-742)
C8	NS5Δ8964(432)as	CTCGGGGTCCTCCACTGCTTCTCGGGCG	75.9	Add Phosphate	Δ 8964-9896 (432-742)
C9	NS5Δ9897(743)s	TAAATGCACCAACCATCTGGGACCAGACAAGACAACAC	74.1	Add Phosphate	Δ 9897-10379 (743-903)
C10	NS5Δ9897(743)as	TGACACTCTTGCCCGCCCCACCAACTCATCTTGGT	77.7	Add Phosphate	Δ 9897-10379 (743-903)
C11	NS5Δ7686(6)PCRs	GTACATCGATATGGGAGGTGCCGAGGGAGTCTCTCGAGGGACGGCTAA	81.7	Add ClaI-start	Δ 7686-7832 (6-54)

		G		codon	
C12	NS5Δ9897(743)PCRas	GTACGGTACCTTATGACACTCTTGCCCGCCCC	71.9	Add KpnI-stop codon	Δ 9897-10379 (743-903)
C13	NS5Δ9897(743-HA)as	GTACGGTACCTTAGGCATAATCTGGGACATCATAAGGGTATGACACTCTTG	65.0	Add KpnI-HA tag-stop codon	Δ 9897-10379 (743-903)
Antigenome/ Subgenomic					
Set D	Primer Name	Sequence	Tm (^{o}C)	Additions	Deleted Region
D1	pPOLRMGs	GTCGGCATTTTGGGCCGCCGGGTTATTAGCGGATGTTTTTTCC	81.9	N/A	N/A
D2	pPOLRMGas	CGACCTCCGAAGTTGGGGGGGAAGATTTTTTTGCACGTGAGTG	81.1	N/A	N/A
D3	pPOLag3UTRas	GATGAGCTGTACAAGTAAATGCACCAACCATCTGGGAC	71.4	N/A	N/A
D4	pPOLagGFPs	CCAGATGGTTGGTGCATTTACTTGTACAGCTCATCC	70.3	N/A	N/A
D5	pPOLagGFPas	ACGGACTGGTATTGATGGTGAGCAAGGGCGCCGAG	78.2	N/A	N/A
D6	pPOLag5CHPs	CTCGGCGCCCTTGCTCACCATCAATACCAGTCCG	78.1	N/A	N/A
D7	MGNeg3UTRas	CAAGATCGCCGTGTAAATGCACCAACCATC	69.4	N/A	N/A

D8	**MGNegLucs**	**AGATGGTTGGTGCATTTACACGGCGATCTTG**	**69.7**	**N/A**	**N/A**
D9	**MGNegLucChias**	**GGACTGGTATTGATGGAAGACGCCAAAAAC**	**66.9**	**N/A**	**N/A**
D10	**MGNegLucChis**	**GTTTTTGGCGTCTTCCATCAATACCAGTCC**	**65.8**	**N/A**	**N/A**
D11	**pTM1-Ags**	**ATAATACCATGGAGCGGATGTTTTTTCC**	**61.3**	**Add NcoI**	**N/A**
D12	**pTM1-Agas**	**TCGACTTAATTAATTAGCTCTCCCTTAGCCATC**	**62.3**	**Add PacI**	**N/A**
D13	**KFDvpNS1s**	**GTACATCGATATGGATATGGGCTGTGCAATTGATGCTAACAGGATG**	**78.2**	**Add ClaI-start codon**	**N/A**
D14	**T7-5UTRs**	**TAATACGACTCACTATAGGGAGATTTTTTTGCACG**	**64.0**	**N/A**	**N/A**
D15	**LUCR2as**	**AGGGTTGGACTCAACGTCTCCTGCCAACTTGAGAAGGTCAAAATTCACGGCGATCTT**	**68.0**	**N/A**	**N/A**
D16	**KFDNSs**	**GAGACGTTGAGTCCAACCCTGGGCCCACCCTTTCAGTCGGCTTTTTGATTACTG**	**69.0**	**N/A**	**N/A**
D17	**pTM1-T7as**	**CCCTATAGTGAGTCGTATTAATTTCGCGGGATCGAGATCAATTCAACAATG**	**63.5**	**N/A**	**N/A**
D18	**LucSeq1s**	**AGCTTGCAGTTCTTCATGCCCGTG**	**64.7**	**N/A**	**N/A**
D19	**LucSeq3as**	**CGTCGAAGATGTTGGGGTGTTGCA**	**65.1**	**N/A**	**N/A**

		G			
KFDV-GFP					
Set E	Primer Name	Sequence	Tm (^{o}C)	Additions	Deleted Region
E1	subGFPAGEs	ACCGGTGGAGGTGCCGAGGGAGAGACTC	72.5	Adding Phosphate and AgeI	N/A
E2	subGFPAGEas	ACCGGTTCTGCGTGTTCCAGTTGTCCTAAGC	70.9	Adding Phosphate and AgeI	N/A
E3	KFDVnsGFPs	GTACACCGGTGGAGGTGCCGAGGGAGTGAGCAAGGGCGCC	86.4	Contains cleavage sites for NS5	N/A
E4	KFDVnsGFPas	GTACACCGGTTCTGCGTGTTCCAGTCTTGTACAGCTCATCCATGCC	66.8	Contains cleavage sites for NS4B	N/A
E5	newGFPage4Bs	GGAGGTGCCGAGGGAGTGAGCAAGGG	70.7	Adding Phosphate	N/A
E6	newGFPage4Bas	TCTGCGTGTTCCAGTTGTCCTAAGCCACAGTC	69.5	Adding Phosphate	N/A
E7	subGFPage5s	GGAGGTGCCGAGGGAGAGACTCTTGGG	69.1	Adding Phosphate	N/A
E8	subGFPage5as	TCTGCGTGTTCCAGTCTTGTACAGCTCATCCATG	70.8	Adding Phosphate	N/A

E9	**NS5nostop GFPas**	**CCTTGCTCACTCCCTCGGCACCTCC TCTGCGTGTTCCAGTTGTGATGATA TTGCTTTC**	**70.2**	**N/A**	**N/A**
E10	**cleGFPs**	**AGAGGAGGTGCCGAGGGAGTGAGC AAGGG**	**72.3**	**N/A**	**N/A**
E11	**clestopGFP as**	**TTCTCTGGGAGGTTTTGGTTACTTG TACAGCTC**	**65.1**	**N/A**	**N/A**
E12	**del3UTRs**	**GATGAGCTGTACAAGTAACCAAAA CCTCCCAG**	**64.6**	**N/A**	**N/A**
E13	**ENS1.1as**	**CGCCCTTGCTCACGTTAGCATCAAT TGCACGCCCATATCAGCACCAACC C**	**69.4**	**N/A**	**N/A**
E14	**ENS1GFPs**	**GCAATTGATGCTAACGTGAGCAAG GGCGCCGAG**	**76.4**	**N/A**	**N/A**
E15	**ENS1GFPa s**	**CTTTTCCAGAACACGCTTGTACAGC TCATCCATGCC**	**73.6**	**N/A**	**N/A**
E16	**ENS1.5s**	**GATGAGCTGTACAAGCGTGTTCTG GAAAAGAC**	**65.6**	**N/A**	**N/A**

Figure A.1. KFDV Genome. The 5′ and 3′ UTR regions are colored in dark grey, the single ORF is colored in light grey and a "/" colored in green has been inserted for every 500 bases.

5′AGATTTTTTTGCACGTGAGTGCTCTCGTTTCAGGCAACGTGAGTGGCGCTTTGTTG
GTATTTCCTTGGTGGGAAAGTGTTGAAGCGTTAACGTGTTGAGGAAAAGACAGCTTA
GGAGAACAAGAGCTGGGGATGGCCAAAGGAGCCGTCCTTAAAGGAAAGGGGGGCG
GTCCCCCTAGGCGAGTGCCGAAAGAGACCGCAAAAAAGACGCGTCAAGGACCAGG
CCGATTGCCAAACGGACTGGTATTGATGCGCATGATGGGAGTGCTGTGGCATATGGT
CGCTGGAACGGCCAGGAATCCGATCCTCAAGCGATTCTGGGCGACTGTTCCGGTAC
GGCAGGCCATTGCAGCGCTCCGTAAAATCCGAAAGACAGTTGGACTGCTATTGGAC
TCTTTAAATAAAAGAAGAGGGAAGAGAAGGTCAACCACCGGATTGCTCACGCCAAT
CTTGCTAGCTTGCCTGGCGACCCTGGTGTTCTCTGCGACAGTTCGCAGAGAG/AGAAC
AGGGAACATGGTGATCAGGGCAGAAGGAAAGGACGCAGCCACGCAAGTGGAAGTC
ATGAATGGAACATGCACCATTCTTGCCACAGACATGGGGAGTTGGTGTGATGATTCA
ATCATGTACGAGTGTGTCACCATTGACTCGGGAGAAGAACCAGTTGATGTGGATTGC
TTCTGCAAAGGCGTTGAGCGAGTGTCACTGGAATACGGAAGGTGTGGGAAACCAGC
TGGCGGTAGAAACAGGAGGTCAGTGTCGATTCCGGTGCATGCTCATAGTGATCTCAC
CGGAAGAGGGCACAAGTGGCTTAAAGGGGACTCAGTCAAGACACATCTGACACGTG
TGGAAGGCTGGGTTTGGAAAAACAAGTTCCTGACAGCGGCCTTTTGTGCAGTTGTGT
GGATGGTAACGGACAGCCTGCCGACAAGGTTCATTGTCATAACGGTGGCCCTTTGCC
TGGCTCCTACATATGCCACACGATGCACACACCTGCAGAACCG/GGACTTTGTCTCA
GGGACCCAAGGGACGACTAGAGTTTCATTGGTGTTGGAATTAGGCGGCTGTGTCACC

CTCACAGCTGAAGGCAAGCCATCAGTGGATGTTTGGCTCGACGACATACACCAGGA

GAACCCGGCCAAGACACGAGAGTATTGTCTTCATGCCAAGCTGGCAAACTCCAAGG

TGGCCGCACGTTGTCCAGCCATGGGTCCAGCGACACTGCCAGAGGAGCACCAGGCG

AGCACAGTCTGTAGACGAGACCAGAGTGACAGAGGCTGGGGTAACCATTGTGGACT

GTTCGGGAAGGGCAGCATTGTGGCTTGTGCCAAGTTTAGCTGTGAGGCCAAAAAGA

AGGCAACTGGATATGTGTACGATGTCAACAAAATCACATATGTGGTGAAGGTGGAA

CCTCACACGGGTGACTATCTAGCGGCCAACGAGTCGCACAGCAACCGGAAGACAGC

ATCTTTCACAACGCAGTCCGAGAAGACCATCTTGACAC/TGGGAGATTATGGAGACA

TCTCCCTCACGTGCCGGGTGACTAGTGGAGTGGATCCTGCCCAGACTGTGGTATTGG

AACTGGACAAGACAGCGGAACACTTGCCCAAGGCTTGGCAGGTACACCGAGACTGG

TTTGAGGACCTCTCCTTGCCATGGCGACACGGGGGTGCCCAGGAATGGAACCATGCT

GACCGGCTCGTGGAATTTGGTGAACCGCACGCTGTGAAAATGGACATTTTTAACCTT

GGGGACCAGACGGGTATCCTGTTGAAGTCTCTGGCTGGAGTGCCCGTGGCTAACATA

GAGGGCAGCAAGTACCATCTCCAGAGTGGTCATGTCACCTGCGATGTGGGCCTTGA

AAAACTTAAGATGAAAGGGATGACATACACGGTTTGTGAGGGATCAAAATTTGCTT

GGAAAAGGCCGCCAACCGACAGTGGACATGATACCGTAGTCATGGAGGTGACTTAC

ACCGGGAGCAAGCCATGCAGAATACCAGTG/AGAGCCGTGGCCCATGGAGAACCCA

ATGTTAACGTGGCAAGTCTAATAACCCCAAACCCATCCATGGAAACAACTGGAGGA

GGGTTCGTTGAGCTACAGCTACCACCAGGAGACAACATCATCTATGTTGGTGAGCTG

AGCCACCAGTGGTTTCAGAAGGGCAGCACAATTGGCCGTGTTCTGGAAAAGACCAG

GAGGGGCATAGAGAGACTCACAGTTGTGGGAGAGCACGCCTGGGACTTCGGTTCGG

TAGGCGGCATGCTATCATCAGTGGGGAAGGCTCTACACACGGCTTTTGGCGCAGCAT

TTAATACCATTTTTGGAGGGGTGGGATTCCTCCCACGCATTCTGCTGGGGGTAGCTC

TGGCTTGGCTGGGGCTCAACTCACGGAACCCCACCCTTTCAGTCGGCTTTTTGATTAC

TGGTGGACTTGTGTTGACAATGACACTGGGGGTTGGTGCTGATATGGGCTGTGCAAT

TGATGCTAACAGGATGGAGCT/ACGATGTGGTGAGGGCCTTGTTGTGTGGAGAGAGG

TCACCGACTGGTATGATGGTTACGCATTCCACCCAGAATCGCCCTCTGTCCTTGCGG

CATCTCTAAAAGAAGCATATGAGGAAGGAATTTGTGGTATTGTGCCCCAGAACCGG

CTTGAGATGGCCATGTGGAGGCGTGTGGAGGCTGTGCTCAACTTGGCCCTCGCAGAG

AGTGATGCTAATCTAACGGTGGTTGTGGACAAAAGAGATCCCAGTGACTACAGGGG

AGGCAAAGTGGGAACCCTAAGGCGTTCAGGCAAGGAAATGAAGACGTCATGGAAG

GGATGGAGCCAATCCTTTGTGTGGAGTGTCCCAGAAGCGCCACGGCGTTTTATGGTT

GGGGTTGAGGGGGCTGGAGAGTGTCCTCTTGACAAACGCCGAACAGGAGTCTTCAC

AGTGGCAGAGTTTGGGATGGGAATGAGGACCAAGGTCTTCTTGGACCTACGTGAGA

CTGCCTCCTCAGACT/GTGATACCGGAGTCATGGGGGCTGCAGTCAAAAGCGGTCAT

GCCGTCCACACCGACCAAAGTCTTTGGATGAGGTCGCACAGGAATGCAACGGGAGT

GTTCATATCTGAGTTGATAGTGACCGACCTACGGAACTGCACATGGCCAGCCAGCCA

CACCTTGGACAACGCCGGTGTCGTGGACTCAAAACTCTTCCTTCCAGCAGGCCTGGC

TGGACCACGGTCGCACTACAATCACATTCCTGGGTACGCAGAACAGGTTAAGGGGC

CATGGAGCCAAACGCCCCTACGGGTGGTAAGGGAACCCTGCCCTGGGACTGCGGTT

AAGATTGACCAGAGTTGTGACAAAAGGGGGGCGTCGCTGCGTAGCACGACGGAAAG

CGGGAAGGCCATACCAGAATGGTGTTGCCGCACATGTGAGCTGCCCCCAGTCACAT

TCCGTAGTGGGACTGATTGCTGGTATGCCATGGAAATTAGACCAGTCCACCAACAGG

GTGGTCTG/GTGAGGTCGATGGTGCTGGCTGACAACGGAGCCATGCTAAGTGAAGGT

GGAGTCCCTGGCATTGTGGCTGTGTTCGTGGTCCTGGAGCTGGTCATCAGGAGACGC

CCAACAACTGGCAGTTCAGTGGTGTGGTGTGGGATGGTTGTCCTTGGCCTTGTTGTG

ACTGGGCTAGTCACCATTGAGGGCCTATGCCGCTATGTGGTGGCCGTCGGCATCTTG

ATGAGCATGGAGCTCGGACCAGAGATTGTGGCACTAGTTCTGCTACAGGCAGTGTTT

GACATGAGGACTGGCCTCCTGGTGGCTTTTGCAGTCAAAAGGGCCTACACAACTAG

AGAGGCTGTGGCAACCTATTTCTTGCTCCTCGTGCTGGAACTTGGGTTTCCGGAGGC

CTCACTGAGTAACATCTGGAAGTGGGCCGACTCCTTGGCAATGGGAGCACTGATTCT

CCAGGCGTGTGGTCAGGAGGGTAGAACTCGAGTGGGCTATCTCCTGGCAGCTAT/GA

TGACCCAAAAGGACATGGTAATAATCCACACAGGCTTGACCATTTTTCTATCAGCTG

CCACGGCAATGGCGGTCTGGAGCATGATCAAGGGTCAACGGGACCAGAAGGGACTT

TCCTGGGCCACACCACTTGCAGGCCTCCTTGGAGGCGAGGGAGTGGGTCTTAGATTG

CTGGCGTTTCGAAAGCTTGCCGAGCGAAGGAACAGACGGTCTTTCAGTGAACCACT

GACGGTGGTGGGAGTCATGCTCACTGTGGCAAGTGGGATGGTGAGACACACATCCC

AGGAAGCACTGTGCGCTCTTGTAGCTGGGGCCTTTCTCCTCCTCATGATGGTACTGG

GAACACGGAAGATGCAGCTCACCGCAGAGTGGTGCGGTGAAGTGGAATGGAACCCA

GACCTAGTGAACGAGGGAGGAGAGGTTAATCTGAAAGTGAGGCAGGACGCCATGG

GGAATCTCCATCTCACTGAGGTGGAGAAGGAAGAACGTGCGATGGCGT/TATGGCTT

CTTGCAGGGTTGGTGGCTTCAGCCTTCCACTGGGCAGGCATTCTAATAGTATTGGCT

GTGTGGACACTTTTTGAGATGCTGGGCTCGGGGCGAAGGTCTGAACTTGTCTTCTCT

GGACAGGAGACCCGGACCGAAAGGAATCGGCCCTTTGAGATCAAGGATGGAGCCTA

TCGCATCTACAGCCCTGGCTTGCTTTGGGGACACCGCCAAATTGGAGTGGGGTATGG

AGCCAAGGGAGTTCTGCACACCATGTGGCACGTCACTAGGGGGGCAGCCCTGGTTG

TGGATGAGGCAATCTCTGGACCCTATTGGGCTGACGTCAGGGAAGACGTTGTGTGCT

ATGGTGGAGCATGGAGTCTTGAGAGCCGGTGGAGGGGTGAGACCGTTCAGGTGCAC

GCGTTTCCACCAGGGAGACCCCAAGAGACACACCAGTGCCAGCCGGGTGAACTCAT

CCTGGAGAATGGCAGGAAACTTGGAGCAGTCCCTATTGAC/CTGAGCAAAGGCACCT

CGGGAAGTCCTATCATTAACGCCCAGGGAGAGGTGGTGGGTCTTTATGGGAACGGC

CTGAAGACCAATGAAGCCTATGTCAGCAGCATAGCACAAGGAGAAGCCGAGAAAA

GCAGACCGGAAATCCCGTTGAGTGTGCAAGGAACAGGCTGGATGTCAAAAGGTCAA

ATCACGGTGCTGGACATGCATCCGGGGTCAGGGAAGACACATCGAGTCCTCCCGGA

GCTTGTGAGGCAGTGTGCAGACCGAGGGATGAGGACTCTAGTTCTTGCCCCCACCCG

GGTGGTCCTGAAGGAGATGGAGAGAGCGCTTGCTGGCAAGAAGGTCCGATTCCACT

CACCCGCGGTGGAAGGGCAGACCACAGCGGGGGCCATTGTTGACGTCATGTGCCAT

GCCACGTACGTCCACAGAAGGCTGCTGCCCCAAGGGAGACAAAATTGGGAAGTCGC

CATAATGGATGAGGCCCATTGGACTGATCCGCACAG/TATCGCGGCAAGAGGGCATC

TTTATTCGCTCGCCAAAGAGAACAGGTGCGCCTTGGTGCTCATGACAGCAACTCCAC

CCGGCCGGGGAGATCCTTTCCCGGAGTCCAATGGAGCCATTATGAGTGAGGAAAGG

GCCATTCCGGACGGAGAGTGGAGAGAGGGCTTTGACTGGATAACAGAGTATGAGGG

TCGAACAGCATGGTTCGTTCCATCCATATCAAAAGGTGGGGCGGTTGCAAGAACCCT

GCGCCAGAGAGGCAAAAGTGTGATCTGTCTCAACAGTAAAACCTTTGAGAAGGATT

ACCTGAGGGTCAGGGAAGAGAAGCCAGATTTTGTGGTGACAACAGATATCTCTGAG

ATGGGTGCCAACCTGGATGTCAGCCGAGTTATTGATGGTAGAACAAACATAAAGCC

AGAGGAGGTGGATGGAAAGGTAGAGTTGACTGGAACCAGGAAGGTCACGACAGCA

TCGGCGGCTCAGCGCCGGGGCAGGGTGGGAA/GGACATCTGGACGCACTGATGAGT

ACATATACTCTGGACAGTGTGATGATGACGACACCAGCCTCGTTCAATGGAAGGAG

GCGCAGATACTCCTGGACAATATCACCACACTGAGGGGTCCGGTCGCAACTTTTTAT

GGACCCGAGCAGGTGAAGATGCCAGAAGTGGCTGGCCACTACAGGCTGAATGAGGA

GAAAAGGAAACACTTCCGGCACTTGATGACTCAATGTGACTTCACTCCCTGGCTGGC

GTGGCATGTCGCCACCAACACCAGCAATGTGTTGGATCGGAGCTGGACCTGGCAGG

GGCCGGAGGAAAATGCCATTGACGGGGCCGACGGAGATCTGGTGCGGTTTAAAACG

CCTGGCGGCTCAGAACGTGTCTTGCAGCCGGTGTGGAAGGACTGCAGAATGTTCCGT

GAGGGACGGGACGTCAAAGACTTCATACTGTACGCCTCCGGGCGTCGCAGTGTTGG

TGATGTTTTGGGTGGTCTGGCGGGG/GTCCCCGGTCTCTTGAGGCACAGGTGCGCCA

GCGCGCTTGACGTAGTTTACACCCTTCTCAATGAGAATCCGGGCAGCAGGGCAATGC

GCATGGCTGAGAGAGATGCACCAGAGGCATTTCTGACTATTGTTGAGGTTGCTGTTT

TAGGAGTGGCCACTCTTGGCATACTCTGGTGCTTTGTGGCAAGAGCTTCGGTCAGCC

GCATGTTCCTGGGCACGGTTGTGCTCTTTGCTGCCCTCTTTCTGCTGTGGATTGGTGG

AGTGGACTATGGACACATGGCAGGGATAGCCCTGATATTTTACACCCTCCTCACTGT

GCTGCAGCCAGAGCCGGGAAAACAGCGAAGTAGCGATGACAACAGACTGGCATAC

TTCCTCCTGGGGCTTTTTAGTTTGGCTGGACTCGTGACGGCCAACGAAATGGGCATG

TTGGACAAGACAAAGGCTGACCTTGCAGGGCTGGTGTGGCGCGGAGAGCAGAGGCA

TCCAGCCTGGGAGGA/GTGGACAAATGTGGACATCCAACCAGCACGATCTTGGGGGA

CGTATGTGCTGATCGTCTCTCTGTTCACTCCCTACATGCTGCACCAGCTTCAGACAAA

AATACAACAACTGGTGAACAGTTCAGTGGCAAGTGGTGCTCAGGCTATGAGAGATC

TTGGGGGTGGGACACCATTCTTCGGGGTGGCCGGCCATGTGATTGCCTTGGGCGTCA

CGTCACTCGTGGGTGCCACTCCCATGTCCTTGGGCTTGGGGGTGGCTTTGGCTGCTTT

CCACTTGGCCATCGTCGCCTCGGGATTGGAAGCAGAGCTGACGCAGAGGGCGCACA

GGGTATTCTTCTCGGCAATGGTTAAAAACCCAATGGTGGATGGAGACGTCATCAATC

CCTTCCCCGATGGAGAGACAAAGCCAGCGCTATACGAGAGAAGGATGAGTTTAATC

CTGGCCATTGCCTTGTGCATGGGTTCAGTGGTCCTCAACCGAACCGCGGCCTCAATG

ACCG/AGGCTGGGGCTGTTGGCCTAGCAGCGCTGGGTCAGCTGGTCCATCCCGAGAC

TGAGACACTCTGGACAATGCCAATGGCGTGTGGTATGGCGGGGCTCGTGCGGGGGA

GCTTCTGGGGCCTGTTGCCCATGGGACACCGACTGTGGCTTAGGACAACTGGAACAC

GCAGAGGAGGTGCCGAGGGAGAGACTCTTGGGGACATCTGGAAGAGGCGGCTGAA

TGGTTGCTCTAGGGAGGAGTTTTTTCAGTACCGGCGAAGTGGAGTCATGGAGACGG

AACGTGACAAGGCTCGAGAGCTTCTGAAGAGAGGTGAGACAAACATGGGACTGGCT

GTCTCTCGAGGGACGGCTAAGCTGGCATGGCTAGAAGAACGGGGCTATGCGACCTT

GAAAGGTGAGGTTGTTGATCTCGGCTGTGGCAGAGGCGGGTGGTCATACTACGCTG

CTTCCAGGCCAGCTGTCATGGGAGTGAAGGCCTACACGATAGGAGGGAAAGGCCAT/

GAGGTCCCAAGACTGATCACAAGCCTCGGATGGAACCTCATCAAGTTTAGGACCGG

AATGGATGTGTACTCCCTAGAGGCACACAGGGCTGACACCATCCTTTGTGACATTGG

TGAGAGTAGTCCGGATCCCCTGGCGGAAGGAGAGAGGAGCCGCCGTGTCATCCTCC

TCATGGAGAAATGGAAACTCCGCAACCCTGACGCGTCCTGCGTGTTCAAGGTTTTGG

CTCCGTACAGACCAGAGGTGCTTGAGGCTCTCCACAGATTCCAGCTTCAATGGGGCG

GGGGGTTGGTCCGCGTCCCTTTCTCCCGCAATTCCACGCATGAGATGTACTTCTCCA

CTGCGATCAGTGGTAACATTATCAACTCAGTGAACACTCAGTCCAGGAAGTTGTTGG

CCAGATTTGGGGATCAGCGGGGACCCACCAAGGTCCCCGAGGTGGATCTGGGAACT

GGCACACGCTGTGTGGTACTGGCAGAAGACAAGGTCAGGGAAGCTGA/TGTGGCCG

AAAGAATAGCTGCCCTCAAGACCCAATATGGTGATTCTTGGCATGTGGACAAAGAA

CATCCATACAGAACATGGCAATATTGGGGAAGCTACAAGACAGAGGCCACAGGTTC

GGCTGCCTCTCTGATCAACGGAGTGGTGAAACTCCTCAGTTGGCCCTGGAATGCTAG

GGAGGATGTGGTGCGCATGGCAATGACGGACACAACGGCCTTTGGCCAGCAGAGGG

TTTTTAAGGAAAAGGTGGACACCAAAGCGCAGGAGCCGCAGGTGGGAACCAAGATC

ATCATGAGGGCCGTTAACGACTGGATCTTTGAAAGACTTGCGGGAAAGAAAACACC

ACGACTGTGCACGCGAGAGGAATTCATCGCAAAGGTGCGCTCAAACGCTGCGCTCG

GAGCCTGGTCAGATGAACAAAATCGCTGGCCAAACGCCCGAGAAGCAGTGGAGGA

CCCCGAGTTTTGGAGGCTCGTTGATGAGGAAAGAGAGAGACATC/TTGGAGGACGGT

GTGCCCAGTGTGTGTACAACATGATGGGTAAGAGAGAGAAGAAACTCGGTGAGTTC

GGTGTCGCCAAGGGGAGCCGTGCCATCTGGTACATGTGGTTGGGGAGCCGGTATCT

GGAATTTGAGGCACTGGGTTTCCTCAATGAAGACCACTGGGCTTCCAGGGACCTCAG

TGGAGCGGGGGTTGAGGGGACCAGTCTTAACTACCTGGGATGGCATTTGAAGAAGC

TGTCCGAACTCGAAGGAGGGCTTTTCTATGCCGACGACACAGCGGGCTGGGACACA

AGAATCACCAATGCAGACCTTGAGGATGAGGAGCAAATTCTGCGTTATCTGGAAGG

CGAACACCGAACCCTCGCAAAGACAATCTTGGAAAAAGCTTACCATGCCAAAGTGG

TCAAAGTGGCGCGCCCCTCCAGCTCGGGAGGCTGCGTCATGGACATCATAACCAGA

AGAGACCAACGTGGTTCAGGCCAGGTGGTGACCTACGCT/CTAAACACCCTCACGAA

CATCAAGGTGCAGCTTATCCGCATGATGGAGGGAGAGGGCGTGATCGGGCCATCTG

ACTCACAGGACCCGCGACTCCTACGTGTGGAAGCCTGGCTGAAAGAGCATGGAGAG

GAGCGCCTGACCCGCATGCTGGTCAGTGGGGATGATTGCGTTGTGAGACCAATTGAC

GACCGCTTCGGGAAGGCCCTCTACTTCCTAAATGACATGGCCAAGGTGAGAAAGGA

CATTGGAGAGTGGGAGCCCTCAGAAGGTTACTCCAGCTGGGAGGAGGTCCCCTTTTG

TTCCCACCATTTCCATGAGTTGACGATGAAGGATGGCAGGGTCATAATCGTCCCATG

CAGAGACCAAGATGAGTTGGTGGGGCGGGCAAGAGTGTCACCTGGGTGTGGCTGGA

GCGTTAGGGAAACAGCATGTCTCTCAAAGGCCTATGGACAGATGTGGCTGCTGAGC

TACTTCCACAGGAGGGACCTGAGGACGCTCGG/CCTGGCAATCTGCTCAGCTGTGCC

CATTGATTGGGTCCCGCAGGGACGAACCACATGGAGCATCCACGCGAGTGGAGCGT

GGATGACCACAGAGGACATGCTGGAAGTGTGGAACCGGGTCTGGATTCTTGACAAC

CCCTTCATGGGGGACAAAGGGAAGGTGAGAGAATGGAGGGACATCCCGTACCTCCC

TAAGTCCCAGGATGGGCTGTGCTCTTCCCTGGTGGGACGCCGAGAACGGGCGGAAT

GGGCAAAGAACATCTGGGGATCAGTGGAGAAAGTGAGGAGAATGATCGGCCCCGA

GAGGTATGCTGATTATCTCTCCTGCATGGACAGGCATGAGCTCCACTGGGACCTGAA

GTTGGAAAGCAATATCATCTAAATGCACCAACCATCTGGGACCAGACAAGACAACA

CCCTCACCGTGTGACAGGGGCAACGCGGTAAGGATTGAAGGAGCCCCAACGACGAA

CTGTGGCAGCACACCATTTGGTGACGGG/AAGCTGGTCGCTCCCGACGCAGGTCGTC

GTAAGAACTTTGTGAGACCAAAACCTCCCAGAGAAGGCCGAACTGGGAGGCCATGA

AGGCCCCTGGCTTTAGCCAGGAGGGGGGAGAGGGAAAATTGGCATTCCCTCTCAGG

AGATTTCCTCCCCCTACAACTAAATTTCCCCCTGCTATGCAGGGGGGGCGGTTCTTGT

TCTCCCCGAACCATCATCACCAAGACACAGATTGTCGGACAAGGAGGTGGTGCATG

TTTCGGAAAAAACATCCGCT**3′**

Literature Cited

Adhikari Prabha, M.R. et al., 1993. Clinical study of 100 cases of Kyasanur Forest disease with clinicopathological correlation. *Indian J Med Sci*, 47(5), pp.124–130.

Ajariyakhajorn, C. et al., 2005. Randomized, placebo-controlled trial of nonpegylated and pegylated forms of recombinant human alpha interferon 2a for suppression of dengue virus viremia in rhesus monkeys. *Antimicrob Agents Chemother*, 49(11), pp.4508–4514.

Alcaraz-Estrada, S.L. et al., 2010. Construction of a dengue virus type 4 reporter replicon and analysis of temperature-sensitive mutations in non-structural proteins 3 and 5. *Journal of General Virology*, 91(11), pp.2713–2718.

Alvarez, D.E., Filomatori, C. V & Gamarnik, A. V, 2008. Functional analysis of dengue virus cyclization sequences located at the 5' and 3'UTRs. *Virology*, 375(1), pp.223–35.

Anderson, C.R. & Singh, K.R., 1971. The Reaction of Cattle to Kyasanur Forest Disease Virus. *Indian J Med Res*, 59(2), pp.195–198.

Anderson, J.F. & Rahal, J.J., 2002. Efficacy of interferon alpha-2b and ribavirin against West Nile virus in vitro. *Emerging infectious diseases*, 8(1), pp.107–108.

Andreou, L.V., 2013. Preparation of genomic DNA from bacteria. *Methods in Enzymology*, 529(January), pp.143–151.

Armstrong, J.A., 1981. Cytopathic effect inhibition assay for interferon: microculture plate assay. *Methods in enzymology*, 78(Pt A), pp.381–387.

Ashour, J. et al., 2009. NS5 of dengue virus mediates STAT2 binding and degradation. *Journal of virology*, 83(11), pp.5408–18.

Baker, D.P. et al., 2010. PEGylated interferon beta-1a: meeting an unmet medical need in the treatment of relapsing multiple sclerosis. *Journal of interferon & cytokine research : the official journal of the International Society for Interferon and Cytokine Research*, 30, pp.777–785.

Berger Rentsch, M. & Zimmer, G., 2011. A vesicular stomatitis virus replicon-based bioassay for the rapid and sensitive determination of multi-species type I interferon. *PloS one*, 6(10), p.e25858.

Best, S.M. et al., 2005. Inhibition of interferon-stimulated JAK-STAT signaling by a tick-borne flavivirus and identification of NS5 as an interferon antagonist. *Journal of virology*, 79(20), pp.12828–12839.

Bhat, H.R. et al., 1978. Antibodies to Kyasanur Forest Disease Virus in Bats in the Epizootic-Epidemic Area and Neighbourhood. *Indian J Med Res*, 68, pp.387–392.

Bonaldo, M.C. et al., 2007. Construction and characterization of recombinant flaviviruses bearing insertions between E and NS1 genes. *Virol J*, 4, p.115.

Boshell, J. & Rajagopalan, P.K., 1968. Observations on the experimental exposure of monkeys, rodents and shrews to infestation of ticks in forest in Kyasanur Forest diseases area. *Indian J Med Res*, 56(4), pp.573–588.

Brinton, M. a, 2014. Replication cycle and molecular biology of the West Nile virus. *Viruses*, 6(1), pp.13–53.

Brooks, A.J. et al., 2002. The interdomain region of dengue NS5 protein that binds to the viral helicase NS3 contains independently functional importin beta 1 and importin alpha/beta-recognized nuclear localization signals. *The Journal of biological chemistry*, 277(39), pp.36399–407.

Brown, K.S., Ebihara, H. & Feldmann, H., 2012. Development of a minigenome system for Andes virus, a New World hantavirus. *Arch Virol*, 157(11), pp.2227–2233.

De Burghgraeve, T. et al., 2012. An analogue of the antibiotic teicoplanin prevents flavivirus entry in vitro. *PloS one*, 7(5), p.e37244.

Caignard, G. et al., 2009. Differential regulation of type I interferon and epidermal growth factor pathways by a human Respirovirus virulence factor. *PLoS Pathogens*, 5(9).

Calisher, C.H. et al., 1989. Antigenic relationships between flaviviruses as determined by cross-neutralization tests with polyclonal antisera. *J Gen Virol*, 70 (Pt 1), pp.37–43.

Calisher, C.H., 2000. West Nile virus in the New World: appearance, persistence, and adaptation to a new econiche--an opportunity taken. *Viral immunology*, 13(4), pp.411–414.

Campbell, G.L. et al., 2002. West Nile virus. *Lancet infectious diseases*, 2(September), pp.519–529.

Carletti, F. et al., 2010. Alkhurma hemorrhagic fever in travelers returning from Egypt, 2010. *Emerg Infect Dis*, 16(12), pp.1979–1982.

Chambers, T.J. et al., 1990. Flavivirus Genome Organization, Expression, and Replication. *annual reviews of Microbiology*, 44, pp.649–688.

Chan-Tack, K.M. & Forrest, G., 2005. Failure of interferon alpha-2b in a patient with West Nile virus meningoencephalitis and acute flaccid paralysis. *Scand J Infect Dis*, 37(11-12), pp.944–946.

Charrel, R.N. et al., 2005. Low diversity of Alkhurma hemorrhagic fever virus, Saudi Arabia, 1994-1999. *Emerg Infect Dis*, 11(5), pp.683–688.

Chernov, V.M. et al., 2014. Mycoplasma Contamination of Cell Cultures : Vesicular Traffic in Bacteria and Control over Infectious Agents. *Acta naturae*, 6(22), pp.6–8.

Clyde, K. & Harris, E., 2006. RNA Secondary Structure in the Coding Region of Dengue Virus Type 2 Directs Translation Start Codon Selection and Is Required for Viral Replication RNA Secondary Structure in the Coding Region of Dengue Virus Type 2 Directs Translation Start Codon Selecti. *Journal of virology*, 80(5), pp.2170–2182.

Cohen, J. & Kupferschmidt, K., 2014. A dose of reality. *Science (New York, N.Y.)*, 346(6212), pp.908–11.

Cook, B.W. et al., 2012. The generation of a reverse genetics system for Kyasanur Forest Disease Virus and the ability to antagonize the induction of the antiviral state in vitro. *Virus Res*, 163(2), pp.431–438.

Cook, B.W.M., 2010. *The Molecular Characterization and the Generation of a Reverse Genetics System for Kyasanur Forest Disease Virus by Master of Science*. Manitoba.

Crance, J.M. et al., 2003. Interferon, ribavirin, 6-azauridine and glycyrrhizin: antiviral compounds active against pathogenic flaviviruses. *Antiviral Res*, 58(1), pp.73–79.

Daffis, S. et al., 2011. The naturally attenuated Kunjin strain of West Nile virus shows enhanced sensitivity to the host type I interferon response. *Journal of virology*, 85(11), pp.5664–8.

Dandawate, C.N., Desai, G.B. & Banerjee, K., 1994. Field Evaluation of Formalin Inactivated Kyasanur Forest Disease Virus Tissue Culture Vaccine in Three Districts of Karnataka State. *Indian J Med Res*, 99, pp.152–158.

Davidson, A.D., 2009. Chapter 2. New insights into flavivirus nonstructural protein 5. *Adv Virus Res*, 74, pp.41–101.

Davis, W.G. et al., 2007. Interaction between the cellular protein eEF1A and the 3'-terminal stem-loop of West Nile virus genomic RNA facilitates viral minus-strand RNA synthesis. *Journal of virology*, 81(18), pp.10172–87.

Deardorff, E.R. et al., 2013. Powassan Virus in and New Mexico ,. , 19(12), pp.1–5.

Diamond, M.S. et al., 2000. Modulation of Dengue virus infection in human cells by alpha, beta, and gamma interferons. *Journal of virology*, 74(11), pp.4957–4966.

Dodd, K. a et al., 2014. Kyasanur Forest disease virus infection in mice is associated with higher morbidity and mortality than infection with the closely related Alkhurma hemorrhagic fever virus. *PloS one*, 9(6), p.e100301.

Dodd, K.A. et al., 2011. Ancient ancestry of KFDV and AHFV revealed by complete genome analyses of viruses isolated from ticks and mammalian hosts. *PLoS neglected tropical diseases*, 5(10), p.e1352.

Egloff, M. et al., 2002. An RNA cap (nucleoside-2'-O-) -methyltransferase in the flavivirus RNA polymerase NS5 : crystal structure and functional characterization. *The EMBO journal*, 21(11), pp.2757–2768.

Falzarano, D. et al., 2013. Inhibition of novel beta coronavirus replication by a combination of interferon-alpha2b and ribavirin. *Scientific reports*, 3, p.1686.

Feldmann, H. et al., 2004. Functional Analysis of the Noncoding Regions of the Uukuniemi Virus (Bunyaviridae) RNA Segments. *Journal of virology*, 78(21), pp.11726–11738.

Filomatori, C. V et al., 2006. A 5' RNA element promotes dengue virus RNA synthesis on a circular genome. *Genes Dev*, 20(16), pp.2238–2249.

Flick, R. & Pettersson, R.F., 2001. Reverse genetics system for Uukuniemi virus (Bunyaviridae): RNA polymerase I-catalyzed expression of chimeric viral RNAs. *Journal of virology*, 75(4), pp.1643–1655.

Flint, M. et al., 2014. Inhibitors of the tick-borne, hemorrhagic Fever-associated flaviviruses. *Antimicrobial Agents and Chemotherapy*, 58(6), pp.3206–3216.

Gaynor, R.B., Hillmant, D. & Berkt, A.J., 1984. Adenovirus early region 1A protein activates transcription of a nonviral gene introduced into mammalian cells by infection or transfection. *Proc Natl Acad Sci U S A*, 81(February), pp.1193–1197.

Ghosh Roy, S. et al., 2014. Regulation of cell survival and death during Flavivirus infections. *World journal of biological chemistry*, 5(2), pp.93–105.

Go, Y.Y., Balasuriya, U.B.R. & Lee, C., 2014. Zoonotic encephalitides caused by arboviruses : transmission and epidemiology of alphaviruses and flaviviruses. *Clinical and experimental vaccine research*, pp.58–77.

Gogate, S.S. et al., 1996. Establishment of a cell line from Indian monkey (Macaca radiata) kidney and its characterization. *Indian journal of experimental biology*, 34(2), pp.151–154.

Gould, E.A., Moss, S.R. & Turner, S.L., 2004. Evolution and dispersal of encephalitic flaviviruses. *Arch Virol Suppl*, (18), pp.65–84.

Grard, G. et al., 2007. Genetic characterization of tick-borne flaviviruses: new insights into evolution, pathogenetic determinants and taxonomy. *Virology*, 361(1), pp.80–92.

Gritsun, T.S. et al., 2003. Characterization of a siberian virus isolated from a patient with progressive chronic tick-borne encephalitis. *J Virol*, 77(1), pp.25–36.

Groseth, A. et al., 2005. RNA Polymerase I-Driven Minigenome System for Ebola Viruses RNA Polymerase I-Driven Minigenome System for Ebola Viruses. *Journal of virology*, 79(7).

Hanley, K.A. & Weaver, S.C., 2010. *Frontiers in Dengue Virus Research*, Norfolk, UK: Caister Academic Press.

Harinasuta, C., Wasi, C. & Vithanomsat, S., 1984. The effect of interferon on Japanese encephalitis virus in vitro. *Southeast Asian J Trop Med Public Health*, 15(4), pp.564–568.

Harris, E. et al., 2006. Molecular biology of flaviviruses. *Novartis Found Symp*, 277, pp.23–39; discussion 40, 71–3, 251–3.

Hayasaka, D. et al., 2004. Sub-genomic replicons of Tick-borne encephalitis virus. *Archives of virology*, 149(6), pp.1245–56.

Heim, R., Cubitt, A.B. & Tsien, R.Y., 1995. Improved green fluorescence. *Nature*, 373(6516), pp.663–664.

Hoffmann, H.-H., Schneider, W.M. & Rice, C.M., 2015. Interferons and viruses: an evolutionary arms race of molecular interactions. *Trends in Immunology*, 36(3), pp.124–138.

Holbrook, M.R., 2012. Kyasanur forest disease. *Antiviral Res*, 96(3), pp.353–362.

Howley, P.M. & Knipe, D.M., 2007. *Fields' Virology*, Lippincott Williams & Wilkins.

Ichiyama, K. et al., 2013. Sulfated polysaccharide, curdlan sulfate, efficiently prevents entry/fusion and restricts antibody-dependent enhancement of dengue virus infection in vitro: a possible candidate for clinical application. *PLoS neglected tropical diseases*, 7(4), p.e2188.

Isaacs, A. & Lindenmann, J., 1957. Virus interference. I. The interferon. *Proc R Soc Lond B Biol Sci*, 147(927), pp.258–267.

Isaacs, A., Lindenmann, J. & Valentine, R.C., 1957. Virus interference. II. Some properties of interferon. *Proc R Soc Lond B Biol Sci*, 147(927), pp.268–273.

Issur, M. et al., 2009. The flavivirus NS5 protein is a true RNA guanylyltransferase that catalyzes a two-step reaction to form the RNA cap structure. *RNA (New York, N.Y.)*, 15(12), pp.2340–50.

Jang, S.K. & Wimmer, E., 1990. Cap-independent translation of encephalomyocarditis virus RNA: Structural elements of the internal ribosomal entry site and involvement of a cellular 57-kD RNA-binding protein. *Genes and Development*, 4, pp.1560–1572.

Johansson, M. et al., 2001. A small region of the dengue virus-encoded RNA-dependent RNA polymerase, NS5, confers interaction with both the nuclear transport receptor importin-beta and the viral helicase, NS3. *J Gen Virol*, 82(Pt 4), pp.735–745.

Jones, C.T., Patkar, C.G. & Kuhn, R.J., 2005. Construction and applications of yellow fever virus replicons. *Virology*, 331(2), pp.247–259.

Jones, K.E. et al., 2008. Global trends in emerging infectious diseases. *Nature*, 451(7181), pp.990–993.

Kalil, A.C. et al., 2005. Use of interferon-alpha in patients with West Nile encephalitis: report of 2 cases. *Clin Infect Dis*, 40(5), pp.764–766.

Kapoor, M. et al., 1995. Association between NS3 and NS5 proteins of dengue virus type 2 in the putative RNA replicase is linked to differential phosphorylation of NS5. *J Biol Chem*, 270(32), pp.19100–19106.

Karan, L.S. et al., 2014. Analysis of the complete genome of the tick-borne flavivirus Omsk hemorrhagic fever virus. *Journal of medical virology*, 1187(October 2013), pp.1181–1187.

Kasabi, G.S., Murhekar, M. V, Sandhya, V.K., et al., 2013. Coverage and effectiveness of Kyasanur forest disease (KFD) vaccine in Karnataka, South India, 2005-10. *PLoS Negl Trop Dis*, 7(1), p.e2025.

Kasabi, G.S., Murhekar, M. V, Yadav, P.D., et al., 2013. Kyasanur Forest Disease, India, 2011–2012. *Emerging Infectious Diseases*, 19(2), pp.2011–2012.

Kaur, S., Sassano, A., Joseph, A.M., et al., 2008. Dual regulatory roles of phosphatidylinositol 3-kinase in IFN signaling. *Journal of immunology (Baltimore, Md. : 1950)*, 181(10), pp.7316–7323.

Kaur, S., Sassano, A., Dolniak, B., et al., 2008. Role of the Akt pathway in mRNA translation of interferon-stimulated genes. *Proceedings of the National Academy of Sciences of the United States of America*, 105(12), pp.4808–4813.

Kieseier, B.C. & Calabresi, P.A., 2012. PEGylation of Interferon-β-1a: A promising strategy in multiple sclerosis. *CNS Drugs*, 26, pp.205–214.

Kiran, S.K. et al., 2015. Kyasanur Forest Disease Outbreak and Vaccination Strategy, Shimoga District, India, 2013–2014. *Emerging Infectious Disease journal*, 21(1), p.146.

Kuby, j., 1997. *Immunlogy*, New York, NY, USA: W. H. Freeman and Company.

Kuhn, J.H. et al., 2014. Nomenclature- and database-compatible names for the two Ebola virus variants that emerged in Guinea and the Democratic Republic of the Congo in 2014. *Viruses*, 6(11), pp.4760–99.

Lanciotti, R.S. et al., 1999. Origin of the West Nile Virus Responsible for an Outbreak of Encephalitis in the Northeastern United States. *Emerging Infectious Diseases*, 286(December), pp.2333–2338.

Laurent-Rolle, M. et al., 2014. The Interferon Signaling Antagonist Function of Yellow Fever Virus NS5 Protein Is Activated by Type I Interferon. *Cell Host & Microbe*, 16(3), pp.314–327.

Laurent-Rolle, M. et al., 2010. The NS5 protein of the virulent West Nile virus NY99 strain is a potent antagonist of type I interferon-mediated JAK-STAT signaling. *Journal of virology*, 84(7), pp.3503–15.

Lavoie, T.B. et al., 2011. Binding and activity of all human alpha interferon subtypes. *Cytokine*, 56(2), pp.282–289.

Leardkamolkarn, V. et al., 2012. Development of Dengue type-2 virus replicons expressing GFP reporter gene in study of viral RNA replication. *Virus Research*, 163, pp.552–562.

Li, H. et al., 1999. The serine protease and RNA-stimulated nucleoside triphosphatase and RNA helicase functional domains of dengue virus type 2 NS3 converge within a region of 20 amino acids. *J Virol*, 73(4), pp.3108–3116.

Li, J.-K. et al., 2012. Autophagy is involved in the early step of Japanese encephalitis virus infection. *Microbes and infection / Institut Pasteur*, 14(2), pp.159–68.

Li, S.H. et al., 2013. Development and characterization of the replicon system of Japanese encephalitis live vaccine virus SA14-14-2. *Virol J*, 10, p.64.

Lin, K., Kwong, A.D. & Lin, C., 2004. Combination of a hepatitis C virus NS3-NS4A protease inhibitor and alpha interferon synergistically inhibits viral RNA replication and facilitates viral RNA clearance in replicon cells. *Antimicrobial Agents and Chemotherapy*, 48(12), pp.4784–4792.

Lin, R.-J. et al., 2006. Blocking of interferon-induced Jak-Stat signaling by Japanese encephalitis virus NS5 through a protein tyrosine phosphatase-mediated mechanism. *Journal of virology*, 80(12), pp.5908–18.

Liu, W.J. et al., 2006. A single amino acid substitution in the West Nile virus nonstructural protein NS2A disables its ability to inhibit alpha/beta interferon induction and attenuates virus virulence in mice. *J Virol*, 80(5), pp.2396–2404.

Lu, G. & Gong, P., 2013. Crystal Structure of the full-length Japanese encephalitis virus NS5 reveals a conserved methyltransferase-polymerase interface. *PLoS pathogens*, 9(8), p.e1003549.

Lubick, K.J. et al., 2015. Flavivirus Antagonism of Type I Interferon Signaling Reveals Prolidase as a Regulator of IFNAR1 Surface Expression. *Cell Host & Microbe*, 18(1), pp.61–74.

Mackenzie, J.M. et al., 1998. Subcellular localization and some biochemical properties of the flavivirus Kunjin nonstructural proteins NS2A and NS4A. *Virology*, 245(2), pp.203–215.

Madani, T.A., 2005. Alkhumra virus infection, a new viral hemorrhagic fever in Saudi Arabia. *J Infect*, 51(2), pp.91–97.

Madani, T.A. et al., 2014. Comparison of RT-PCR Assay and Virus Isolation in Cell Culture for the Detection of Alkhumra Hemorrhagic Fever Virus. *Journal of medical virology*, 1180(November 2013), pp.1176–1180.

Mansharamani, H.J. & Dandawate, C.N., 1967. Experimental Vaccine Against Kyasanur Forest Disease (KFD) Virus From Tissue Culture Source II. *Indian journal of pathology and bacteriology*, 10(1), pp.25–32.

Mansharamani, H.J., Dandawate, C.N. & Krishnamurthy, B.G., 1967. Experimental Vaccine Against Kyasanur Forest Disease (KFD) Virus From Tissue Culture Source I. *Indian journal of pathology and bacteriology*, 10(1), pp.9–24.

Massé, N. et al., 2010. Dengue virus replicons: Production of an interserotypic chimera and cell lines from different species, and establishment of a cell-based fluorescent assay to screen inhibitors, validated by the evaluation of ribavirin's activity. *Antiviral Research*, 86(3), pp.296–305.

McGee, C.E. et al., 2010. Infection, dissemination, and transmission of a West Nile virus green fluorescent protein infectious clone by Culex pipiens quinquefasciatus mosquitoes. *Vector borne and zoonotic diseases (Larchmont, N.Y.)*, 10(3), pp.267–274.

McLean, J.E. et al., 2011. Flavivirus NS4A-induced autophagy protects cells against death and enhances virus replication. *The Journal of biological chemistry*, 286(25), pp.22147–59.

Meager, A., 2002. Biological assays for interferons. *J Immunol Methods*, 261(1-2), pp.21–36.

Medin, C.L., Fitzgerald, K. a & Rothman, A.L., 2005. Dengue virus nonstructural protein NS5 induces interleukin-8 transcription and secretion. *Journal of virology*, 79(17), pp.11053–61.

Mehla, R. et al., 2009. Recent ancestry of Kyasanur Forest disease virus. *Emerg Infect Dis*, 15(9), pp.1431–1437.

Memish, Z. a et al., 2014. Is the epidemiology of alkhurma hemorrhagic fever changing?: A three-year overview in Saudi Arabia. *PloS one*, 9(2), p.e85564.

Moritoh, K. et al., 2011. Development and application of West Nile virus subgenomic replicon RNA expressing secreted alkaline phosphatase. *The Journal of veterinary medical science / the Japanese Society of Veterinary Science*, 73(5), pp.683–686.

Morrey, J.D. et al., 2002. Identification of active antiviral compounds against a New York isolate of West Nile virus. *Antiviral Research*, 55(1), pp.107–116.

Morrison, J. et al., 2013. Dengue virus co-opts UBR4 to degrade STAT2 and antagonize type I interferon signaling. *PLoS pathogens*, 9(3), p.e1003265.

Moss, B. et al., 1990. Product review. New mammalian expression vectors. *Nature*, 348(6296), pp.91–92.

Mourya, D.T. et al., 2013. Spread of Kyasanur Forest Disease, Bandipur Tiger Reserve, India, 2012-2013. *Emerging Infectious Diseases*, 19(9), pp.1540–1541.

Munoz-Jordan, J.L. et al., 2005. Inhibition of alpha/beta interferon signaling by the NS4B protein of flaviviruses. *J Virol*, 79(13), pp.8004–8013.

Musso, M. et al., 2015. A case of Alkhumra virus infection. *Journal of Clinical Virology*, 66, pp.12–14.

Ng, C.Y. et al., 2007. Construction and characterization of a stable subgenomic dengue virus type 2 replicon system for antiviral compound and siRNA testing. *Antiviral Research*, 76(3), pp.222–231.

Park, G.S. et al., 2007. Identification of Residues Critical for the Interferon Antagonist Function of Langat Virus NS5 Reveals a Role for the RNA-Dependent RNA Polymerase Domain. *Journal of virology*, 81(13), pp.6936–6946.

Pattnaik, P., 2006. Kyasanur forest disease: an epidemiological view in India. *Rev Med Virol*, 16(3), pp.151–165.

Pestka, S., 2007. The interferons: 50 Years after their discovery, there is much more to learn. *Journal of Biological Chemistry*, 282(28), pp.20047–20051.

Petersen, L.R. & Barrett, A.D., 2009. Arthropod-Borne Flaviviruses. In D. D. Richman, R. J. Whitley, & F. G. Hayden, eds. *Clinical Virology*. Washington, D. C. USA: ASM Press, pp. 1173–1208.

Pierson, T.C. et al., 2005. An infectious West Nile virus that expresses a GFP reporter gene. *Virology*, 334(1), pp.28–40.

ProMED-mail, 2015. Kyasanur forest disease - India (GA). *ProMED-mail*, 9. Available at: http://www.promedmail.org/direct.php?id=3306895 [Accessed April 18, 2015].

Rahal, J.J. et al., 2004. Effect of interferon-alpha2b therapy on St. Louis viral meningoencephalitis: clinical and laboratory results of a pilot study. *J Infect Dis*, 190(6), pp.1084–1087.

Randall, R.E. & Goodbourn, S., 2008. Interferons and viruses: an interplay between induction, signalling, antiviral responses and virus countermeasures. *J Gen Virol*, 89(Pt 1), pp.1–47.

Ravanini, P. et al., 2011. Rhabdomyolysis and severe muscular weakness in a traveler diagnosed with Alkhurma hemorrhagic fever virus infection. *J Clin Virol*, doi: 10.10.

Ray, D. et al., 2006. West Nile virus 5'-cap structure is formed by sequential guanine N-7 and ribose 2'-O methylations by nonstructural protein 5. *Journal of virology*, 80(17), pp.8362–70.

Reed, L.J. & Muench, H., 1938. A Simple Method of Estimating Fifty Per cent Endpoints. *The American Journal of Hygiene*, 27(3), pp.493–497.

Reid, S.P. et al., 2006. Ebola virus VP24 binds karyopherin alpha1 and blocks STAT1 nuclear accumulation. *J Virol*, 80(11), pp.5156–5167.

Ritchie, S.A. & Rochester, W., 1998. Wind-Blown Mosquitoes and Introduction of Japanese Encephalitis into Australia. *Emerging Infectious Diseases*, 7(5), pp.1996–1999.

Robertson, S.J. et al., 2014. Tick-Borne Flaviviruses Antagonize Both IRF-1 and Type I IFN Signaling To Inhibit Dendritic Cell Function. *The Journal of Immunology*, 192(6), pp.2744–2755.

Robertson, S.J. et al., 2009. Tick-borne flaviviruses: dissecting host immune responses and virus countermeasures. *Immunol Res*, 43(1-3), pp.172–186.

Rocha-Pereira, J. et al., 2013. The viral polymerase inhibitor 2'-C-methylcytidine inhibits Norwalk virus replication and protects against norovirus-induced diarrhea and mortality in a mouse model. *Journal of virology*, 87(21), pp.11798–805.

Samsa, M.M. et al., 2009. Dengue virus capsid protein usurps lipid droplets for viral particle formation. *PLoS Pathog*, 5(10), p.e1000632.

Samuel, M.A. et al., 2006. PKR and RNase L contribute to protection against lethal West Nile Virus infection by controlling early viral spread in the periphery and replication in neurons. *J Virol*, 80(14), pp.7009–7019.

Samuel, M.A. & Diamond, M.S., 2005. Alpha/beta interferon protects against lethal West Nile virus infection by restricting cellular tropism and enhancing neuronal survival. *Journal of virology*, 79(21), pp.13350–13361.

Schoggins, J.W. et al., 2011. A diverse range of gene products are effectors of the type I interferon antiviral response. *Nature*, 472(7344), pp.481–5.

Schoggins, J.W. et al., 2014. Pan-viral specificity of IFN-induced genes reveals new roles for cGAS in innate immunity. *Nature*, 505(7485), pp.691–5.

Shah, K. V, Dandawate, C.N. & Bhatt, P.N., 2012. Kyasanur forest disease virus: viremia and challenge studies in monkeys with evidence of cross-protection by Langat virus infection. *F1000Research*, 1, p.61.

Shaner, N.C., Patterson, G.H. & Davidson, M.W., 2007. Advances in fluorescent protein technology. *J Cell Sci*, 120(Pt 24), pp.4247–4260.

Shimomura, O., Johnson, F.H. & Saiga, Y., 1962. Extraction, Purification and Properties of Aequorin, a Bioluminescent Protein from the Luminous Hydromedusan Aequorea. *Journal of Cellular and Comparative Physiology*, 59(3), pp.223–239.

Singh, B.B. & Gajadhar, a a, 2014. Role of India's wildlife in the emergence and re-emergence of zoonotic pathogens, risk factors and public health implications. *Acta tropica*, 138C, pp.67–77.

Sleifer, S. et al., 2005. Side effects of interferon-alpha therapy. *Pharm World Sci*, 27, pp.423–431.

Solomon, T. et al., 2003. Interferon alfa-2a in Japanese encephalitis: a randomised double-blind placebo-controlled trial. *Lancet*, 361(9360), pp.821–826.

Sperber, S.J. et al., 1992. Anti-HIV-1 activity of recombinant and hybrid species of interferon-alpha. *J Interferon Res*, 12(5), pp.363–368.

Sperber, S.J. et al., 1993. Anti-rhinoviral activity of recombinant and hybrid species of interferon alpha. *Antiviral Res*, 22(2-3), pp.121–129.

Stone, R., 2014. Monkey fever unbound. *Science (New York, N.Y.)*, 345(6193), pp.130–1, 133.

Takeuchi, O. & Akira, S., 2009. Innate immunity to virus infection. *Immunol Rev*, 227(1), pp.75–86.

Talavera, D. et al., 2004. IL8 release, tight junction and cytoskeleton dynamic reorganization conducive to permeability increase are induced by dengue virus infection of microvascular endothelial monolayers. *The Journal of general virology*, 85(Pt 7), pp.1801–13.

Tandale, B. V et al., 2015. New focus of Kyasanur Forest disease virus activity in a tribal area in Kerala, India, 2014. *Infectious diseases of poverty*, 4, p.12.

Taylor, R.T. et al., 2011. TRIM79??, an interferon-stimulated gene product, restricts tick-borne encephalitis virus replication by degrading the viral RNA polymerase. *Cell Host and Microbe*, 10(3), pp.185–196.

Theriault, S. et al., 2004. Rescue of Ebola virus from cDNA using heterologous support proteins. *Virus Research*, 106(1), pp.43–50.

Trapido, H. et al., 1959. Kyasanur Forest disease. VIII. Isolation of Kyasanur Forest disease virus from naturally infected ticks of the genus Haemaphysalis. *Indian J Med Res*, 47(2), pp.133–138.

Trapido, H. et al., 1964. Ticks Ectoparasitic on Monkeys in the Kyasanur Forest Disease Area of Shimoga District, Mysore State, India. *Am J Trop Med Hyg*, 13, pp.763–772.

Tsien, R.Y., 1998. The green fluorescent protein. *Annu Rev Biochem*, 67, pp.509–544.

Uchil, P.D., Kumar, A. V & Satchidanandam, V., 2006. Nuclear localization of flavivirus RNA synthesis in infected cells. *J Virol*, 80(11), pp.5451–5464.

Velado Fernández, I. et al., 2014. Development of a novel protocol for generating flavivirus reporter particles. *Journal of virological methods*, 208, pp.96–101.

Verhelst, J., Hulpiau, P. & Saelens, X., 2013. Mx proteins: antiviral gatekeepers that restrain the uninvited. *Microbiology and molecular biology reviews : MMBR*, 77(4), pp.551–66.

Villordo, S.M. & Gamarnik, A. V, 2009. Genome cyclization as strategy for flavivirus RNA replication. *Virus Res*, 139(2), pp.230–239.

Voigt, E. et al., 2013. A quantitative infection assay for human type I, II, and III interferon antiviral activities. *Virology journal*, 10, p.224.

Wang, J. et al., 2009. Isolation of kyasanur forest disease virus from febrile patient, Yunnan, China. *Emerging Infectious Diseases*, 15(2), pp.326–328.

Webb, H.E. & Chaterjea, J.B., 1962. Clinico-pathological observations on monkeys infected with Kyasanur Forest disease virus, with special reference to the haemopoietic system. *Br J Haematol*, 8, pp.401–413.

Werme, K., Wigerius, M. & Johansson, M., 2008. Tick-borne encephalitis virus NS5 associates with membrane protein scribble and impairs interferon-stimulated JAK-STAT signalling. *Cell Microbiol*, 10(3), pp.696–712.

Westaway, E.G. et al., 1997. Ultrastructure of Kunjin virus-infected cells: colocalization of NS1 and NS3 with double-stranded RNA, and of NS2B with NS3, in virus-induced membrane structures. *Journal of virology*, 71(9), pp.6650–6661.

Work, T.H. et al., 1957. Kyasanur forest disease. III. A preliminary report on the nature of the infection and clinical manifestations in human beings. *Indian J Med Sci*, 11(8), pp.619–645.

Work, T.H., Roderiguez, F.R. & Bhatt, P.N., 1959. Virological epidemiology of the 1958 epidemic of Kyasanur Forest disease. *Am J Public Health Nations Health*, 49(7), pp.869–874.

Yap, T.L. et al., 2007. Crystal structure of the dengue virus RNA-dependent RNA polymerase catalytic domain at 1.85-angstrom resolution. *J Virol*, 81(9), pp.4753–4765.

Yoshii, K. et al., 2014. A critical determinant of neurological disease associated with highly pathogenic tick-borne flavivirus in mice. *Journal of virology*, 88(10), pp.5406–20.

Yoshii, K. et al., 2005. Packaging the replicon RNA of the Far-Eastern subtype of tick-borne encephalitis virus into single-round infectious particles: development of a heterologous gene delivery system. *Vaccine*, 23(30), pp.3946–56.

Yoshii, K. & Holbrook, M.R., 2009. Sub-genomic replicon and virus-like particles of Omsk hemorrhagic fever virus. *Arch Virol*, 154(4), pp.573–580.

Youn, S. et al., 2013. Non-structural protein-1 is required for West Nile virus replication complex formation and viral RNA synthesis. *Virology journal*, 10, p.339.

Yu, L., Takeda, K. & Markoff, L., 2013. Protein-protein interactions among West Nile non-structural proteins and transmembrane complex formation in mammalian cells. *Virology*, 446(1-2), pp.365–77.

Zou, G. et al., 2011. Development and characterization of a stable luciferase dengue virus for high-throughput screening. *Antiviral Res*, 91(1), pp.11–19.